Towards a Rational Design of Commercial Maltodextrins: a Mechanistic Approach

Leon M. Marchal

Promotor: Dr. ir. J. Tramper
Hoogleraar in de bioprocestechnologie

Co-promotoren: Dr. J. Bergsma
Senior scientist Avebe, Foxhol

Dr. ir. C.D. de Gooijer
Universitair hoofddocent bij de sectie proceskunde

Leon M. Marchal

Towards a Rational Design of Commercial Maltodextrins: a Mechanistic Approach

Proefschrift
ter verkrijging van de graad van doctor
op gezag van de rector magnificus
van de Wageningen Universiteit,
dr. C.M. Karssen,
in het openbaar te verdedigen
op maandag 4 oktober 1999
des namiddags te vier uur in de Aula.

This study was funded by Avebe and the Dutch Ministry of Economic Affairs (PBTS Biotechnology Project No. BIO94043)

ISBN 90-5808-107-9

Voorwoord

Een nawoordje van de schrijver als voorwoord voor de lezer.

Een proefschrift voltooien is over het algemeen geen solo-actie meer. Velen hebben eraan bijgedragen, die ik hiervoor wil bedanken. Allereerst mijn promotor, Hans Tramper, die ik wil bedanken voor alle vrijheid die je me gaf om deze promotie vorm te geven. Je hebt me nooit iets dwingend proberen op te leggen en je stond altijd open voor nieuwe denkbeelden en voorstellen met betrekking tot het onderzoek. Je was voorts nooit te beroerd om beargumenteerd commentaar te leveren. Deze zaken gelden trouwens voor de gehele begeleidingscommissie; bestaande uit Kees de Gooijer, Rik Beeftink, Jack Bergsma en Bert Franke. Ik heb de 6 à 8 wekelijkse bijeenkomsten als zeer nuttig ervaren. Het gaf de benodigde deadlines en zorgde voor een goede reflectie van het uitgevoerde onderzoek.
Voorts wil ik jullie bedanken voor het kritisch doorworstelen van de conceptartikelen. Iedereen wist altijd weer andere verbeteringen aan te dragen en over sommige (spellings)zaken werd door de verschillende mensen duidelijk anders gedacht.

Niet te vergeten, wil ik uiteraard ook de studenten bedanken die bijgedragen hebben aan de totstandkoming van dit proefschrift. In volgorde van aankomst: Jan Jonkers, Monique Keultjes, Elwin Wolters, Teun van de Laar, Eef Schimmelpennink, Joost Zondervan, Earl Goetheer, Rein Ulijn en Stefan van der Burgh. Mensen bedankt, zonder jullie bijdrage zou dit boekje een stuk dunner geworden zijn.

Ook wil ik de mensen bij Avebe bedanken. In het bijzonder Stoffer Rustebiel voor het vele HPLC werk dat je voor me hebt uitgevoerd. Voorts de mensen bij de afdeling Process Research voor de gezellige open sfeer en de vele leuke (lunch)discussies. Alhoewel ik formeel onder de sectie Proceskunde van de LUW viel, heb de volledige 4 jaar in Veendam gesleten. De vakgroepsfeer heb ik meegekregen van dagbezoekjes aan Wageningen en uiteraard de 2 studiereizen en een aantal labuitjes. Mensen bedankt voor deze leuke tijd.

leon

Contents

Chapter 1

General Introduction

Starch

Almost all green plants produce starch as a source of energy storage. The starch is deposited in special organelles (chloroplasts and amyloplasts) as small granules ranging from 1 to 100 μm. These tiny white granules occur in various parts of plants, for example in cereal grains (maize, wheat), in roots (tapioca) and in tubers (potatoes). The granules vary in size and shape depending on the plant source, and are insoluble in cold water (Swinkels, 1985). Starch is a polymer composed of glucose units primarily linked by α(1→4) glucosidic bonds, with some additional α(1→6) linkages (Figure 1).

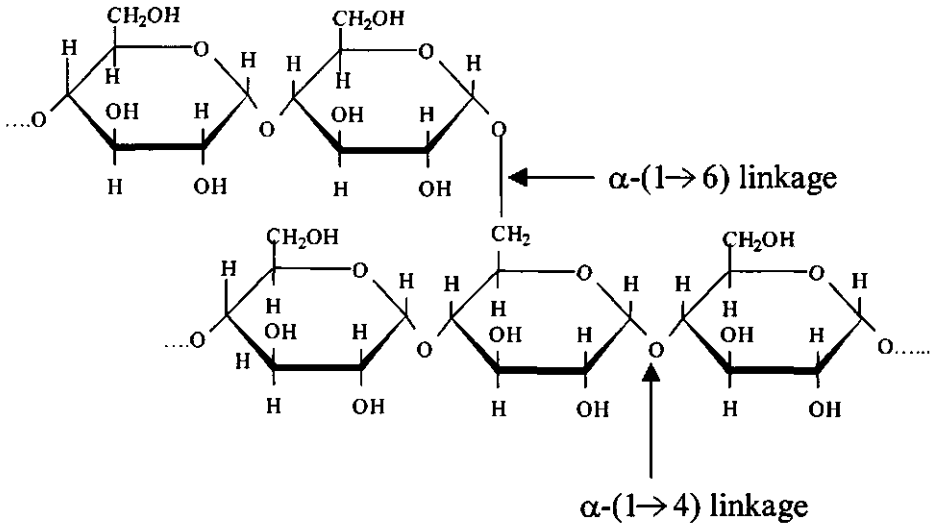

Figure 1: Schematic representation of α-(1→4) and α-(1→6) linked glucose units in starch.

It consists of a mixture of two types of polymers: amylose and amylopectin. The relative mass contribution of amylose and amylopectin varies but normally lies around 20-30% [w/w] for amylose and 70-80% [w/w] for amylopectin. Varieties with deviating compositions also exist, for example nearly 100% pure amylopectin potato and maize starch. Amylopectin is a branched polymer in which linear chains, containing on average 20-24 $\alpha(1\rightarrow4)$-linked D-glucose residues, are linked by $\alpha(1\rightarrow6)$-D-glucosidic linkages to form a multiple-branched structure. More information on the structure of amylopectin can be found in chapter 5.

The percentage of $\alpha(1\rightarrow6)$ linkages in amylose (0.2-0.7%) is much smaller than in amylopectin (4-5%), resulting in a more linear polymer (Hizukuri, 1996).

The worldwide production of industrial starch showed a steady increase over the last two decades (Table I). Primary triggers for this increase were increased demand for high fructose syrups (specially in the USA and to a lesser extent in Europe due to high taxes), glucose syrups for fermentation purposes, and wheat gluten (resulting in starch as a by-product). Despite this increase in demand there currently is a worldwide overproduction of starch.

Table I: Annual worldwide production of commercial starches in million metric tons.

Botanical source	1980*	1990*	1993*	1995/1996†
Maize	11.6	20	26.3	35.2
Potato	1.4	2.4	2.5	2.1
Tapioca & others	1.5	1.7	3.2	3.8
Wheat	0.6	1.5	1.7	2.8
Total	15.1	25.6	33.7	43.9

*Courtesy of Avebe, Veendam, the Netherlands. †(HRA, 1997)

Starch is used for various applications mainly in the food, paper and textile industries (Whistler et al., 1984). A significant quantity of this starch is modified (chemically, physically, or enzymatically) before use. The main modifications are polymer degradation,

oxidation, cross-linking, and substitution with various groups, and combinations thereof. This thesis deals with one of these modifications, the partial enzymatic degradation of starch to a saccharide mixture.

Historic perspective of enzymatic starch hydrolysis

Payen and Persoz were the first to become aware of enzymatic starch hydrolysis in 1833, when a malt extract was found to convert starch to sugar (Payen and Persoz, 1833).

A fungal amylase preparation was first employed for commercial syrup manufacture in 1938 (Dale and Langlois, 1940). The enzyme preparation contained a mixture of glucoamylase and α-amylase and was used to further hydrolyse an acid hydrolysate (Schenck, 1992). Glucoamylases are capable of cleaving both α(1→4) and α(1→6) linked glucose units and can convert starch to glucose. Glucoamylase is a so-called exo-enzyme, cleaving off glucose units from the non-reducing ends of saccharides (Figure 2).

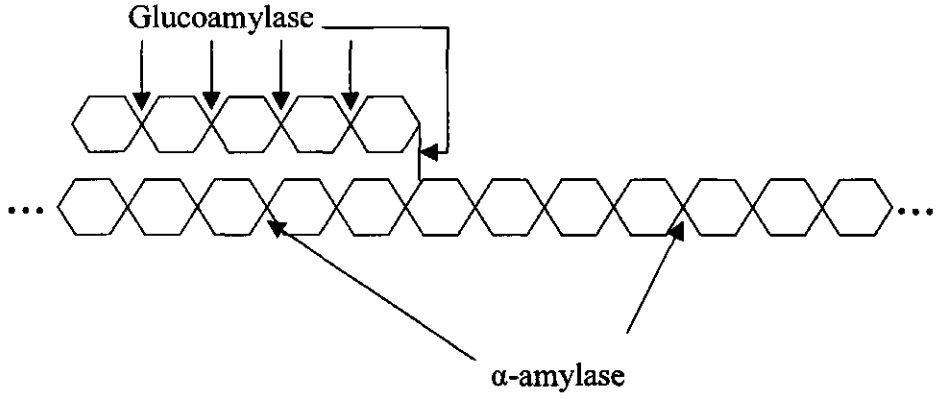

Figure 2: Schematic representation of the way in which α-amylase and glucoamylase hydrolyze starch.

An α-amylase is only capable of cleaving α(1→4) linked glucose units, but, in contrast to a glucoamylase, can hydrolyze inside a saccharide polymer. An α-amylase is therefore a so-called endo-enzyme. In 1951, glucoamylases from both *Aspergillus niger* (Kerr et al., 1951)

and *Rhizopus delemar* (Phillips and Caldwell, 1951a,b) were characterized. The enzyme from the *Rhizopus* strain was called glucoamylase and the *Aspergillus* enzyme amyloglucosidase. Both terms are still in use although the official trivial name for the enzyme is glucoamylase. Investigations continued, especially on the removal of the contaminating enzyme transglucosidase (that reduces the yield of glucose attained), and commercial operation, for the production of crystalline glucose, was initiated by 1960 (Schenck, 1992). Having reached commercial success with enzymatic saccharification, the next goal was to replace acid hydrolysis completely by developing a high temperature amylase that could efficiently liquefy starch. Thermostable bacterial α-amylases had been developed in the early 1900s by Boidin and Effront (1917a,b) and were used since that time in the brewing, textile and paper industries. So, it was a logical step to use these heat-stable α-amylases for starch liquefaction, and the first commercial processes were implemented in the early 1960s (Schenck, 1992).

Maltodextrin production

In the early 1950s, researchers had coined the term maltodextrin for saccharide mixtures that consist of maltose, maltotriose, maltotetraose, maltopentaose etc (Walker and Whelan, 1957; Whelan and Roberts, 1952). The first commercial maltodextrin was Frodex 15 (later called Lo-Dex 15), introduced by American Maize Products Company in 1959 (Alexander, 1992). In the 40 years that followed, a range of commercial maltodextrins became available and maltodextrins are now used in a wide range of applications. Maltodextrins are used for example as carrier or bulk agent, texture provider, spray-drying aid, fat replacer, film former, freeze control agent, to prevent crystallization, or to supply nutritional value. The last chapter of this thesis gives more information on the saccharide composition of a starch hydrolysate in relation to its physical and biological properties in various applications. The total world market of starch hydrolysate products (excluding dextrose, glucose and fructose syrups, and polyols) was estimated at some 2 million metric tons in 1995/1996 (HRA, 1997). Figure 3 gives the basic production scheme for maltodextrins.

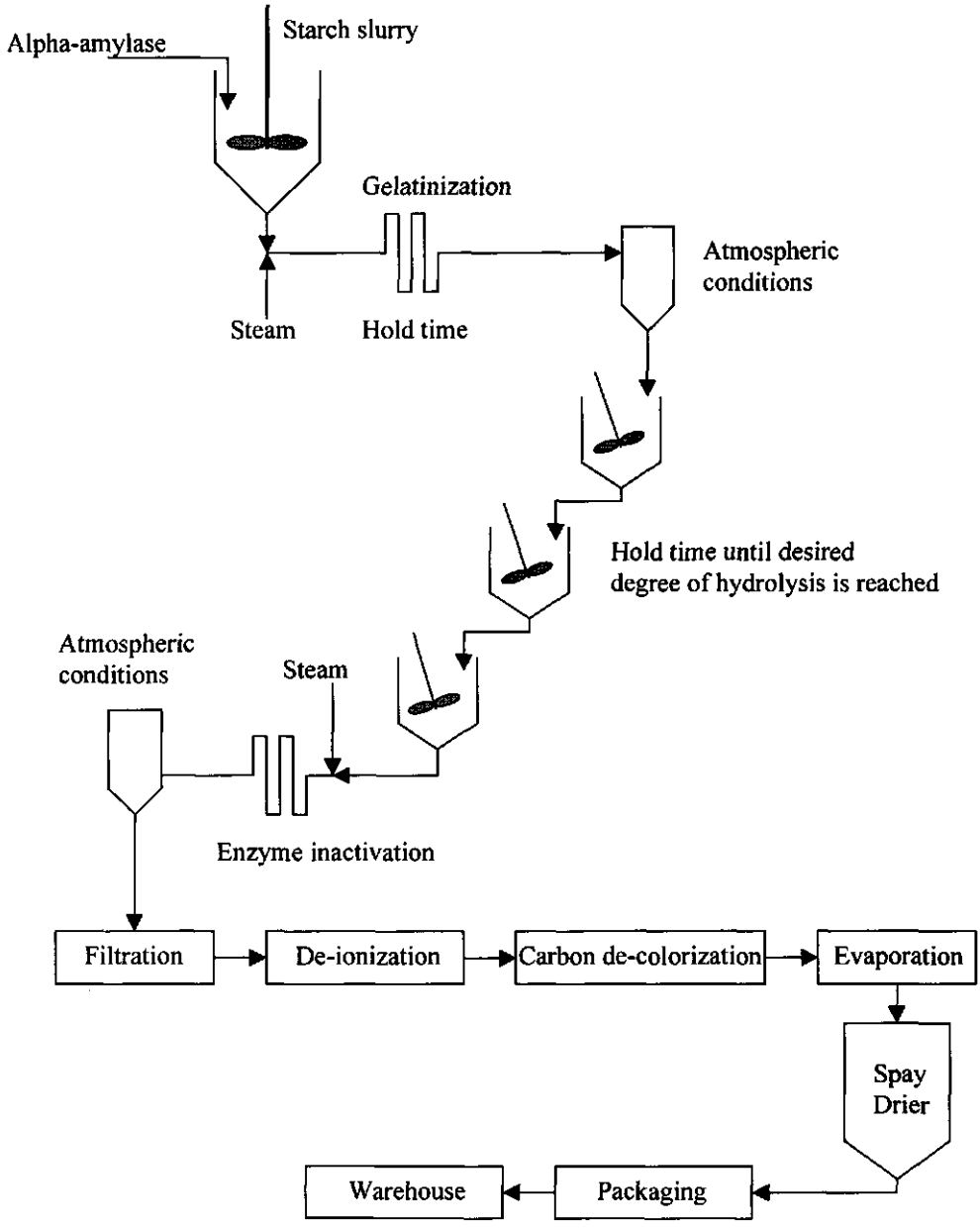

Figure 3: Schematic representation of the process for the conversion of starch to maltodextrins.

Of course, many variations to this basic theme exist. A starch slurry (40% dry weight [w/w]) with added heat-stable α-amylase (usual liquid enzyme preparation dosage 0.01% [v/w] on dry starch basis) is dissolved at neutral pH (6-7) by steam injection in a jetcooker. After a holding time (2-3 minutes), the pressure is reduced to atmospheric conditions cools down the starch solution. The hydrolysis reaction is continued at 85-90°C until the desired degree of hydrolysis is reached. Hereafter the enzyme is inactivated by a second heat treatment. Impurities are removed by filtration, and after de-ionization and carbon decolorization the dry weight concentration is increased in an evaporator to about 70% [w/w] before spray drying to the final product. Starch hydrolysis products (i.e. maltodextrins) are normally characterized by their dextrose equivalent (DE) value, which is a related to the degree of hydrolysis. The theoretical definition of dextrose equivalent is:

$$DE \equiv \frac{\text{Molecular weight dextrose}}{\text{Number - average molecular weight starch hydrolysat e}} \times 100 \qquad (1)$$

Starch, which has a very high molecular weight, has a dextrose equivalent of virtually zero. Totally converted starch (dextrose, the trivial name for glucose) has a dextrose equivalent of 100. So, the dextrose equivalent is convenient number between zero and 100, to easily characterize the mean-average molecular weight of a starch hydrolysate. The USA Food and Drug Administration defined maltodextrins as non-sweet starch hydrolysate products with a dextrose equivalent of less than 20 (Schenck, 1992). This arbitrarily fixed limited value is not always taken absolute in this thesis and higher degrees of hydrolysis are also evaluated.

Outline of this thesis

The central issue at the start of this research project was: Is the actual production process for maltodextrins optimal or can it be improved?

To answer this question, evaluation of a considerable number of hydrolysis experiments is necessary. The traditional titration methods (Lane and Eynon, 1923; Schoorl, 1929) to determine the degree of hydrolysis (DE) are not only time-consuming, but also inaccurate

(Commerford and Scallet, 1969). Therefore in chapter two, the use of osmometry (freezing-point depression) is described to determine the degree of hydrolysis of starch in a fast, reliable and above all accurate way. Throughout the work presented in this thesis osmometry was used. Six parameters (including their interactions), notably temperature, dry weight concentration, calcium addition, enzyme dosage, pH and the stirring speed were investigated with respect to their effects on the rate of hydrolysis (chapter 3). This was done by a set up of experiments according to a central composite design, to restrict the number of experiments to an acceptable level. Special emphasis in this kinetic study was placed on the use of industrially relevant high dry-weight concentrations. Research reports on this range were scarce, probably due to difficulties in handling these highly viscous starch solutions, and the special equipment required (i.e. stirred autoclave, jetcooker). An accurate description (within the investigated process ranges) of the enzymatic hydrolysis could be given, suitable for better control of the process. The most remarkable outcome of this kinetic study was, however, not related to enzyme activity, but to enzyme specificity. The temperature at which hydrolysis took place was found to influence the saccharide composition obtained at the end of the hydrolysis. The mean-average molecular weight of these hydrolysates was the same, but their saccharide composition differed. This was investigated in more detail, by posing four questions about this phenomenon (chapter 4):

1) How does the influence of temperature on the oligosaccharide composition evolve during hydrolysis?
2) Is there a temperature influence on the overall molecular weight distribution in the initial hydrolysis?
3) What are the mechanisms underlying this temperature phenomenon?
4) Do other bacterial α-amylases also show a similar temperature influence?

The reaction temperature proved to be a valuable tool for the production of starch hydrolysate products with a better-defined saccharide composition. Gradually, it became evident that advances in maltodextrin production are not so much related to a cheaper production process for the current maltodextrins (already quite optimal in industrial practice), but to the development of maltodextrins with a more defined saccharide

composition for specific applications (so-called tailor-made maltodextrins). A model, capable of describing the hydrolysis of starch with respect to the saccharide produced, can be a potent tool in the development of tailor-made maltodextrins. Since no suitable models were available, work was initiated on the development of such a model. In first instance, the structure of amylopectin in solution was modeled in a computer matrix (chapter 5). When this modeled amylopectin structure was evaluated with independent literature values related to the structure of amylopectin (i.e. percentage β-hydrolysis), it was recognized that these values were not corrected for the hydrolytic gain during hydrolysis. This overestimation of the actual percentage of β-hydrolysis can be corrected for, however (chapter 6). The resulting model of amylopectin in solution can be used very well to simulate all kind of enzymatic or chemical reactions. This is demonstrated in chapter 7 by evaluation of the saccharides produced upon hydrolysis with an α-amylase, the principal enzyme used in maltodextrin production. The final chapter deals with the design procedure for more tailor-made starch hydrolysate products. Both defining an optimal saccharide composition and ways of producing this at acceptable cost are discussed. Furthermore, future research needs are pointed out.

References

Alexander, R.J. 1992. Maltodextrins:production, properties and applications, pp.233-276.In: Schenck FW and Hebeda RE (eds.), Starch hydrolysis products; Worldwide technology, production, and applications, VCH Publishers, New York.

Boidin, A., Effront, J. Process for treating amylaceous substances. United States Patent. 1,227,374. 1917a.

Boidin, A., Effront, J. Process of manufacturing diastases and toxins by oxidizing ferments. United States Patent. 1,227,525. 1917b.

Commerford, J.D., Scallet, B.L. 1969. Reaction of oligosaccharides II Dextrose equivalents. Cereal. Chem. **46:** 172-176.

Dale, J.K., Langlois, D.P. Sirup and method of making the same. United States Patent. 2,201,609. 1940.

Hizukuri, S. 1996. Starch:Analytical Aspects, pp.347-429.In: Eliasson AC (eds.), Carbohydrates in food, Marcel Dekker, inc., New York.

HRA, 1997 Starches & Hydrolyzates: A Worldwide Review of Manufacturers & Production. Prairie Village, USA.

Kerr, R.W., Cleveland, F.C., Katzbeck, W.J. 1951. The action of amylo-glucosidase on amylose and amylopectin. J. Am. Chem. Soc. **73:** 3916-3921.

Lane, J.H., Eynon, L. 1923. Determination of reducing sugars by means of Fehling's solution with methylene blue as internal indicator. J. Soc. Chem. Ind. Trans. 32-36.

Payen, A., Persoz, J.F. 1833. Mémoire sur la Diastase, les principaux Produits de ses Réactions, et leurs applications aux arts industriels. Ann. Chim. (Phys.). **53:** 73-92.

Phillips, L.L., Caldwell, M.L. 1951a. A study of the action of gluc amylase, a glucose-producing amylase, formed by the mold, *Rhizopus delemar*. J. Am. Chem. Soc. **73:** 3563-3568.

Phillips, L.L., Caldwell, M.L. 1951b. A study of the purification and properties of a glucose-forming amylase from *Rhizopus delemar*, gluc amylase. J. Am. Chem. Soc. **73:** 3559-3563.

Schenck, F.W. 1992. Starch hydrolysis products; an introduction and history, pp.1-22.In: Schenck FW and Hebeda RE (eds.), Starch hydrolysis products; Worldwide technology, production, and applications, VCH Publishers, New York.

Schoorl, N. 1929. Suiker titratie. Chemisch weekblad. 130-134.

Swinkels, J.J.M. 1985. Composition and properties of commercial native starches. Starch. **37:** 1-5.

Walker, G.W., Whelan, W.J. 1957. The mechanism of carbohydrase action 4. The mechanism of D-enzyme action. Biochem. J. **67:** 548-551.

Whelan, W.J., Roberts, P.J. 1952. Action of salivary α-amylase on amylopectin and glycogen. Nature. **170:** 748-749.

Whistler, R.L., Bemiller, J.N., and Paschall, E.F. 1984. Starch Chemistry and Technology. 2nd: Academic Press, Orlando.

Chapter 2

The use of Freezing-Point Depression for the Theoretical Dextrose Equivalent Measurement

L. M. Marchal, J. Jonkers and J. Tramper

Starch (1996), **48**, 220-224

Abstract

The determination of the theoretical dextrose equivalent (DE) was investigated, by measuring the osmolality (mol dissolved particles / kg H_2O) by freezing-point depression. Relations for DE and increase in dry weight during hydrolysis were derived as a function of molality and amount of dry weight at the start of the hydrolysis. With freezing-point depression it was possible to determine the theoretical DE of oligosaccharides (dextrose to maltoheptaose), whereas a traditional titration method (Luff-Schoorl) overestimates 20-50%. The overestimation of DE by Luff-Schoorl titration was also evident during the hydrolysis of amylopectin potato starch. With freezing-point depression it was possible to determine the degree of hydrolysis in a fast, reliable and above all accurate way. The relation for the increase of dry weight during the hydrolysis of starch with an α-amylase was experimentally validated.

Introduction

Starch mostly consists of a mixture of amylopectin (70-80% w/w) and amylose (20-30% w/w). Amylopectin is a branched macromolecule (M_w 10^7- 5.10^8 [g/mol]) of which on average one in 20-25 α(1→4)-bound glucose units are branched by α(1→6)-D-glucosidic bonds. Amylose (M_w 10^5-10^7 [g/mol]) consists of much longer linear chains of which on average one in several hundreds α(1→4)-bound glucose units are branched by α(1→6)-D-glucosidic bonds (Banks and Greenwood, 1975). An important parameter for the degree of hydrolysis of starch is the dextrose equivalent (DE), which is defined as:

$$DE \equiv \frac{\text{Molecular weight dextrose}}{\text{Number - average molecular weight starch hydrolysate}} \times 100 \qquad (1)$$

Most commonly used determinations are titration methods such as Lane and Eynon (1923) and Luff-Schoorl (1929). Both methods are based on the reduction of Cu^{2+} to copper(I)oxide by the reducing sugars. Although quite commonly used, there are some disadvantages (Fitton, 1979; Swinkels, 1985b). The most important disadvantage is the overestimation of the exact dextrose equivalent. This overestimation varies for different saccharides (Commerford and Scallet, 1969), which makes it hard to correct for this. Attempts have been made to use HPLC for measurement of syrups with a DE above 40 (Delheye and Moreels, 1988; Kiser and Hagy, 1979; Mariller et al., 1985). With HPLC (depending on the method and column used) the amount of oligosaccharides with a degree of polymerisation of 1 up to 12 can be detected separately. A problem even with highly hydrolysed starch is the contribution of the oligosaccharides with a higher degree of polymerisation (16-70% w/w), which appear as one peak in the chromatogram, to the total dextrose equivalent. The use of freezing-point depression to determine the dextrose equivalent has been reported by Kearsley (1978) and Fitton (1979). Some characteristics of dextrose equivalent measurement with the freezing-point depression or titration methods like Luff-Schoorl and Lane-Eynon are summarized in Table I.

Table I: Some properties of measuring the dextrose equivalent by freezing-point depression or titration methods like Luff-Schoorl and Lane-Eynon.

	Freezing-point depression	Luff-Schoorl / Lane-Eynon
Time for measurement (min)	2	15-30
Variation between operators	Standard error	Standard error
	0.05-0.09	0.2-0.8
Chemical costs per measurement	0.02 $	2$ (of which 1.2$ disposable)
Environmental friendly	Yes	No

With a calibration table of known Lane-Eynon dextrose equivalents and corresponding dry weight, the measured osmolality is converted to Lane-Eynon DE. A different substrate or production method (for example enzyme or acid) leads to a different spectrum of molecules and therefore to a different Lane-Eynon DE. So a calibration curve has to be made for each different substrate or production method. The research presented in this paper focused on the development of a simple and fast technique, suitable for process control, to measure the dextrose equivalent as accurate as possible during a liquefaction experiment, without the need to make a new calibration curve each time.

Theory

When 1 mol of a non-dissociating solute such as dextrose is dissolved in 1 kg of water, the freezing-point is depressed by 1.86°C. For a non-dissociating compound, the measured osmolality equals the molality. The use of freezing-point depression is in theory applicable to each measurement that involves an increase or decrease in the amount of moles present in a solution (Nijpels et al., 1980; Ramet et al., 1979; Rayner and Noack, 1994). To determine the theoretical dextrose equivalent of a starch solution by measuring the osmolality and dry weight

a number of relations had to be derived (Appendix I). The dextrose equivalent (DE) as a function of the dry weight (dw_o) and osmolality (osm_o) of the gelatinized starch and the measured osmolality (osm_m) during the hydrolysis (I.11) thus is:

$$DE = \frac{18(osm_m - osm_o)(1 - dw_o)}{dw_o + 18.10^{-3}(osm_m - osm_o(1 - dw_o))} \qquad (2)$$

The dry weight (dw) as a function of the dry weight and osmolality of the gelatinized starch and the measured osmolality during the hydrolysis (I.12) then is:

$$dw = \frac{dw_o + 18.10^{-3} osm_m - 18.10^{-3} osm_o(1 - dw_o)}{1 + 18.10^{-3} osm_m} \qquad (3)$$

To determine the dextrose equivalent during a starch hydrolysis with the classical titration methods, the actual dry weight (at that moment) needs to be known. Refraction index measurement is often used to correct for the increase in dry weight (hydrolytic gain) during a starch hydrolysis (ISO, 1982). A disadvantage of this method is that it is designed to determine sugar (dextrose) concentrations. Since the refraction of sugars is dependent on their structure, there is a deviation between the actual dry weight of the starch hydrolysates and the one derived from the measured refraction index. Often calibration curves are made to convert the dry weight (as measured by refraction index) to the actual dry weight (Wartman et al., 1976). A disadvantage is that for each different substrate or enzyme or (process) condition, which results in a different spectrum of molecules, a different calibration curve has to be made. The method presented here was not influenced by the factors mentioned above and only the dry weight of the gelatinized starch had to be measured. If this was done by refraction index, only one calibration table (to convert dry weight of the gelatinized starch given by the refraction index to the actual dry weight) had to be made for each different substrate.

Chapter 2

Material and Methods

Equipment

The osmolality was measured with The Advanced Osmometer Model 3D3 (Advanced Instruments, Norwood, MA), using a sample volume of 0.2 ml and an analysis time of about two minutes. The conductivity was measured with a WTW LF95 (Wissenschaf TL, Weilheim, Germany) conductivity meter. Determination of dry weight was always done in triplicate by drying in an oven at 130°C for at least two hours. With highly hydrolysed starch this should be lowered to 100°C under reduced pressure to decrease Maillard reactions.

The oligosaccharides

The oligosaccharides (maltotriose to maltoheptaose, Nihon Shokuhin Kako Co. Ltd., Tokyo) were checked for their purity on HPLC. All oligosaccharides were at least 99% pure (results not shown). The moisture content of these oligosaccharides was determined with the Karl Fischer method (ISO, 1978). Dextrose (Merck 8337) and maltose (Merck 5910, Darmstadt, Germany) were at least 99.5% pure. The dextrose equivalent of the dissolved oligosaccharides was determined by both freezing-point depression and Luff-Schoorl titration.

Salts

Salts present in the starch or in the water, or added to enhance enzyme stability, also contribute to the depression of the freezing-point. Correction for these salts, which determine measured osmolality of gelatinized starch (offset of the hydrolysis), was done in three different ways:

1) In starch hydrolysis the abundant salts are $CaCl_2$, NaCl and KCl. In the relevant concentration ranges there is a linear relation between the conductivity and the osmolality (Fitton, 1979). Conductivity (at 25°C) and osmolality of different calcium chloride concentrations in demi (0-1.5 g/l) were measured.
2) The initial increase in dextrose equivalent due to α-amylolytic activity is linear (DE 0-5). By extrapolating the initial increase in osmolality to the y-axis, the offset due to the salts present was calculated.

3) Since potato starch is composed of large polymers, the maximal contribution to the initial osmolality was negligible. The osmolality of the gelatinized starch solution was therefore approximated by the contribution of the salts (offset). Direct measurement of the gelatinized starch solution was, at high dry weight concentrations, not possible because of the high viscosity. After dilution with warm demi water (to prevent retrogradation) the osmolality was measured and the offset calculated.

Liquefaction experiment.

Amylopectin potato starch (Avebe, Veendam, the Netherlands) was obtained from transgenic potatoes (amylose content < 1%, calcium content 481 [µg/g]). The starch suspension (10% w/w) in demi water was gelatinized in a stirred autoclave (30 minutes, 140°C). The gelatinized starch (pH 6.28) was transferred into a 2 liter stirred reactor and the temperature was adjusted to 90.8°C. Calcium (25.8 ppm [µg/g]) was added to stabilize the enzyme. α-Amylase from *Bacillus licheniformis* (Maxamyl, Gist-brocades, presently Genencor, Delft, the Netherlands) was added (0.01% v/w) and the dextrose equivalent was determined as a function of time by both Luff-Schoorl titration and freezing-point depression. To further investigate the observed ratio between Luff-Schoorl titration and freezing-point depression at higher hydrolysis levels (more toward dextrose) a saccharification experiment with glucoamylase from *Aspergillus niger* (Spezyme GA 300N, Genencor, Finland) was done (pH 4.5, 60°C) in duplo. To compare the DE as determined by HPLC with that from freezing-point depression, 34 highly hydrolysed amylopectin starch samples of a liquefaction experiment (Maxamyl) were analysed. In these liquefaction experiments the dry weight ranged from 2.8 to 37% (w/w), the pH from 5.6 to 7.6 and the temperature from 63 to 97°C. The HPLC used was an Aminex HPX-42A (300 mm x 7.8 mm) carbohydrate analysis column (Bio-rad, Veenendaal, The Netherlands) operated at 85°C, with water as eluents and a flow of 0.4 ml/min. The average degree of polymerisation of the higher saccharides (>Dp12) after complete hydrolysis of amylopectin waxy-maize starch with an α-amylase from *Bacillus amyloliquefaciens* is between 67-165 (Bertoft, 1991). The dextrose equivalent determined by either freezing-point depression or calculated from the

HPLC data were compared (paired T-test) using a degree of polymerisation of the higher saccharides of 50, 125 and 200.

Results and Discussion

Oligosaccharides

To investigate the accuracy of the dextrose equivalent measurement with freezing-point depression, several pure oligosaccharides were tested. Figure 1 gives the theoretical (by definition) and the dextrose equivalent determined by Luff-Schoorl titration and freezing-point depression.

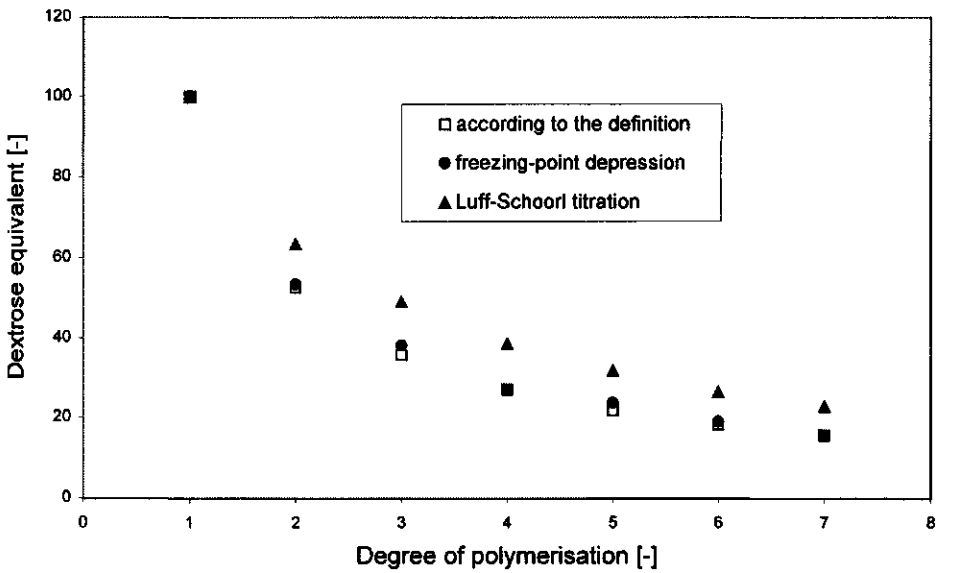

Figure 1: Dextrose equivalent of several oligosaccharides (dextrose - maltoheptaose) determined by both Luff-Schoorl titration and freezing-point depression.

Luff-Schoorl titration overestimated the theoretical dextrose equivalent by a factor 1.21-1.5 as reported earlier (Swinkels, 1985b). The dextrose equivalent determined by freezing-point depression correlated well with the theoretical dextrose equivalent (according to the definition).

Salts

The relation found between the conductivity and osmolality for different calcium chloride concentrations (results not shown) was in accordance with the results found earlier (Fitton, 1979). A disadvantage of this method is that the measured conductivity of a solution is also depending on the viscosity (Atkins, 1987). Dilution of the gelatinized starch before liquefaction at high dry weight and low salt concentrations gave inaccurate results (results not shown). The influence of the resolution (1 mosm) of the osmometer on the offset at very low molalities is relatively large. Of the three methods described in the material and methods section, the extrapolation of the initial increase in osmolality to the y-axis was the most convenient way to determine the offset due to the salts (Figure 2).

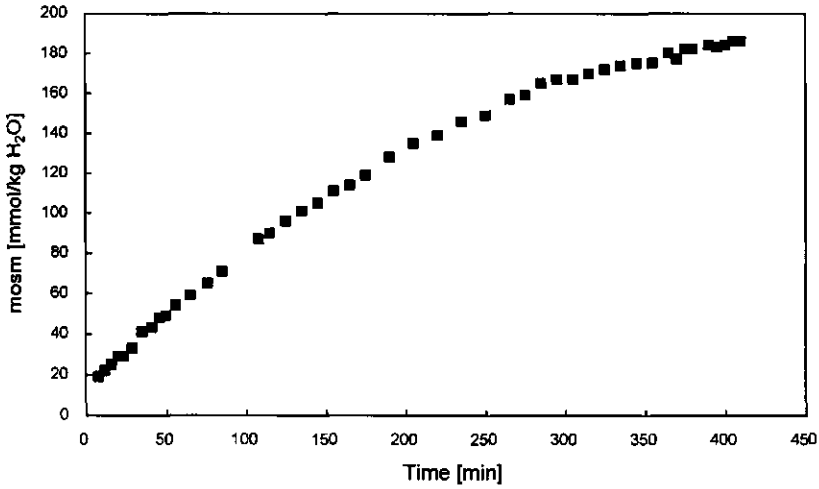

Figure 2: The measured osmolality as a function of time during the hydrolysis of amylopectin potato starch with an α-amylase.

Liquefaction experiment.

During the hydrolysis of starch, the amount of dry weight increased with increasing dextrose equivalent. The model predicted (equation 3) dry weight increase was as a function of the initial dry weight (dw_0) and osmolality (osm_o) and the measured osmolality (osm_m) during the liquefaction. Figure 3 gives the model predicted (equation 3) and the actual measured dry weight as a function dextrose equivalent.

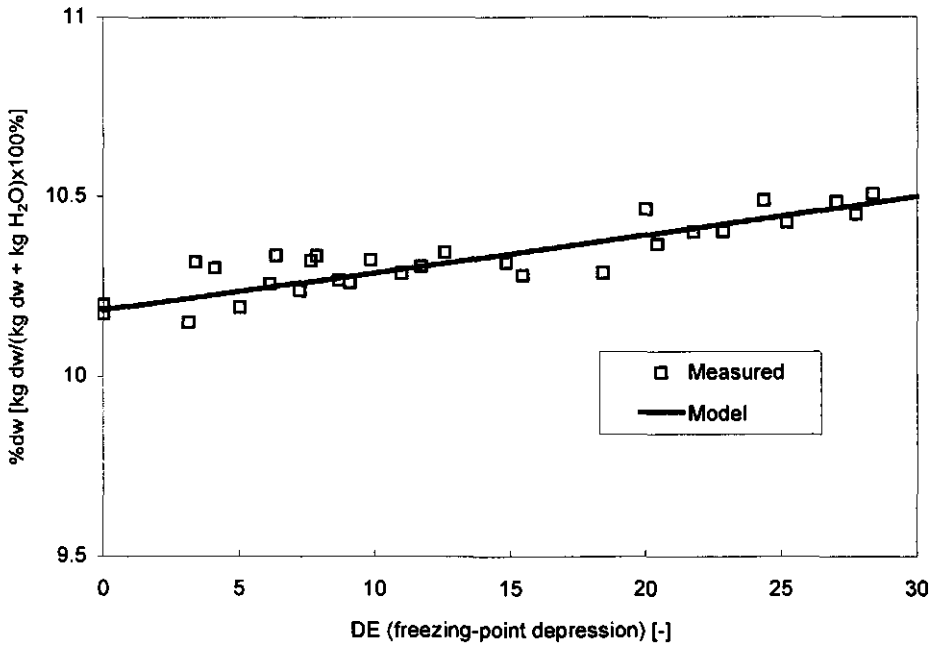

Figure 3: Model predicted (equation 3) and measured dry weight as a function of dextrose equivalent during liquefaction of amylopectin potato starch.

Although it is of course possible to measure the dry weight at each point during a liquefaction experiment, this is quite laborious. The measurement of only one dry weight concentration (dw_o) is more efficient.

Figure 4 shows the increase in dextrose equivalent followed by both Luff-Schoorl titration and by freezing-point depression. The overestimation of the dextrose equivalent by the Luff-Schoorl titration is evident.

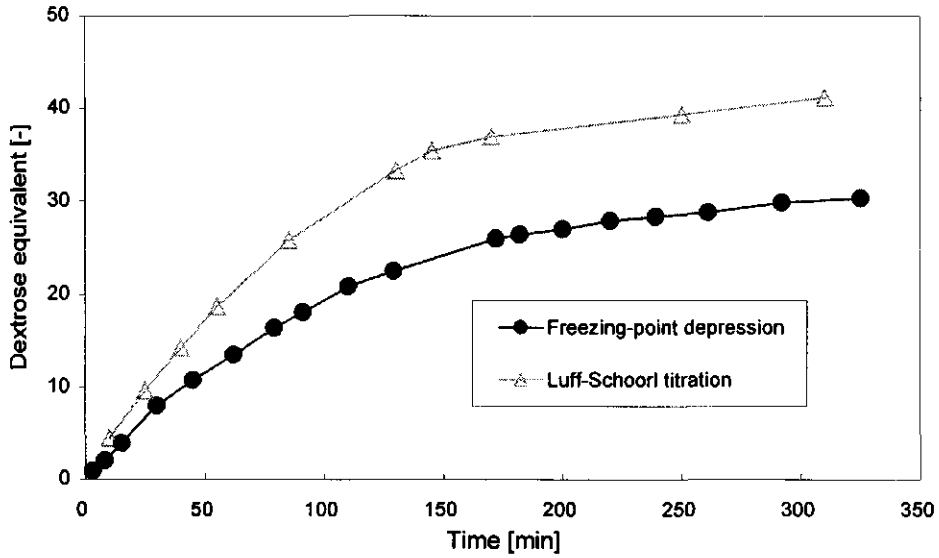

Figure 4: Dextrose equivalent as a function of time as determined by both Luff-Schoorl titration and freezing-point depression during a liquefaction experiment of amylopectin potato starch (10% dw) with an α-amylase (enzyme dosage 0.01% [v/w], pH 6.28, 90.8°C). The data points are connected for ease of comparison only.

The ratios between DE's as determined by Luff-Schoorl titration and calculated from freezing-point depression for two liquefaction and two saccharification experiments are shown in Figure 5. The ratio between dextrose equivalent as determined by Luff-Schoorl and freezing-point depression was up to DE values of 20 around 1.5. With the increase in dextrose equivalent the contribution of smaller oligosaccharides increases and the ratio did go toward 1 for dextrose (DE 100) as expected.

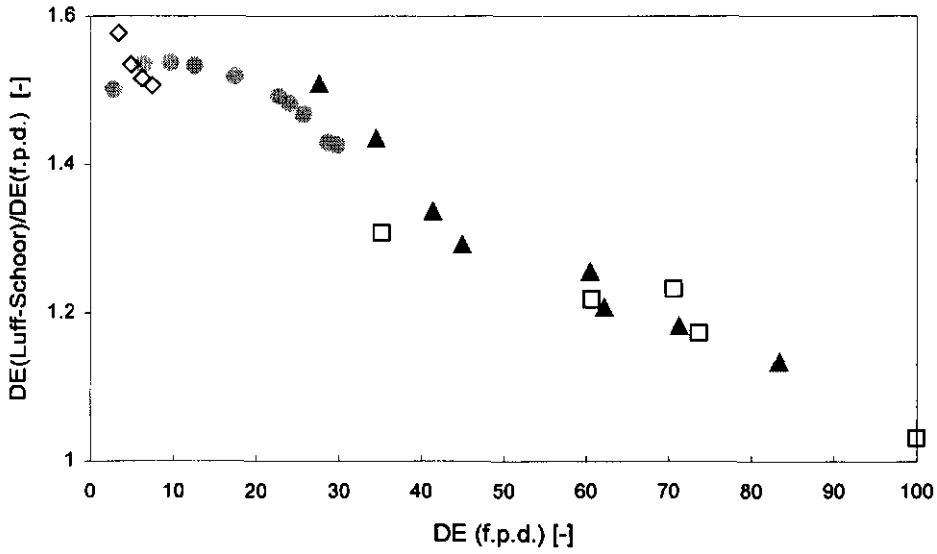

Figure 5: The ratio between dextrose equivalent as determined by Luff-Schoorl and freezing-point depression (f.p.d.) for liquefaction (● and ◊) and saccharification (▲ and □) experiments.

In Figure 6 the dextrose equivalent as determined by freezing point depression and calculated from HPLC-data for 34 different samples are given. There was no significant difference in dextrose equivalent between these two methods. The probability values from the paired T-test ranged from 0.54 for an average degree of polymerisation for the higher saccharides (>DP12) of 200 to 0.43 and 0.3 for respectively 125 and 50.

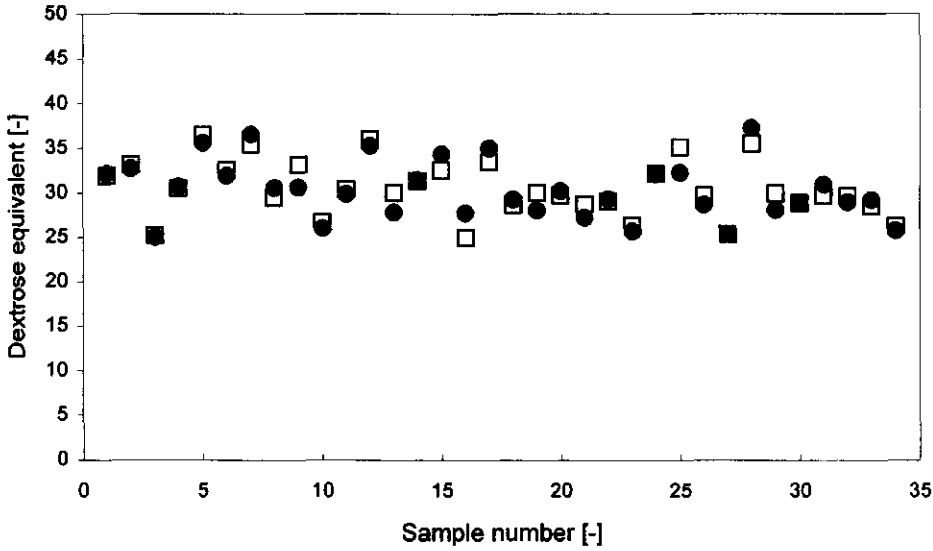

Figure 6: The dextrose equivalent for 34 different liquefaction experiments of highly hydrolysed (α-amylase) amylopectin potato starch as determined by freezing-point depression (●) and calculated from HPLC-data (□). The average degree of polymerisation for the higher saccharides (>DP12) taken here is 125.

Conclusion

With freezing-point depression it was possible to measure the theoretical (by definition) dextrose equivalent accurately. Only one dry weight determination, before the start of the liquefaction, was necessary to know the dry weight during the whole hydrolysis. Its use as an easy, fast and exact method to follow the enzymatic hydrolysis of a biological polymer (starch) was shown here.

Nomenclature

DE	=	dextrose equivalent	[-]
DP_n	=	degree of polymerisation	[-]
dw	=	dry weight	[kg dw/(kg dw + H_2O)]
dw_o	=	dry weight gelatinized starch	[kg dw/(kg dw + H_2O)]
dw_{kgH2O}	=	dry weight	[kg dw/kg H_2O]
M_n	=	number-average molecular weight	[kg dw/mol]
M_w	=	weight-average molecular weight	[g/mol]
osm	=	osmolality	[mol/kg H_2O]
osm_m	=	measured osmolality	[mol/kg H_2O]
osm_o	=	osmolality due to salts	[mol/kg H_2O]

Appendix I

An important characteristic of polymers is their number-average molecular weight. If the amount of dry weight present in the solution per kg of H_2O is known and the osmolality is measured, the number-average molecular weight can be calculated according to:

$$M_n = \frac{dw_{kgH_2O}}{osm}. \qquad (I.1)$$

Dry weight is mostly defined as kg of weight per kg solution (water and dry weight), which leads to:

$$M_n = \frac{dw/(1-dw)}{osm}. \qquad (I.2)$$

The dextrose equivalent is directly related to the number-average molecular weight:

$$DE \equiv \frac{0.18}{M_n} \times 100 . \qquad (I.3)$$

So the dextrose equivalent of the starch hydrolysate is equal to (equation I.2 in I.3):

$$DE = \frac{18osm(1-dw)}{dw} . \qquad (I.4)$$

Table II shows the dextrose equivalent, degree of polymerisation, and number-average molecular weight of some oligosaccharides and starch.

Table II: Molecular weight, dextrose equivalent (according to the definition), and degree of polymerisation of some carbohydrates.

Carbohydrate	M_n [kg/mol]	Dextrose equivalent [-]	Degree of polymerisation [-]
Dextrose	0.18	100	1
Maltose	0.342	52.63	2
Maltotriose	0.504	35.71	3
Maltotetraose	0.666	27.03	4
Potato starch (Swinkels, 1985a)	$\approx 2.3 \times 10^3$	≈0.008	≈14,000

The degree of polymerisation of the starch hydrolysate (DP_n) can be calculated from the number-average molecular weight:

$$DP_n = \frac{M_n - 0.18}{0.162} + 1 . \qquad (I.5)$$

During hydrolysis, each time when a glycosidic linkage is hydrolysed, water is added to the hydrolysate and the mass of the solute increases. When 0.162 kg of starch is totally converted to dextrose (DE=100) the dry mass becomes 0.18 kg. If the amount of gelatinized starch before liquefaction (dw_o) is known, the amount of dry weight during the hydrolysis is a function of the degree of polymerisation:

$$dw(DP_n) = dw_o \frac{0.162(DP_n - 1) + 0.18}{0.162DP_n} . \qquad (I.6)$$

Substitution of equation I.5 in I.6 gives the relation of dry weight as a function of M_n:

$$dw(M_n) = dw_o \left(\frac{M_n}{M_n - 18.10^{-3}} \right) . \qquad (I.7)$$

Substitution of equation I.3 in I.7 gives the relation of dry weight during the hydrolysis as a function of dextrose equivalent:

$$dw(DE) = dw_o \left(\frac{1}{1 - 1.10^{-3} DE} \right) . \qquad (I.8)$$

The amount free water decreases during hydrolysis. This means that the amount of salts present at the start of a liquefaction experiment (osm_o) are slightly concentrated during hydrolysis. The osmolality due to the hydrolysis of starch (osm) is the measured osmolality (osm_m) minus the osmolality due to the salts present (osm_o) times the concentration factor:

$$osm = osm_m - osm_o \frac{(1 - dw_o)}{(1 - dw)} . \qquad (I.9)$$

Substituting (I.9) in (I.4) gives the dextrose equivalent as a function of the dry weight and

osmolality of the gelatinized starch and the measured osmolality and dry weight during the hydrolysis:

$$DE = \frac{18(osm_m(1-dw_o) - osm_o(1-dw_o))}{dw}. \qquad (I.10)$$

Substitution of equation I.8 in I.10 gives the dextrose equivalent as a function of the dry weight and osmolality of the gelatinized starch and the measured osmolality during the hydrolysis:

$$DE = \frac{18(osm_m - osm_o)(1-dw_o)}{dw_o + 18.10^{-3}(osm_m - osm_o(1-dw_o))}. \qquad (I.11)$$

Substitution of equation I.10 in I.8 gives the dry weight as a function of the dry weight and osmolality of the gelatinized starch and the measured osmolality during the hydrolysis:

$$dw = \frac{dw_o + 18.10^{-3} osm_m - 18.10^{-3} osm_o(1-dw_o)}{1+18.10^{-3} osm_m}. \qquad (I.12)$$

Acknowledgement

The authors thank Jack Bergsma, Bert Franke and Nico Oosterhuis (Avebe), Rik Beeftink and Kees de Gooijer (WAU) for careful reading of the manuscript and their useful comments. Avebe and the Dutch Ministry of Economic Affairs (PBTS Biotechnology Project No. BIO94043) funded this research.

References

Atkins, P.W. 1987. Physical chemistry. 3rd: Oxford University press, Oxford.

Banks, W., Greenwood, C.T. 1975. Starch and its Components. Edinburgh University Press, Edinburgh.

Bertoft, E. 1991. Investigation of the fine structure of alpha-dextrins derived from amylopectin and their relation to the structure of waxy- maize starch. Carbohydr. Res. **212:** 229-244.

Commerford, J.D., Scallet, B.L. 1969. Reaction of oligosaccharides II: Dextrose equivalents. Cereal. Chem. **46:** 172-176.

Delheye, G., Moreels, E. 1988. Dextrose equivalent measurements on commercial syrups. Starch. **40:** 430-432.

Fitton, M.G. 1979. Rapid determination of dextrose equivalent by cryoscopy. Starch. **31:** 381-384.

ISO, 1982 Glucose Syrup - Determination of dry matter content - Refraction index method. ISO 1743.

ISO, 1978 Determination of water - Karl Fischer method. International organization for standarization, ISO 760.

Kearsley, M.W. 1978. The rapid Determination of dextrose equivalent of glucose syrups. J. Assoc. Publ. Analysts. **16:** 85-88.

Kiser, D.L., Hagy, R.L. 1979. Estimation of dextrose equivalent value of starch hydrolysates from liqued chromatographic profiles, pp.363-378.In: Charalambous G (eds.), Liquid chromatographic analysis of food beverages: Volume 2, Academic press, New York.

Lane, J.H., Eynon, L. 1923. Determination of reducing sugars by means of Fehling's solution with methylene blue as internal indicator. J. Soc. Chem. Ind. Trans. 32-36.

Mariller, P., Ciurea, I.C., Humbert, B. 1985. An optimized attempt for dextrose equivalent evaluation of corn syrups from HPLC-data. Mitt. Gebiete Lebensm. Hyg. **76:** 553-562.

Nijpels, H.H., Evers, P.H., Novak, G., Ramet, J.P. 1980. Application of cryoscopy for the measurement of enzymatic hydrolysis of lactrose. Journal of Food Science. **45:** 1684-1687.

Ramet, J.P., Novak, G., Evers, P.A., Nijpels, H.H. 1979. Application de la cryométrie à la mesure de l'hydrolyse enzymatique du lactose. Le Lait. **581-582:** 46-55.

Rayner, M.H., Noack, K. 1994. Biosensors based on cryoscopic osmometry: a preliminary investigation. Biosensors. Bioelectron. **9:** 301-304.

Schoorl, N. 1929. Suiker titratie. Chemisch weekblad. 130-134.

Swinkels, J.J.M. 1985a. Composition and properties of commercial native starches. Starch. **37:** 1-5.

Swinkels, J.J.M. 1985b. Karakterisering van zetmeelhydrolysaten. Glucose informatie band. **8:** 71-93.

Wartman, A.M., Hagberg, C., Eliasion, M.A. 1976. Refractive index - dry substance relationships for commercial corn syrups. Journal of Chemical and. **21:** 459-468.

Chapter 3

The Effect of Process Conditions on the α-Amylolytic Hydrolysis of Amylopectin Potato Starch: an Experimental Design Approach

L.M. Marchal, J. Jonkers, G.Th. Franke, C.D. de Gooijer, J. Tramper

Biotechnology & Bioengineering (1999), **62**, 348-357

Abstract

The hydrolysis of amylopectin potato starch with *Bacillus licheniformis* α-amylase (Maxamyl) was studied under industrially relevant conditions (i.e. high dry-weight concentrations). The following ranges of process conditions were chosen and investigated by means of an experimental design: pH [5.6-7.6]; calcium addition [0-120 μg/g]; temperature [63-97°C]; dry-weight concentration [3-37% [w/w]]; enzyme dosage 27.6-372.4 μl/kg] and stirring [0-200 rpm]. The rate of hydrolysis was followed as a function of the theoretical dextrose equivalent. The highest rate (at a dextrose equivalent of 10) was observed at high temperature (90°C) and low pH (6). At a higher pH (7.2), the maximum temperature of hydrolysis shifted to a lower value. Also, high levels of calcium resulted in a decrease of the maximum temperature of hydrolysis. The pH, temperature, and the amount of enzyme added showed interactive effects on the observed rate of hydrolysis. No product or substrate inhibition was observed. Stirring did not effect the rate of hydrolysis. The oligosaccharide composition after hydrolysis (at a certain dextrose equivalent) did depend on the reaction temperature. The level of maltopentaose [15-24% [w/w]], a major product of starch hydrolysis by *B. licheniformis* α-amylase, was influenced mostly by temperature.

Chapter 3

Introduction

The hydrolysis of starch to products with a low molecular weight, catalyzed by an α-amylase, is one of the most important commercial enzyme processes. The hydrolyzed products are widely applied in the food, paper, and textile industries (Nigam and Singh, 1995). Although numerous papers have appeared in the past years describing catalytic and mechanistic aspects as well as product profiles the information on interpretation of α-amylolysis under industrial conditions (i.e. high dry-weight concentrations) is scarce (Henderson and Teague, 1988; Madsen et al., 1973; Rosendal et al., 1979). Most of the kinetic research is primarily carried out at low (typically around 1% w/w) dry-weight concentrations (Annous and Blaschek, 1994; Babu and Satyanarayana, 1993; Chiang et al., 1979; De Cordt et al., 1992; Dobreva et al., 1994; Fujii et al., 1988; Gorinstein, 1993; Kennedy and White, 1979; Krishnan and Chandra, 1983; Kumar et al., 1990; Ramesh and Lonsane, 1990; Saito, 1973; Violet and Meunier, 1989). The influence of dry-weight concentration (possible substrate (Yankov et al., 1986) and product inhibition (Fujii et al., 1988; Park and Rollings, 1994; Steverson et al., 1984)) has been given little attention.

The object of this study was to investigate, in general terms, the process conditions relevant in industrial practice, aiming at a better control of the amylolytic process. In industrial applications, pH and temperature are controlled and calcium is often added to enhance enzyme stability. Knowledge of interactions between factors such as pH and calcium (Antrim et al., 1991) or pH and temperature (Henderson and Teague, 1988) is limited. Furthermore, the effect of stirring on the enzymatic conversion is not known. To study these process conditions (including interactions), a considerable number of experiments are required. This number can be reduced to a minimum by doing the experiments according to an experimental design (Box et al., 1978). To study the effects of pH, temperature, added calcium, enzyme dosage, dry-weight, and stirring speed on the enzymatic conversion a central composite experimental design was used. The rate of hydrolysis (number of bonds hydrolyzed per minute by the enzyme) was taken as the response variable. Amylopectin potato starch, lacking amylose, was used as a substrate because of its low tendency for retrogradation. Since in industry starch is liquefied without buffers, which are known to

influence the α-amylolytic hydrolysis of starch (Kennedy and White, 1979; Krishnan and Chandra, 1983; Rosendal et al., 1979), a nonbuffered system was used. Potato starch has some buffering capacity due to the phosphate groups on the amylopectin. Since no base or acid is produced during the reaction of α-amylase, the pH remains constant during liquefaction.

Material and methods

Liquefaction experiments

Amylopectin potato starch (Avebe, Veendam, the Netherlands) was obtained from transgenic potatoes (amylose content of starch <1%, calcium content 481 [μg/g]). Since a nonbuffered system was used, there was a drop in pH after gelatinization. Adjusting the pH after gelatinization gives practical problems due to the high viscosity of gelatinized starch, especially at high dry weight concentrations. The pH was therefore set in suspension before gelatinization. From preliminary experiments, a relationship between the pH in suspension and after gelatinization was derived for our experimental setup. The starch was suspended in demineralized water and the pH was adjusted to obtain the desired value after gelatinization. The starch was gelatinized in a stirred autoclave by heating for 30 minutes at 140°C. The gelatinized starch was transferred to a double vesseled 2 dm^3 stirred reactor with a diameter of 0.2 m (diameter: height ratio 0.5). A four-blade 45° pitched turbine (diameter 0.1 m) was placed at one third of the reactor height from the bottom. With the variable calcium addition (as $CaCl_2$), the total ionic strength was kept constant. When less than 120 μg/g calcium was added, enough sodium chloride was added to keep the total ionic strength constant. The temperature was adjusted to the settings of the experimental design before the start of the experiment. The exact dry weight concentration of the starch at the start of the liquefaction was determined in triplicate by drying at 130°C for two hours. The dry weight concentration at the end of the liquefaction was measured again, in triplicate overnight at 100°C (to reduce Maillard reactions), to be able to correct for dry weight increase caused by evaporation during sampling. α-Amylase from *Bacillus licheniformis* was used (Maxamyl; Gist-brocades, presently Genencor, Delft, the

Netherlands). Specific density of the enzyme preparation is 1.2 g/ml with an α-amylase protein content of 2% (20 mg/g). The actvivity of the enzyme digest was 11,200 μmol bonds hydrolysed per minute per gram enzyme preparation (substrate 2.5% [w/w] Lintner-starch, pH 6, 90°C). The commercial enzyme preparation Maxamyl is sufficiently pure (Rozie et al., 1991), so no purification steps were necessary. The degree of enzymatic hydrolysis was followed by measuring the osmolality as a measure for the number of bonds hydrolyzed (Appendix I). A detailed description of the procedures used has been given previously (Marchal et al., 1996). The osmometer used was an Advanced osmometer model 3D3 (Advanced Instruments, Norwood, MA). During the first 5 min of each experiment, a standard high stirring speed (158 rpm) was used to homogenize the system. When the starch solution became less viscous (dextrose equivalent ≈ 1), the pH was measured. This pH was taken as actual setting for the experimental design.

Number of bonds hydrolyzed by the enzyme

The increase in osmolality was measured in each individual experiment. With this osmolality both the number of bonds hydrolyzed by the enzyme and the dextrose equivalent were calculated (see Appendix I). An exponential function was fitted through the data points (mmol bonds hydrolyzed per kg dry weight and water, as a function of time) for each experiment:

$$b_h(t) = A(1 - e^{-Bt}), \qquad (1)$$

in which

b_h	=	number of bonds hydrolyzed	[mmol/(kg dw + H_2O)]
A	=	maximum number of bonds hydrolyzed	[mmol/(kg dw + H_2O)]
B	=	pseudo-first-order reaction constant	[min^{-1}].

The differentiated form of equation 1 gives the rate of hydrolysis at any given time [mmol / ((kg dw + H_2O)×min)]. The variable A gives the maximum number of bonds hydrolyzed by the enzyme for each experiment.

The dextrose equivalent (an important parameter in the starch industry) is a measure for the average chain length of a starch hydrolysate. To investigate the rate of hydrolysis at defined DE-values, the time to reach such a dextrose equivalent has to be known for each individual experiment. For this, through the DE(t) data for each experiment, the following function was fitted:

$$DE(t) = C(1 - e^{-Dt}), \qquad (2)$$

in which

C	=	maximum dextrose equivalent reached	[-]
D	=	pseudo-first-order reaction constant	[min^{-1}].

The timbe to reach a certain DE could be calculated for each experiment when rewriting this equation to:

$$t = \frac{\ln\left(\frac{DE}{-C} + 1\right)}{-D}. \qquad (3)$$

These times were used in the differentiated form of equation 1 to calculate $d(b_h)/dt$ [mmol/((kg dw + H_2O)×min)] at different DE's (5,10,15,20) for each experiment.

These hydrolysis speeds were used as response variables in the regression analysis.

Experimental design and analysis

The experiments were done according to a central composite design, consisting of a star design and a two-level half-factorial design (Box et al., 1978). The actual and coded settings of each of the six experimental factors are given in Table I.

Table I: Settings for the six experimental factors of the central composite experimental design.

	Settings per factor				
Factor	-α (-1.72)	-1	0	1	α (1.72)
pH	5.6	6.0	6.6	7.2	7.6
Ca (ppm [µg/g])	0	25	60	95	120
T (°C)	63	70	80	90	97
dw (kg/kg total)	0.028	0.10	0.20	0.30	0.37
enzyme (µl/kg total)	27.6	100	200	300	372.4
stirring (rpm)	0	42	100	158	200

The rate of hydrolysis ($d(b_h)/dt$) at a certain dextrose equivalent was analyzed with linear regression and described as (regression model, n = 6):

$$\frac{d(b_h)}{dt} = a_0 + \sum_{1}^{n} a_i x_i + \sum_{1}^{n} a_{ii} x_i^2 + \sum_{1, i<j}^{n} a_{i,j} x_i x_j + \varepsilon, \qquad (4)$$

in which a_{ij} are the fitted regression coefficients of the independent variables x (pH, dw, temperature, etc.) and ε is the error. Residual plots were made to test the data for normal distribution. The terms were grouped in three categories depending on their probability or p-value. Highly significant terms ($p \leq 0.0001$) were marked with **, significant terms ($0.0001 < p \leq 0.05$) with *, and insignificant terms ($p > 0.05$) without asterisk (Schlotzhauer and Littell, 1991). Only the (highly) significant terms ($p \leq 0.05$) were considered for the final reduced model. If a quadratic term or cross-term was significant, the single terms were always taken into the model. If this term had a $p > 0.05$, it was marked with a dagger. For the final reduced model residual plots were again made to test the data for normal distribution.
In these kinds of experimental design the reliability decreases when going from the center towards the edge of the design. Inside the design the reliability is quite acceptable. Outside

the design the reliability decreases rapidly (Box et al., 1978). In this particular case (six variables), whenever the sum of the length of the coordinates is ≤6, the model description is considered to be inside the design. In between the coded areas -1 and 1, all the investigated variables (pH, temperature, etc.) can be changed freely, and described results will always be inside the design. Therefore this article discusses only the coded areas between -1 and 1.

Influence of process conditions on the oligosaccharide composition

To investigate the effect of the process conditions on the composition of the oligosaccharide mixture after the hydrolysis, 24 hydrolyzed amylopectin-starch samples from different experiments were analyzed. The HPLC column used was an Aminex HPX-42A (300 mm x 7.8 mm) carbohydrate analysis (Bio-rad, Veenendaal, the Netherlands) operated at 85°C, with water as eluent at a flow of 0.4 ml/min. Sample size used was 50 µl of an 2% (w/w) solution and the carbohydrates were analyzed by an index refraction detector. Contributions of the individual oligosaccharides, expressed as percentage of total carbohydrate, was calculated according to the 100% method.

Results and discussion

Correlation matrix

It was not always possible to obtain exactly the required settings (Table I) due to experimental difficulties, especially with controlling the pH after gelatinization. The correlation matrix for the experimental settings was calculated (results not shown) and none of the factors had a significant correlation with any other factor. This means that each regression coefficient can be estimated and independent conclusions can be drawn for each investigated factor.

Data Transformation

The absolute errors of the hydrolysis speed ($d(b_h)/dt$) increased at higher rates of hydrolysis (results not shown). The usual statistical analysis assumes a constant variance of the absolute errors. The observed heteroscedasticity could adequately be corrected by choosing the log-transformation as variance stabilizing transformation. Therefore, the natural logarithm of the hydrolysis speed ($\ln(d(b_h)/dt)$) was taken as the response variable in the statistical analysis. This means that the regression model has the form of

$$\ln\left(\frac{d(b_h)}{dt}\right) = a_0 + \sum_{1}^{n} a_i x_i + \sum_{1}^{n} a_{ii} x_i^2 + \sum_{1, i<j}^{n} a_{i,j} x_i x_j + \varepsilon . \qquad (5)$$

The residual plots of the final reduced models showed that the response data were normally distributed (results not shown).

Number of bonds hydrolyzed by the enzyme

General trends

Figure 1 shows a typical hydrolysis experiment, in which the number of bonds hydrolyzed [mmol/(kg dw + H_2O)] increases with time. In addition, an exponential fit (equation 1) of the data is given. The process conditions significantly effecting the rate of hydrolysis (at certain DE's) are given in Table II. The number of significant factors increases as the reaction proceeds (in DE and time). The dominant factor with respect to enzymatic hydrolysis was the enzyme dosage, which was not surprising. At higher conversions (DE = 10 and higher), pH, and temperature (effecting activity and stability) became significant. At DE = 20, dry weight (increased stability) and calcium addition also became significant for the reaction rate. For the maximum number of bonds hydrolyzed at the end of the reaction (at different reaction times), only the amount of dry weight (substrate) was significant. Stirring at the beginning of the reaction was essential to mix enzyme and substrate well. However, after this initial mixing, stirring (in the range investigated here 0-200 rpm) had no

Table II: Factors (+) of significant influence ($p \leq 0.05$) during different moments of hydrolysis of amylopectin potato starch.

	Initial	DE = 5	DE = 10	DE = 15	DE = 20	Max_{bh}
pH			+	+	+	
Calcium					+	
Temp			+	+	+	
Dry weight					+	+
Enzyme	+	+	+	+	+	
Stirring						

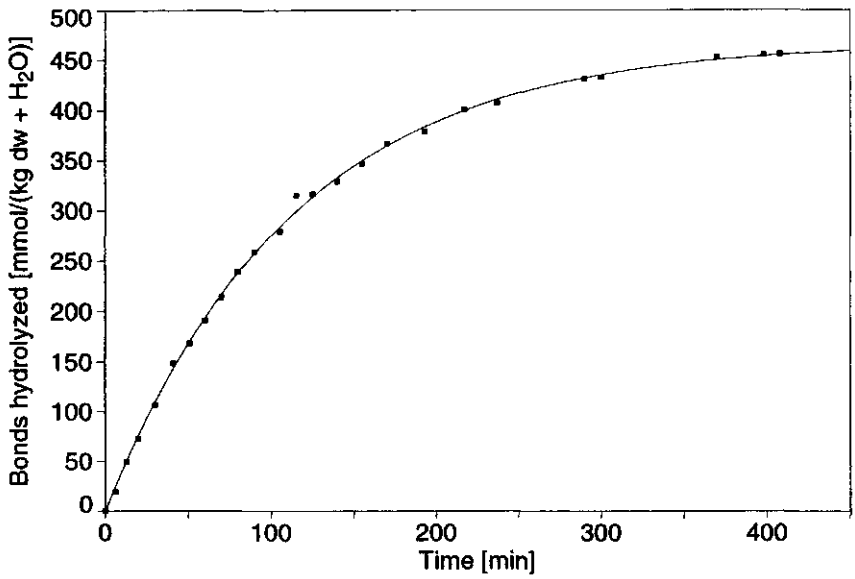

Figure 1: The number of bonds hydrolyzed [mmol/(kg dw + H_2O)] versus time for a typical experiment. Experimental conditions were: pH 6.6, temperature 70°C, calcium addition 25 ppm [µg/g], dry weight 0.307 kg/(kg dw + H2O), and enzyme dosage 300 µl/(kg dw + H_2O). The exponential fit (equation 1) data were: $r^2 = 0.999$, A = 467 [mmol/(kg dw + H_2O)] and $B = 8.9 \times 10^{-3}$ [min^{-1}].

significant influence on the enzymatic activity. So, in this two liter batch, besides initial mixing of enzyme and substrate, mixing was not essential. Some factors will be discussed in more detail below.

pH, temperature, and dry weight

The initial rate of hydrolysis and the rate at dextrose equivalent five were significantly determined only by the enzyme concentration. It may be surprising that the initial hydrolysis was not significantly influenced by pH or temperature. However, the reported maximum pH activity range for *B. licheniformis* α-amylase is quite broad and in the investigated range (pH 6 - pH 7.2) about constant (Antrim et al., 1991; Anyangwa et al., 1993; Bajpai and Bajpai, 1989; Dobreva et al., 1994; Madsen et al., 1973; Morgan and Priest, 1981; Ramesh and Lonsane, 1990; Rosendal et al., 1979; Saito, 1973). This may explain why there was no significant influence of pH on the initial rate of hydrolysis. Most of the studies on temperature and pH activity relations for *B. licheniformis* α-amylase are carried out at low substrate concentrations (0.1-1% [w/w]) and in buffered media (Chiang et al., 1979; Ivanova et al., 1993; Kumar et al., 1990; Madsen et al., 1973; Ramesh and Lonsane, 1990; Saito, 1973; Violet and Meunier, 1989). These studies report an increase of 4-30% in activity in the temperature range 70-90°C. In our experimental setup, the temperature did not significantly influence the initial hydrolysis. At a dextrose equivalent of 10, however, temperature and pH did significantly influence the rate of hydrolysis. The regression coefficients (Table III) can be used to produce graphs, which visualize this rate of hydrolysis. Figure 2 shows the statistically analyzed (regression coefficients) influence of pH and temperature (including the interactions observed) in a 3-dimensional graph. The highest rate of hydrolysis was observed at high temperatures (90°C) and low pH (6). At a higher pH, the maximum temperature shifted towards a lower value. The lowest rate of hydrolysis was found at high temperature (90°C) and pH 7.2. At a high temperature (90°C) the influence of the pH (6.0-7.2) on the rate of hydrolysis was much more pronounced then at a lower temperature (70°C). This is in agreement with the findings of a broader pH

maximum at lower temperatures (30-67°C) as compared to a higher temperature (90°C) (Dobreva et al., 1994; Madsen et al., 1973).

Table III: The significant terms for the natural logarithm of the rate of hydrolysis, $\ln(d(b_h)/dt)$, at different dextrose equivalents (initial, 5, 10, 15, 20), and maximal number of bonds hydrolyzed (max_{bh}). The model-predicted rate of hydrolysis ($\ln(d(b_h)/dt)$) can be calculated for any given set of process conditions, using these regression coefficients and the coded process conditions (Table I).

	ln $d(b_h)/dt$					
	Initial	DE = 5	DE = 10	DE = 15	DE = 20	Max_{bh}
r^2	0.89	0.88	0.91	0.84	0.75	0.95
P>F	0.0001	0.0001	0.0001	0.0001	0.0001	0.0001
Intercept	1.1310**	1.0786**	1.0066**	0.6787**	-0.0120†	347.9**
pH (P)	—	—	-0.1055*	-0.1039†	-0.7302*	—
Calcium (C)	—	—	—	—	-0.0154†	—
Temp. (T)	—	—	0.0147†	0.0367†	0.0358†	—
Dry weight	—	—	—	—	0.2194*	162.6**
Enzyme (E)	0.6083**	0.6092**	0.5838**	0.6151**	0.6339**	—
E^2	-0.2290**	-0.2098**	-0.1352*	-0.1880*	-0.2990*	—
T^2	—	—	-0.0991*	—	—	—
P^2	—	—	—	—	0.5561*	—
TC	—	—	—	—	-0.5245**	—
EP	—	—	—	—	0.3727*	—
ET	—	—	—	—	0.2885*	—
PT	—	—	-0.1359*	-0.1849*	—	—

**$p \leq 0.0001$, *$0.0001 < p \leq 0.05$, †$p > 0.05$.

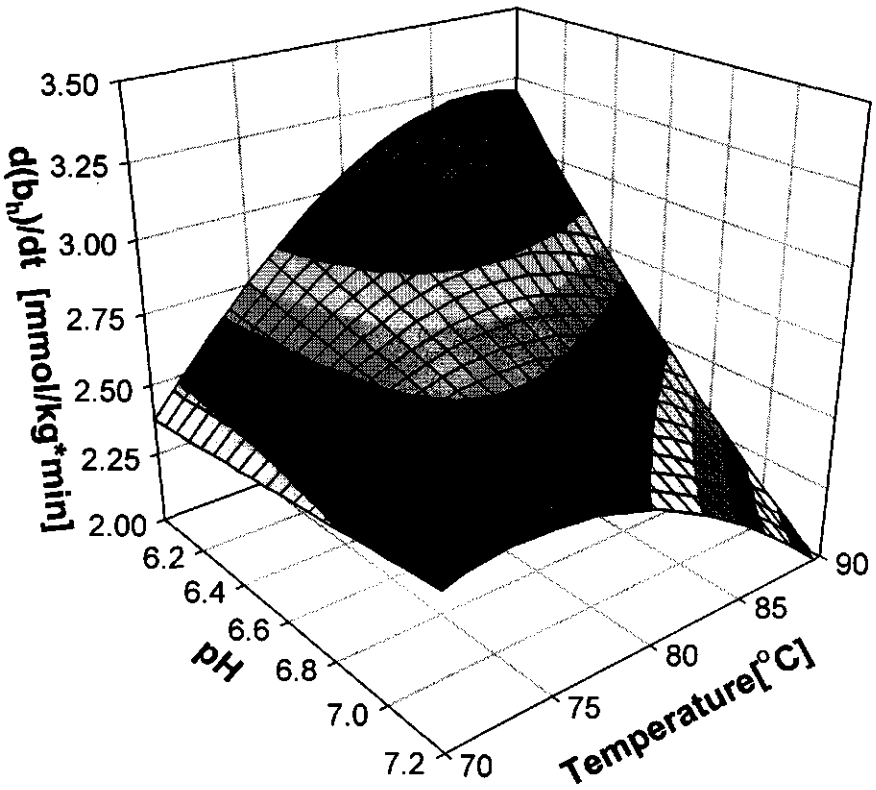

Figure 2: The regression model (Table III) influence of temperature and pH on the rate of hydrolysis at DE = 10. The enzyme dosage here is coded zero, which is 200 µl/(kg dw + H_2O).

At higher levels of conversion (DE = 20) the enzyme dosage showed an interactive effect with both pH and temperature (Figures 3 and 4). The influence of temperature on the rate of hydrolysis was much stronger at higher enzyme dosages (300 µl/kg) than at lower enzyme dosages (100 µl/kg). The rate of hydrolysis increased with the enzyme dosage. So, a low enzyme dosage (longer reaction time) results in a higher (temperature-dependent) inactivation of the enzyme (Rosendal et al., 1979; Violet and Meunier, 1989). This resulted in a smaller overall influence of temperature on the rate of hydrolysis at lower enzyme

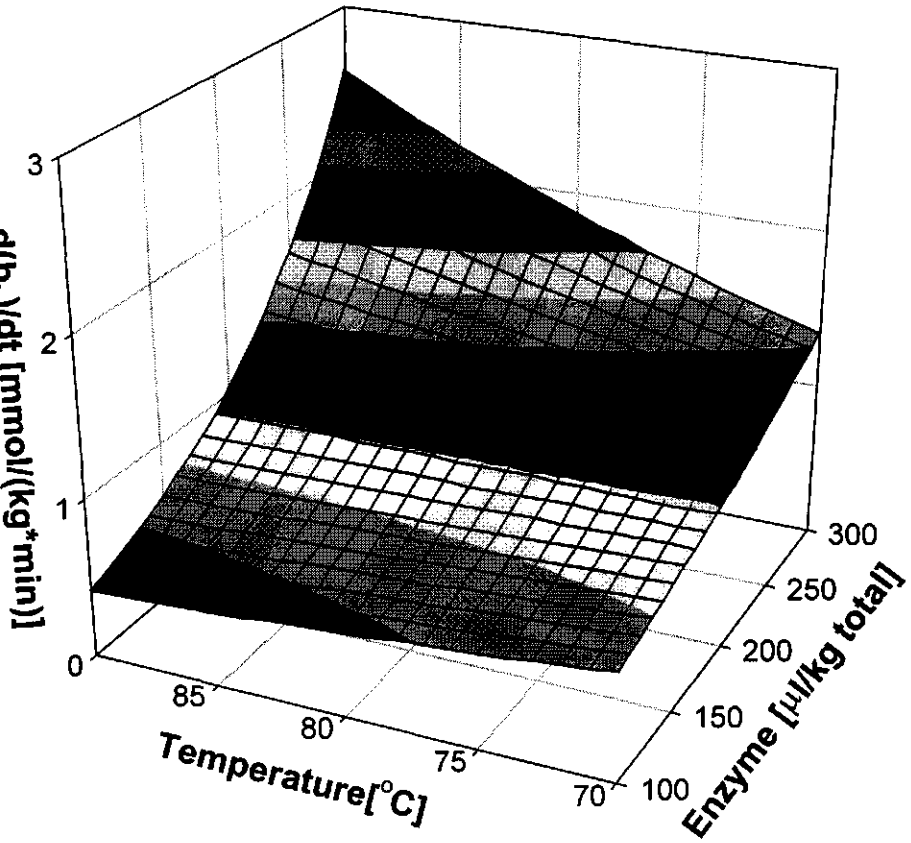

Figure 3: The regression model (Table III) influence of temperature and enzyme dosage on the rate of hydrolysis at DE = 20. Other process conditions are coded zero: pH 6.6, calcium addition 60 ppm [µg/g], and dry weight 0.2 kg/(kg dw + H_2O).

dosages. Enzyme dosage and pH also had an interactive effect on the rate of hydrolysis. This effect however, was less pronounced than the interactive effect between temperature and enzyme dosage. The inactivation of the enzyme also depends on the pH (Rosendal et al., 1979; Violet and Meunier, 1989). Rosendal et al. (1979) reported a drop in the stability of *B. licheniformis* α-amylase above pH 6.8. A higher pH (7.2) led to a higher inactivation

of the enzyme, resulting in a lower rate of hydrolysis as compared to a low pH (6.0). A higher dry weight concentration resulted in higher rates of hydrolysis at DE = 20 (Table III). Starch is known to stabilize α-amylase activity (De Cordt et al., 1994; Gorinstein, 1993; Rosendal et al., 1979; Shetty and Allen, 1988; Tomazic and Klibanov, 1988). The observed increase in enzyme activity at higher dry weight concentrations is most likely caused by this stabilization phenomenon.

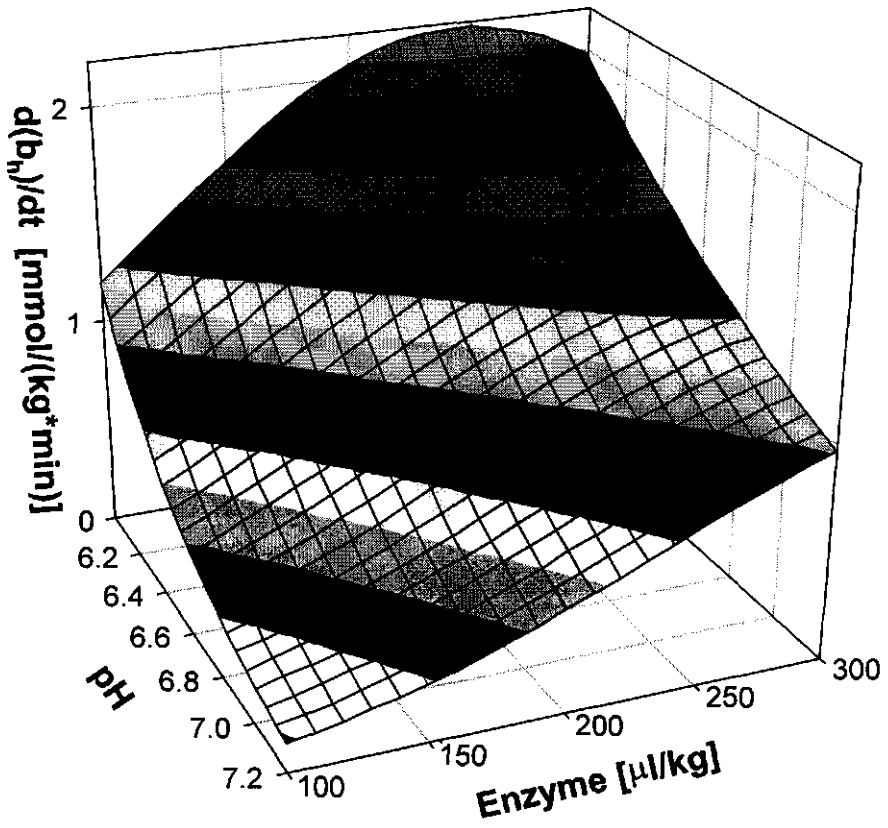

Figure 4: The regression model (Table III) influence of enzyme dosage and pH on the rate of hydrolysis at DE = 20. Other process conditions are coded zero: temperature 80°C, calcium addition 60 ppm [µg/g], and dry weight 0.2 kg/(kg dw + H_2O).

Calcium addition

Calcium addition showed, at the end of the reaction, an interactive effect with the temperature of hydrolysis. The addition of a small amount of calcium resulted in increased rates of hydrolysis at a higher temperature (Figure 5).

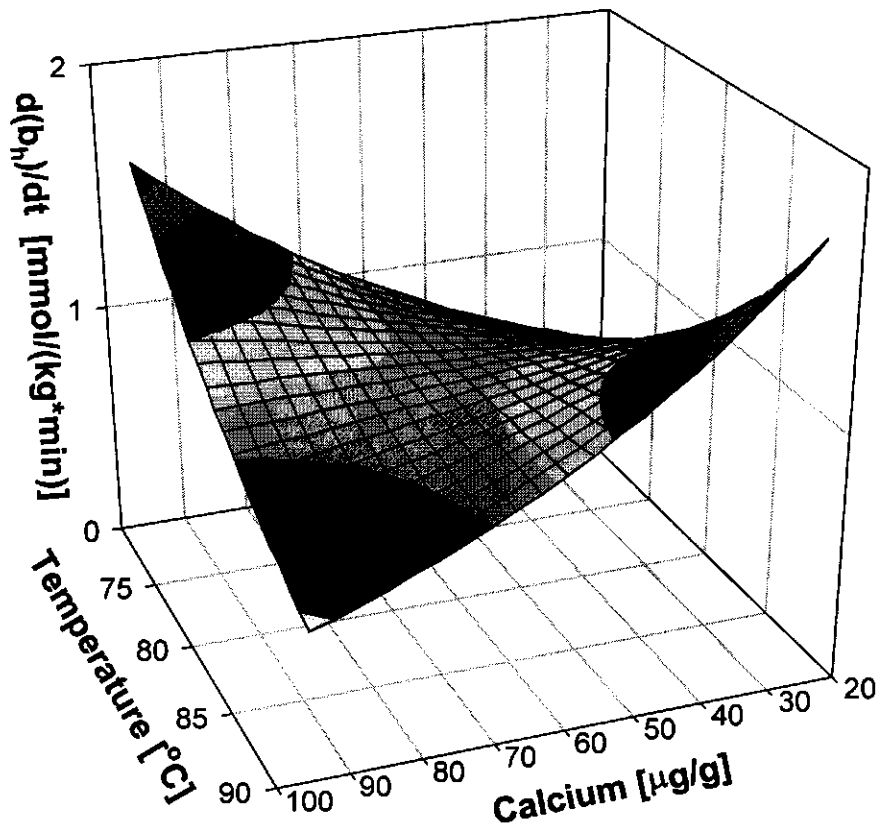

Figure 5: The regression model (Table III) influence of temperature and calcium addition on the rate of hydrolysis at DE = 20. Other process conditions are coded zero: pH 6.6, enzyme dosage 200 µl/(kg dw + H_2O), and dry weight 0.2 kg/(kg dw + H_2O).

High calcium levels resulted in a shift of the maximum temperature of hydrolysis towards a lower value. Calcium is known to play an important role in the structure and activity of α-amylases (Buisson et al., 1987; Hsiu and Fischer, 1964; Machius et al., 1998). Normally the stability of α-amylases is increased by the addition of small amounts of calcium (Atkinson and Mavituna, 1991). Destabilizing effects of calcium addition at higher concentrations are also reported (see Table IV). For the chloride dependent α-amylase from sea urchin a shift in maximum pH was reported after sodium chloride addition (Nakatani and Kobayashi, 1996). For an α-amylase from *Bacillus subtilis*, the addition of 400 ppm calcium resulted in a change in the activity-temperature curve, resulting in decreased enzyme activity below 65°C (Kennedy and White, 1979). Furthermore it is known that calcium can bind to the phosphorylated oligosaccharides present in potato starch (Kamasaka et al., 1995). The possible effect of this calcium binding on the hydrolysis reaction is unknown to date. The exact mechanism behind the observed shift of the maximum temperature of hydrolysis with increased addition of calcium is not clear.

Table IV: Literature data on observed destabilizing effect of calcium addition on α-amylase activity.

Source	No inhibition	Inhibition	Ionic strength kept constant?	Reference
B. licheniformis	0-200 ppm	500 ppm	No	De Cordt et al., 1992
B. coagulans B49	0 ppm	2000 ppm	No	Babu and Satyanarayana, 1993
B. licheniformis MY 10	0 ppm	200-2000 ppm	Yes	Kumar et al., 1990
A. niger	0 ppm	200-400 ppm	No	Boel et al., 1990
B. subtilis	0 ppm	40-400 ppm	No	Kennedy and White, 1979
Porcine pancreatic	0 ppm	240-1200 ppm	No	Deshpande and Cheryan, 1984
C. acetobutylicum	0-120 ppm	200-800 ppm	No	Annous and Blaschek, 1994

Maximum number of bonds hydrolyzed

The maximum number of bonds hydrolyzed at the end of an experiment was linearly dependent on the initial dry weight concentration (Table III). This implicates the absence of product inhibition, which would otherwise lead to incomplete conversion at high substrate concentrations. In Figure 6 both the experimental data and the model prediction (Table III) are given.

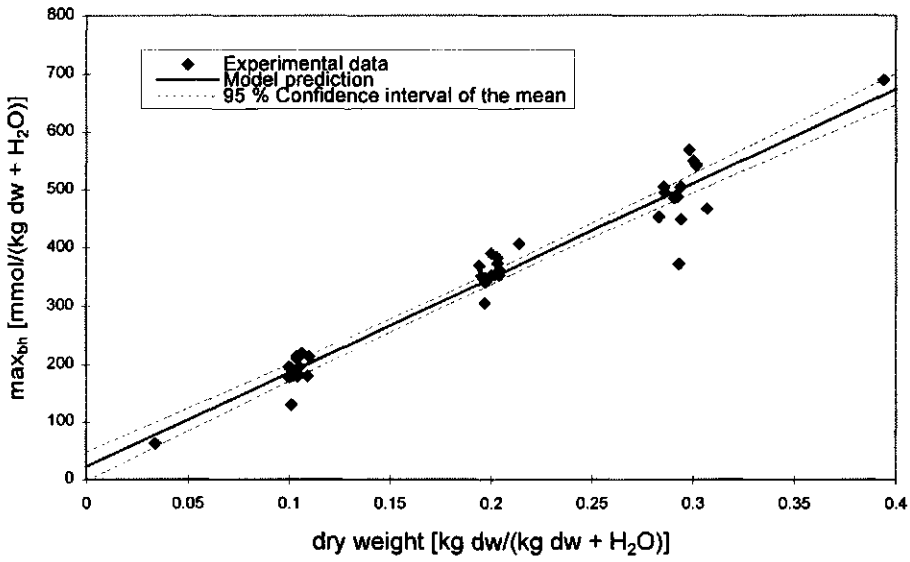

Figure 6: The maximum number of bonds hydrolyzed at the end of an experiment as a function of dry weight. The line (—) is the statistical model (Table III) predicted value with the 95% confidence intervals of the mean predicted values (---).

Influence of process conditions on the oligosaccharide composition

The dextrose equivalent of the hydrolysis products analyzed ranged from about 28 to 33. These hydrolyses were all done under different process conditions (pH, temperature, dry weight, enzyme dosage, calcium addition, and stirring speed). With HPLC the samples

were analyzed for their oligosaccharide composition, ranging from glucose (Degree of polymerization (DP) of one) up to maltoundecaose (DP11). In Figure 7, the amounts (as percentage dry weight of total sugars) of glucose (DP1), maltotetraose (DP4) and maltopentaose (DP5) are given as an example.

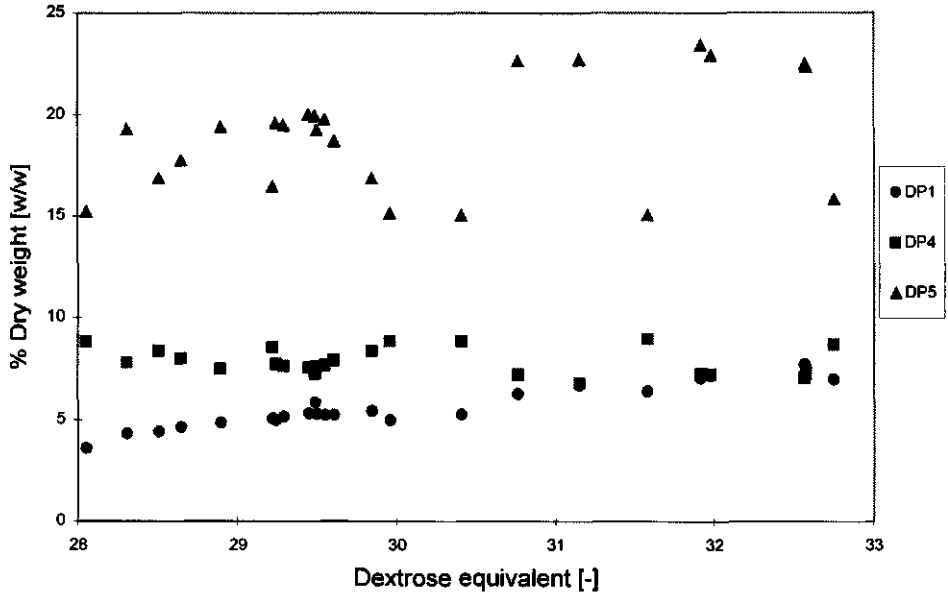

Figure 7: Percentage dry weight (as percentage dry weight of total sugars) of glucose (DP1), maltotetraose (DP4) and maltopentaose (DP5) versus dextrose equivalent.

The correlation between DE and the percentage dry weight of glucose and maltotetraose (DP4) seems rather strong. Maltopentaose showed a cloud of data points as a function of DE, which may be caused by other factors involved. Unfortunately only 24 samples were analyzed on HPLC, which means that the experimental design was far from complete (Box et al., 1978). Another complicated factor was that the dextrose equivalents of the samples were differed, which meant that the dextrose equivalent had to be brought into the design.

Table V: Statistical analysis of the influence of the temperature of hydrolysis and dextrose equivalent on the percentage [w/w] of a specific oligosaccharide. The oligosaccharides range from glucose (DP1) to maltoundecaose (DP11) and a rest fraction (>DP11) of the HPLC analysis. The coded values are DE (-1=28, 0=30.5, and 1=33) and temperature (-1=70°C, 0=80°C and 1=90°C).
The amount (% w/w) of a saccharide is given by:

$$DP_x = a_o + a_1[\text{ temperature(coded)}] + a_2[\text{DE (coded)}]. \qquad \text{(V.I)}$$

DP	Intercept (a_o)	Temp (a_1)	p value	DE (a_2)	p value	r^2
1	5.91	-0.29	0.0002	1.70	0.0001	0.96
2	17.65	1.38	0.0001	1.94	0.0001	0.86
3	16.56	-0.45	0.0001	0.40	0.0001	0.82
4	7.80	0.81	0.0001	0.03	0.7896	0.87
5	19.38	-3.31	0.0001	0.61	0.0631	0.92
6	5.41	1.19	0.0001	-2.71	0.0001	0.96
7	3.36	-0.06	0.0305	0.46	0.0001	0.90
8	3.45	0.10	0.0001	0.12	0.0001	0.66
9	3.24	0.04	0.1057	-0.24	0.0001	0.77
10	2.30	0.12	0.0001	-0.15	0.0002	0.75
11	2.55	-0.24	0.0505	-0.33	0.0492	0.24
>11	12.33	0.65	0.0001	-1.87	0.0001	0.91

Of this design (with now 7 variables) all cross and quadratic terms showed correlation with other variables. Also, dry weight was correlated with the dextrose equivalent. If variables are correlated this means that no independent conclusions can be drawn (Schlotzhauer and Littell, 1991). So, in this statistical analysis only the single process variables were investigated (pH, temperature, enzyme dosage, calcium addition, stirring speed, and dextrose equivalent) and no conclusion was drawn considering the influence (or not) of dry

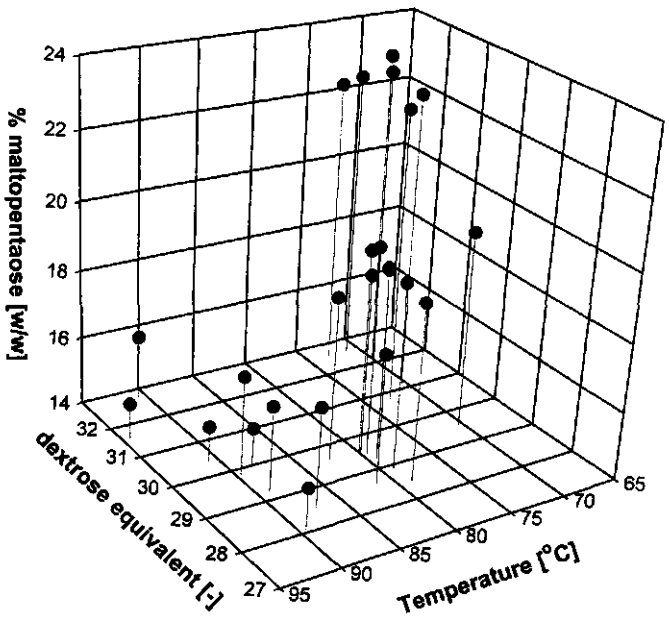

Figure 8: The percentage dry weight (as percentage dry weight of total sugars) of maltopentaose (DP5) as function of the temperature of hydrolysis (70-95°C) and dextrose equivalent.

weight on the saccharide composition. Statistical analysis of the effect of process conditions and DE showed that only temperature and DE significantly influenced the percentage of a specific oligosaccharide obtained after hydrolysis (Table V). Besides a pronounced influence of temperature on maltopentaose (DP5), there was also a significant influence of temperature on the other saccharides. This implies that the temperature of the reaction influences the composition of oligosaccharides. A higher temperature of hydrolysis increased the amount of DP2, DP4, and DP6. Increasing temperature on the other hand, decreased the amount of DP1, DP3, and DP5. The influence of the reaction temperature on the saccharides with a higher degree of polymerization was less

pronounced. The influence of the temperature on the product composition after hydrolysis with *B. licheniformis* α-amylases has been reported earlier (Dobreva et al., 1994; Ramesh and Lonsane, 1989). In both researches, however, there were substantial differences in the degree of hydrolysis between the different temperatures investigated. The influence of temperature was the strongest for maltopentaose (DP5), which is a primary end product of *B. licheniformis* α-amylase hydrolysis (Atkinson and Mavituna, 1991). In Figure 8, the percentage [w/w] of maltopentaose (DP5) as function of the hydrolysis temperature (70-90°C) and dextrose equivalent is given. The decrease in maltopentaose (DP5) with an increasing temperature of hydrolysis is evident, but more research is needed to study the mechanisms involved.

Conclusion

An accurate description (within the investigated process ranges) of the enzymatic hydrolysis could be given, suitable for better control of the process. Enzyme dosage, pH, and temperature predominantly determined the conversion process. Stirring had no influence on the rate of hydrolysis. Calcium addition was not beneficial with respect to increased enzyme stability or activity at higher temperature. High levels of calcium addition even resulted in a shift of the maximum temperature of hydrolysis towards a lower value. The pH, temperature, and amount of enzyme added showed interactive effects on the observed rate of hydrolysis. Furthermore, temperature had an effect on the amount (% dry weight) of specific oligosaccharides (especially maltopentaose) obtained during hydrolysis. The influence of temperature on the saccharide composition can be used as a new tool (besides different α-amylases and starches) to influence the composition of a starch hydrolysate, thus offering good prospects for development of tailor-made starch hydrolysates using (commercially available) α-amylases. Product composition (oligosaccharides) as function of temperature is presently investigated further.

Nomenclature

A	=	maximum number of bonds hydrolyzed	[mmol/(kg dw + H_2O)]
B	=	pseudo-first-order reaction constant	[min^{-1}]
C	=	maximum DE reached	[-]
D	=	pseudo-first-order reaction constant	[min^{-1}]
b_h	=	bonds hydrolyzed	[(m)mol/(kg dw + H_2O)]
DE	=	dextrose equivalent	[-]
dw	=	dry weight	[kg dw/(kg dw + H_2O)]
dw_{kgH2O}	=	dry weight per kg H_2O	[kg dw/kg H_2O]
dw_o	=	dry weight gelatinized starch	[kg dw/(kg dw + H_2O)]
max_{bh}	=	maximum bonds hydrolyzed	[mmol/(kg dw + H_2O)]
osm	=	osmolality	[mol/kg H_2O]
osm_m	=	measured osmolality	[mol/kg H_2O]
osm_o	=	osmolality due to salts	[mol/kg H_2O]

Acknowledgements

The authors thank Stoffer Rustebiel (Avebe) for his HPLC analysis and Rik Beeftink, Albert Otten (WAU), and Jack Bergsma (Avebe) for careful reading of the manuscript and their useful comments. Avebe and the Dutch Ministry of Economic Affairs (PBTS Biotechnology Project No. BIO94043) funded this research.

Appendix I

Measurement of enzymatic activity

An important and often used parameter for the degree of hydrolysis of starch is the dextrose equivalent (DE). A theoretical definition of the dextrose equivalent is

$$DE \equiv \frac{\text{Molecular weight dextrose}}{\text{Number - average molecular weight starch hydrolysate}} \times 100. \quad (I.1)$$

When in this article the term DE or dextrose equivalent is used, the theoretical dextrose equivalent as defined above is meant. The theoretical dextrose equivalent can be obtained from (Marchal et al., 1996)

$$DE = \frac{0.18}{dw_{kgH2O}/osm} \times 100, \quad (I.2)$$

in which osm is the osmolality (= molality here) directly obtained from the freezing- point depression and dw_{kgH2O} is the amount of dry weight per kg of water. Starting from gelatinized starch (osmolality ≈ 0), the number of bonds hydrolyzed per kg water and starch is directly proportional to the osmolality (osm) times the amount of water present :

$$b_h = osm(1 - dw). \quad (I.3)$$

During a hydrolysis, each time when a glycosidic bond is hydrolyzed, water is added to the hydrolysate and the mass of the solute increases. When 0.162 kg of starch is totally converted to dextrose (DE = 100), the dry mass of the solute increases to 0.180 kg. This means that the amount of salts present at the start of a liquefaction experiment (osm_o) is slightly concentrated during the hydrolysis. The osmolality due to the hydrolysis of starch (osm) is the measured osmolality (osm_m) minus the osmolality due to the salts present (osm_o) times the concentration factor:

$$osm = osm_m - osm_o \frac{(1 - dw_o)}{(1 - dw)}, \quad (I.4)$$

in which dw_o is the initial dry weight of the gelatinized starch before liquefaction. Substituting equation I.4 in I.3 gives

$$b_h = osm_m(1-dw) - osm_o(1-dw_o). \qquad (I.5)$$

Previously a relation for the increase in dry weight during the hydrolysis was derived (Marchal et al., 1996):

$$dw = \frac{dw_o + 18.10^{-3} osm_m - 18.10^{-3} osm_o(1-dw_o)}{1+18.10^{-3} osm_m}. \qquad (I.6)$$

Substituting this equation I.6 in I.5 gives the number of bonds hydrolyzed as a function of the measured osmolality (osm_m) and the initial dry weight (dw_o) and osmolality (osm_o).

$$b_h = \frac{(osm_m - osm_o)(1-dw_o)}{1+0.018osm_m}. \qquad (I.7)$$

Previously also a similar relation was derived for measuring the dextrose equivalent during a hydrolysis (Marchal et al., 1996):

$$DE = \frac{18(osm_m - osm_o)(1-dw_o)}{dw_o + 18.10^{-3}(osm_m - osm_o(1-dw_o))}. \qquad (I.8)$$

Thus, by measuring the increase in osmolality during an experiment, both the numbers of bonds hydrolyzed (I.7) and the dextrose equivalent (I.8) were determined and used for further analysis.

References

Annous, B.A., Blaschek, H.P. 1994. Isolation and characterization of alpha-amylase derived from starch-grown *Clostridium acetobutylicum* ATCC 824. J. Ind. Microbiol. **13:** 10-16.

Antrim, R.L., Solheim, B.A., Solheim, L., Auterinen, A.L., Cunefare, J., Karppelin, S. 1991. A new *Bacillus licheniformis* alpha-amylase capable of low pH liquefaction. Starch. **43:** 355-360.

Anyangwa, E.M., Kapseu, C., Elemva, Musonge, P. 1993. The effect and removal of starch in the sugar refining industry. International-Sugar-Journal. **95:** 210-213.

Atkinson, B., Mavituna, F. 1991. Biochemical engineering and biotechnology handbook. 2: Stockton press, New York.

Babu, K.R., Satyanarayana, T. 1993. Extracellular calcium-inhibited alpha-amylase of *Bacillus coagulans* B-49. Enzyme Microb. Technol. **15:** 1066-1069.

Bajpai, P., Bajpai, P.K. 1989. High-temperature alkaline alpha-amylase from *Bacillus licheniformis* TCRDC-B13. Biotechnol. Bioeng. **33:** 72-78.

Boel, E., Bradley, L., Brzozowski, A.M., Derewenda, Z., Dodson, G.G., Jensen, V.J., Petersen, S.B., Thim, L., Woldlike, H.F. 1990. Calcium binding in α-amylse: an x-ray diffraction study at 2.1-Å resolution of two enzymes from *Aspergillus.* Biochemistry. **29:** 6244-6249.

Box, G.E.P., Hunter, G.W., and Hunter, J.S. 1978. Statistics for experiments. John Wiley & Sons, New York.

Buisson, G., Ducee, E., Haser, R., Payan, F. 1987. Three dimensional structure of porcine pancreatic α-amylase at 2.9 Å resolution. Role of calcium in structure and activity. The EMBO Journal. **6:** 3909-3916.

Chiang, J.P., Alter, J.E., Stemberg, M. 1979. Purification and characterization of a thermostable alpha-amylase from *Bacillus licheniformis*. Starch. **31:** 86-92.

De Cordt, S., Hendrickx, M., Maesmans, G., Tobback, P. 1994. The influence of polyalcohols and carbohydrates on the thermostability of alpha-amylase. Biotechnol. Bioeng. **43:** 107-114.

De Cordt, S., Vanhoof, K., Hu, J., Maesmans, G., Hendrickx, M., Tobback, P. 1992. Thermostability of soluble and immobilized alpha-amylase from *Bacillus licheniformis*. Biotechnol. Bioeng. **40:** 396-402.

Deshpande, S.S., Cheryan, M. 1984. Effects of phytic acid, divalent cations, and their interactions on α-amylase activity. Journal of Food Science. **49:** 516-524.

Dobreva, E., Ivanova, V., Emanuilova, E. 1994. Effect of temperature on some characteristics of the thermostable alpha-amylase from *Bacillus licheniformis*. World J. Microbiol. Biotechnol. **10:** 547-550.

Fujii, M., Homma, T., Taniguchi, M. 1988. Synergism of alpha-amylase and glucoamylase on hydrolysis of native starch granules. Biotechnol. Bioeng. **32:** 910-915.

Gorinstein, S. 1993. Kinetic studies during enzyme hydrolysis of potato and cassava starches. Starch. **45:** 91-95.

Henderson, W.E., Teague, W.M. 1988. A kinetic model of *Bacillus stearothermophilus* alpha-amylase under process conditions. Starch. **40:** 412-418.

Hsiu, J., Fischer, E.H. 1964. Alpha-amylases as calcium-metalloenzymes. II Calcium and the catalytic activity. Biochemistry. **3:** 61-66.

Ivanova, V.N., Dobreva, E.P., Emanuilova, E.I. 1993. Purification and characterization of a thermostable alpha-amylase from *Bacillus licheniformis*. J. Biotechnology. **28:** 277-289.

Kamasaka, H., Uchida, M., Kusaka, K., Yoshokawa, K., Yamamoto, K., Okada, S., Ichikawa, T. 1995. Inhibitory effect of phosphorylated oligosaccharides prepared from potato starch on the formation of calcium phosphate. Biosci. Biotechnol. Biochem. **59:** 1412-1416.

Kennedy, J.F., White, C.A. 1979. Characteristics of alpha-amylase K, a novel amylase from a strain of *Bacillus subtilis*. Starch. **31:** 93-99.

Krishnan, T., Chandra, A.K. 1983. Purification and characterization of alpha-amylase from *Bacillus licheniformis* CUMC305. Appl. Environ. Microbiol. **46:** 430-437.

Kumar, S.U., Rehana, F., Nand, K. 1990. Production of an extracellular thermostable calcium-inhibited alpha-amylase by *Bacillus licheniformis* MY 10. Enzyme Microb. Technol. **12:** 714-716.

Machius, M., Declerck, N., Huber, R., Wiegand, G. 1998. Activation of *Bacillus licheniformis* alpha-amylase through a disorder->order transition of the substrate-binding site mediated by a calcium-sodium-calcium metal triad. Structure. **6:** 281-292.

Madsen, G.B., Norman, B.E., Slott, S. 1973. A new heat stable bacterial amylase and its use in high temperaure liquefaction. Starch. **25:** 304-308.

Marchal, L.M., Jonkers, J., Tramper, J. 1996. The use of freezing point depression to determine the theoretical dextrose equivalent. Starch. **48:** 220-224.

Morgan, F.J., Priest, F.G. 1981. Characterization of a thermostable alpha-amylase from *Bacillus licheniformis* NCIB 6346. J. Appl. Bacteriol. **50:** 107-114.

Nakatani, H., Kobayashi, I. 1996. Enzymatic properties of α-amylase from Sea Urchin, *Strongylocentrotus*. Comp. Biochem. Physiol. **113B:** 383-386.

Nigam, P., Singh, D. 1995. Enzyme and microbial systems involved in starch processing. Enzyme Microb. Technol. **17:** 770-778.

Park, J.T., Rollings, J.E. 1994. Effects of substrate branching characteristics on kinetics of enzymatic depolymerization of mixed linear and branched polysaccharides: I. Amylose/Amylopectine alpha-amylolysis. Biotechnol. Bioeng. **44:** 792-800.

Ramesh, M.V., Lonsane, B.K. 1989. End product profiles of starch hydrolysis by bacterial alpha-amylases at different temperatures and pH values. Biotechnol. Lett. **11:** 649-652.

Ramesh, M.V., Lonsane, B.K. 1990. Characteristics and novel features of thermostable alpha-amylase produced by *Bacillus licheniformis* M27 under solid-state fermentation. Starch. **42:** 233-238.

Rosendal, P., Nielsen, B.H., Lange, N.K. 1979. Stability of bacterial alpha-amylase in the starch liquefaction process. Starch. **31:** 368-372.

Rozie, H., Somers, W., Bonte, A., van', t.R.K., Visser, J., Rombouts, F.M. 1991. Adsorption and desorption characteristics of bacterial alpha-amylases on cross-linked potato starch. Biotechnol. Appl. Biochem. **13:** 181-195.

Saito, N. 1973. A Thermophilic Extracellular α-Amylase from *Bacillus licheniformis*. Archs. Biochem. Biophys. **155:** 290-298.

Schlotzhauer, S.D., Littell, R.C. 1991. SAS System for Elementary Statistical Analysis. SAS Institute Inc., Cary, NC.

Shetty, J.K., Allen, W.G. 1988. An Acid-stable, thermostable alpha-amylase for starch liquefaction. Cereal-Food-World. **33:** 929-934.

Steverson, E.M., Korus, R.A., Admassu, W., Heimsch, R.C. 1984. Kinetics of the amylase system of *Saccharomycopsis fibuliger*. Enzyme Microb. Technol. **6:** 549-554.

Tomazic, S.J., Klibanov, A.M. 1988. Mechanisms of irreversible thermal inactivation of Bacillus alpha-amylases. J. Biol. Chem. **263:** 3086-3091.

Violet, M., Meunier, J.C. 1989. Kinetic study of the irreversible thermal denaturation of *Bacillus licheniformis* alpha-amylase. Biochem. J. **263:** 665-670.

Yankov, D., Dobreva, E., Beschkov, V., Emanuilova, E. 1986. Study of optimum conditions and kinetics of starch hydrolysis by means of thermostable alpha-amylase. Enzyme Microb. Technol. **8:** 665-667.

Chapter 4

The Effect of Temperature on the Saccharide Composition Obtained after α-Amylolysis of Starch

L.M. Marchal, A.M.J. van de Laar, E. Goetheer, E.B. Schimmelpennink,
J. Bergsma, H.H. Beeftink, J. Tramper
Biotechnology & Bioengineering (1999), **63**, 344-355

Abstract

The hydrolysis of starch to low-molecular-weight products (normally characterised by their dextrose equivalent (DE), which is directly related to the number-average molecular mass) was studied at different temperatures. Amylopectin potato starch, lacking amylose, was selected because of its low tendency towards retrogradation at lower temperatures. *Bacillus licheniformis* α-amylase was added to 10% [w/w] gelatinised starch solutions. The hydrolysis experiments were done at 50, 70, and 90°C. Samples were taken at defined DE-values and these were analysed with respect to their saccharide composition. At the same DE the oligosaccharide composition depended on the hydrolysis temperature. This implies that at the same net number of bonds hydrolysed by the enzyme, the saccharide composition was different. The hydrolysis temperature also influenced the initial overall molecular-weight distribution. Higher temperatures led to a more homogenous molecular weight distribution. Similar effects were observed for α-amylases from other microbial sources such as *Bacillus amyloliquefaciens* and *Bacillus stearothermophilus*. Varying the pH (5.1, 6.2, and 7.6) at 70°C did not significantly influence the saccharide composition obtained during *B. licheniformis* α-amylase hydrolysis. The underlying mechanisms for *B. licheniformis* α-amylase were studied using pure linear oligosaccharides, ranging from

maltotriose to maltoheptaose as substrates. Activation energies for the hydrolysis of individual oligosaccharides were calculated from Arrhenius plots at 60, 70, 80, and 90°C. Oligosaccharides with a degree of polymerisation exceeding that of the substrate could be detected. The contribution of these oligosaccharides increased as the degree of polymerisation of the substrate decreased and the temperature of hydrolysis increased. The product specificity decreased with increasing temperature of hydrolysis, which led to a more equal distribution between the possible products formed. Calculations with the subsite map as determined for the closely related α-amylase from *B. amyloliquefaciens* reconfirmed this finding of a decreased substrate specificity with increased temperature of hydrolysis.

Introduction

The hydrolysis of starch is one of the most preponderant commercial enzyme processes. In general, the resulting low-molecular-weight products are characterized by their dextrose equivalent (DE), which is directly related to the number-average molecular mass. In a previous study, temperature was found to influence the saccharide composition after hydrolysis with *Bacillus licheniformis* α-amylase (Marchal et al., 1999). This effect of temperature can be used as one of the tools (beside the type of α-amylase and starch) to influence the composition of a starch hydrolysate, thus offering good prospects for development of tailor-made starch hydrolysates using commercially available α-amylases.

In this study we subsequently tried to address the following questions:

1) How does the oligosaccharide composition evolve during hydrolysis at different temperatures?
2) Is there a temperature effect on the overall molecular weight distribution in the initial hydrolysis?
3) What are the mechanisms underlying this temperature phenomenon?
4) Do other bacterial α-amylases also show a similar effect of temperature?

Amylopectin potato starch, lacking amylose, was selected because of its low tendency towards retrogradation. During the course of hydrolysis the oligosaccharide compositions and molecular weight distributions at 50, 70, and 90°C were monitored by HPLC measurements and GPC analysis, respectively. The underlying mechanisms for *B. licheniformis* α-amylase were studied with linear oligosaccharides as substrates, ranging from maltotetraose to maltoheptaose. The temperature sensitivity, substrate specificity, and the transglycosylation activities of the hydrolysis reaction of these oligosaccharides were studied at 60, 70, 80, and 90°C. To study the influence of pH, amylopectin potato starch was hydrolyzed at 70°C and at three pH's (5.1, 6.2, and 7.6). Two other commercial widely used, themostable bacterial α-amylases (from *Bacillus amyloliquefaciens* and *Bacillus stearothermophilus*) were also investigated with respect to the temperature dependency of the oligosaccharide composition.

Material & Methods

Liquefaction experiments

Amylopectin potato starch (Avebe, Veendam, the Netherlands) was obtained from transgenic potatoes (amylose content of starch < 1%, calcium content 481 ([μg/g]). A 10% dry weight [w/w] starch solution was made with demineralized water. Calcium (as $CaCl_2$) and sodium (as NaCl) were both added at a concentration of 60 ppm [μg/g] to respectively enhance enzyme stability and more or less mimic tap water. The starch was gelatinized in a stirred autoclave by heating for 30 minutes at 140°C. The gelatinized starch (pH 6) was transferred to a 2 dm^3 stirred reactor. The temperature was adjusted to the desired setting before the start of the experiment. Sodium azide (0.02% w/w) was added to prevent microbial growth. The hydrolysis reaction was started by addition of the enzyme solution (normal dosage 75 μl/kg solution). The α-amylase from *B. licheniformis* used was Maxamyl (Gist-brocades, presently Genencor, Delft, the Netherlands). The other α-

amylases used were *B. amyloliquefaciens* (BAN 240L, Novo Nordisk, Bagsvaerd, Denmark) and *B. stearothermophilus* (G-zyme 995, Rhône-Poulenc, Stockport, UK). Commercial α-amylase preparations are known to be pure (Helbert et. al., 1996; Rozie et al., 1991). The enzyme preparations used gave a single band on a gradient gel, so no further purification steps were performed. During the first five minutes of each experiment, a high stirring speed (158 rpm) was used to homogenize the system. The hydrolysis reaction was followed by measuring the increase in osmolality as a measure for the theoretical dextrose equivalent (Marchal et al., 1996,1999). The osmometer used was an Advanced osmometer model 3D3 (Advanced Instruments, Norwood, MA). Whenever in this article the term dextrose equivalent or DE is mentioned, the theoretical dextrose equivalent defined as: (180/number-average molecular mass of the starch hydrolysate)×100 is meant. Samples were taken for further analysis at constant dextrose equivalent intervals. The samples were lowered to pH 3 and immediately frozen, in order to stop the hydrolysis reaction. If the dextrose equivalent was less than five, the samples were diluted to 1% w/w to inhibit retrogradation. Several individual experiments were done at each temperature of hydrolysis with *B. licheniformis* α-amylase. At 50°C, two series were done and two additional experimental points at a dextrose equivalent of 5 and 10. At 70°C, three series were done and two additional experimental points at a DE≈3. At 90°C, one serie was done and two additional experimental points at a DE≈30. The experiments with *B. amyloliquefaciens* α-amylase were done at 50°C (two experiments), 70, 74, and 80°C. The experiments with *B. stearothermophilus* α-amylase were done at 50, 70, and 90°C.

Linear oligosaccharides

The oligosaccharides (maltotetraose to maltoheptaose, Nihon Shokuhin Kako Co. Ltd., Tokyo) were checked for their purity by HPLC. All oligosaccharides were at least 99% pure. The moisture content of these oligosaccharides was determined with the Karl Fischer method (ISO, 1978). These oligosaccharides (0.08 M) were hydrolyzed at 60, 70, 80, and 90°C. Calcium (as $CaCl_2$) and sodium (as NaCl) were each added at a concentration of 60

ppm. HPLC analysis was used to follow both the rate of hydrolysis and the formation of the hydrolysis products.

Analysis

The HPLC column was an Aminex HPX-42A (300 mm x 7.8 mm) carbohydrate analysis (Bio-rad, Veenendaal, the Netherlands) operated at 85°C, with water as eluent at 0.4 ml/min. The carbohydrates were analyzed by an index refraction detector and the concentration (w/w) was calculated according to the 100% method. The HPLC method does not provide information on the linkage pattern (branched or linear) of oligosaccharides with a defined degree of polymerization (DP). The molecular weight distribution was analysed on a gel permeation chromatography system with a index refraction detector. The columns were: TSK Quard column PWH + TSK PMPWXL + TSK G 6000 PW + TSK G 4000 PW + TSK G 3000 PW (Tosoh) operated at 40°C with 0.05M NaOH as eluent at a flow rate of 0.6 ml/min. Dextran solutions (Pharmacia, Sweden) were used as molecular weight standards.

Results and discussion

Oligosaccharide composition

Figure 1 represents the contribution of maltopentaose (as weight % of total) during the progress of hydrolysis as represented by the dextrose equivalent (DE). The amount of maltopentaose increases with decreasing temperature. At the same DE, the number-average molecular mass of the hydrolysate is the same. This implies that the net total amount of bonds hydrolyzed by the enzyme is the same, but the composition is different. The previously observed (Marchal et al, 1999) influence of the temperature of hydrolysis on the weight fraction of maltopentaose at the end of the hydrolysis (around a DE of 30) is obviously a phenomenon that evolves gradually at increasing dextrose equivalent. For a good understanding of the phenomena involved one should bear in mind that the dextrose

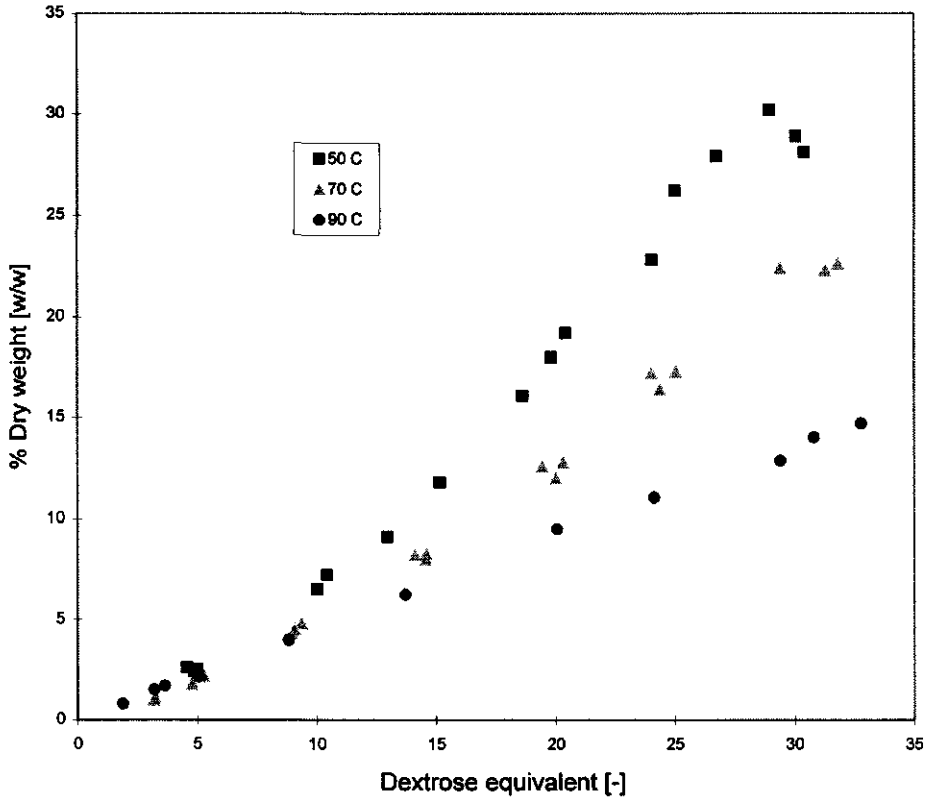

Figure 1: The amount of maltopentaose (as weight % of total) as a function of the dextrose equivalent for the hydrolysis of amylopectin potato starch (10% w/w) with *B. licheniformis* α-amylase at 50, 70, and 90°C.

equivalent on the x-axis is not linear with the time of hydrolysis. The DE versus time shows an exponential shape curve (A×(1-exp(-B×time))) with zero order kinetics up to a DE around 10 and a plateau at a DE of around 30. At a dextrose equivalent of around 30, it is difficult for the α-amylase to hydrolyse more α(1→4) linked glucose units and the hydrolysis virtually stops. As opposed to maltopentaose, the amount of maltotetraose (however with some more experimental scatter) was found to decrease with decreasing temperatures of hydrolysis (Figure 2).

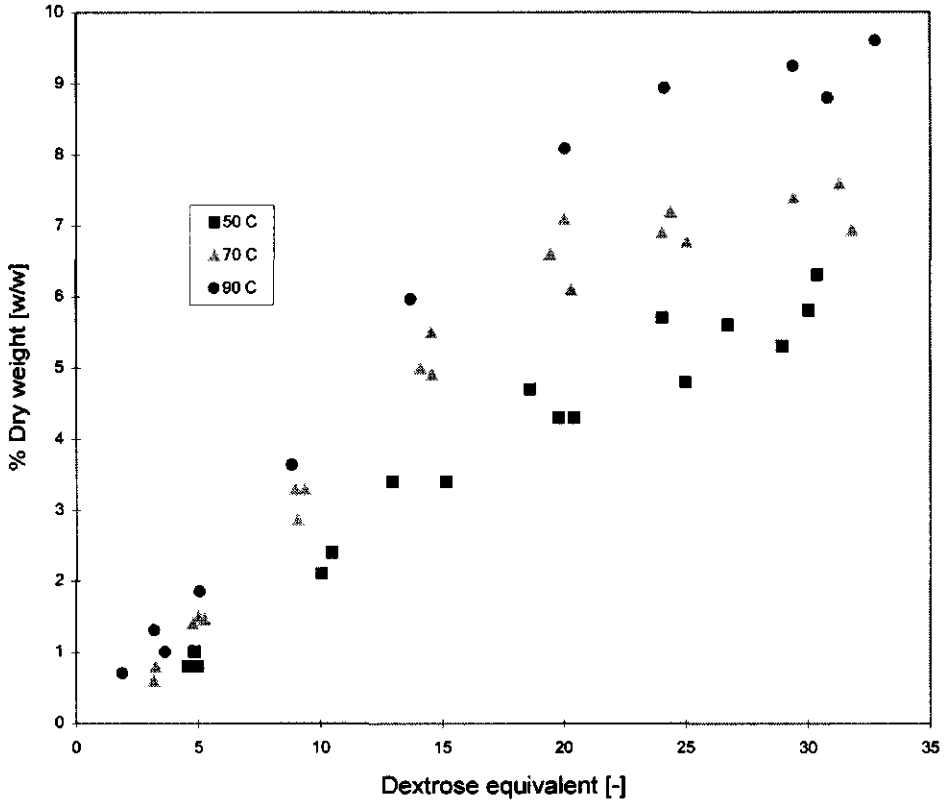

Figure 2: The amount of maltotetraose (as weight % of total) as a function of the dextrose equivalent for the hydrolysis of amylopectin potato starch (10% w/w) with *B. licheniformis* α-amylase at 50, 70, and 90°C.

Figure 3 gives the weight percentage of the oligosaccharides glucose to maltopentaose at a dextrose equivalent of 20. A significant effect of temperature on the amount of the oligosaccharides maltose to maltopentaose can be observed, which strongly indicates a dependence which alternates with degree of polymerization of the saccharide. This alternating effect with the degree of polymerization of the temperature of hydrolysis on the saccharide composition was already observed at the end of the hydrolysis reaction (Marchal et al, 1999).

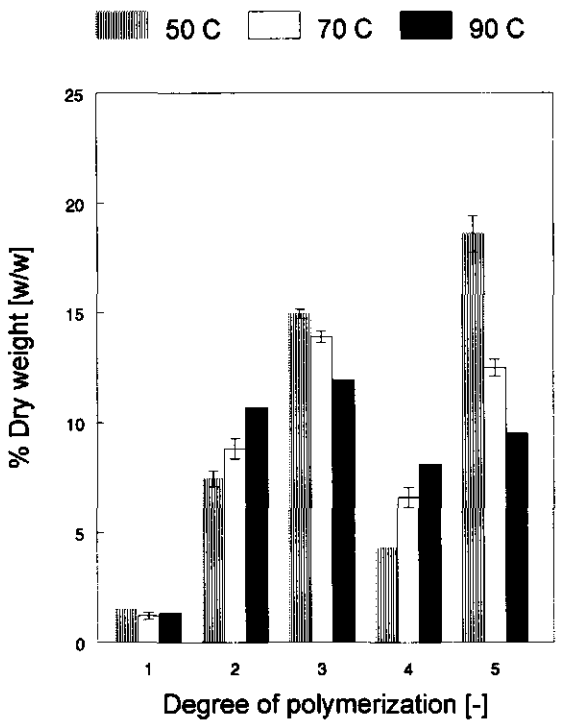

Figure 3: The weight fraction of the oligosaccharides glucose (DP1) to maltopentaose (DP5) at a dextrose equivalent of 20 for the hydrolysis of amylopectin potato starch (10% w/w) with *B. licheniformis* α-amylase at 50, 70, and 90°C. The hydrolysis at 50 and 70°C are given with the 95% confidence interval of the mean predicted value. The values for glucose and maltotetraose at 50°C were exactly the same.

The weight percentage of maltose and maltotriose (Figure 4) increased gradually during the hydrolysis, whereas the level of glucose rose at the end of the hydrolysis (above DE ≈ 20). The amount of maltose (w/w) is increased with increasing temperature of hydrolysis, as opposed to the amount of maltotriose (w/w) which is decreased with increasing temperature of hydrolysis. The temperature of hydrolysis does not have a strong influence on the amount (w/w) of glucose (Figure 4).

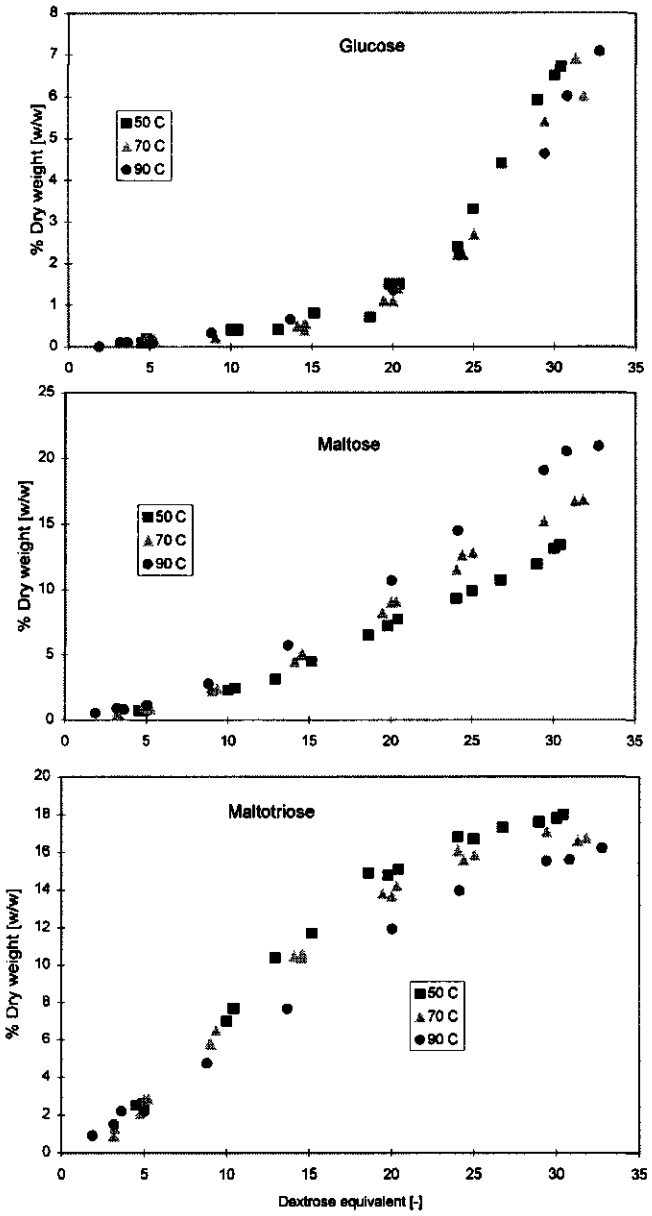

Figure 4: The amount of glucose, maltose, and maltotriose (as weight % of total) as a function of the dextrose equivalent for the hydrolysis of amylopectin potato starch (10% w/w) with *B. licheniformis* α-amylase at 50, 70, and 90°C.

Different profiles, showing peaks, were observed for maltohexaose and maltoheptaose (Figure 5). The net amount of a saccharide is always the production minus further hydrolysis. A peak in the amount of maltohexaose and maltoheptaose has also been

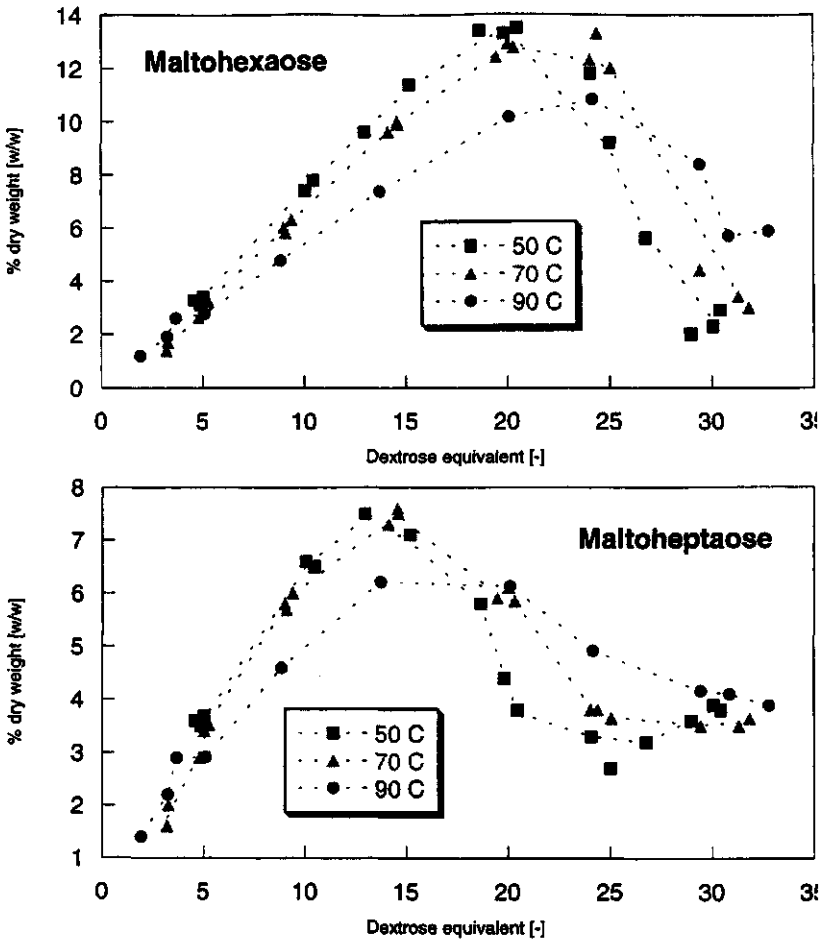

Figure 5: The amount of maltohexaose and maltoheptaose (as weight % of total) as a function of the dextrose equivalent for the hydrolysis of amylopectin potato starch (10% w/w) with *B. licheniformis* α-amylase at 50, 70, and 90°C. The data points are connected for ease of comparison only.

reported during the hydrolysis with *B. licheniformis* 44MB82 α-amylase by Ivanova et al. (1991). At 50°C, the amount of maltoheptaose rises again above a dextrose equivalent of around 25. Linear maltoheptaose is hydrolyzed very easy by *B. licheniformis* α-amylase (see section on linear oligosaccharides). Branched oligosaccharides, liberated from the hydrolysis of amylopectin with *B. amyloliquefaciens* α-amylase, are reported for a degree of polymerization of five and higher (French et al., 1972; Hizukuri, 1996; Hughes et al., 1963). Because the net amount of maltoheptaose (is production minus further hydrolysis) rises again after a minimum, the net production of linear maltoheptaose is very unlikely at a DE above 25. This second increase is most likely due to the net production of branched maltoheptaose from the hydrolysis of branched structures with a higher degree of polymerization. For the higher saccharides (malto-octaose to maltodecaose) such a second increase is also clearly visible at a temperature of hydrolysis of 50 and 70°C (Figure 6). A higher temperature of hydrolysis leads to a higher first peak (around a dextrose equivalent of 10) for all three oligosaccharides (malto-octaose to maltodecaose). The profile for the saccharides with a degree of polymerization of 11 resembled that of malto-octaose to maltodecaose, although with a higher experimental scatter (results not shown). There was no significant effect of the temperature of hydrolysis on the amount of saccharides with a degree of polymerization exceeding 11 (rest fraction of the HPLC-analysis), which decreases gradually with increasing dextrose equivalent (results not shown). The pH (in the range 5.1-7.6) did not significantly influence the saccharide composition during the hydrolysis of starch with *B. licheniformis* α-amylase (results not shown). The pH was found to slightly influence the hydrolysis of small oligosaccharides (maltotriose and maltotetraose) with porcine pancreatic α-amylase, but no influence of the pH was found for the higher saccharides (maltopentaose and higher) by Ishikawa et al. (1991).

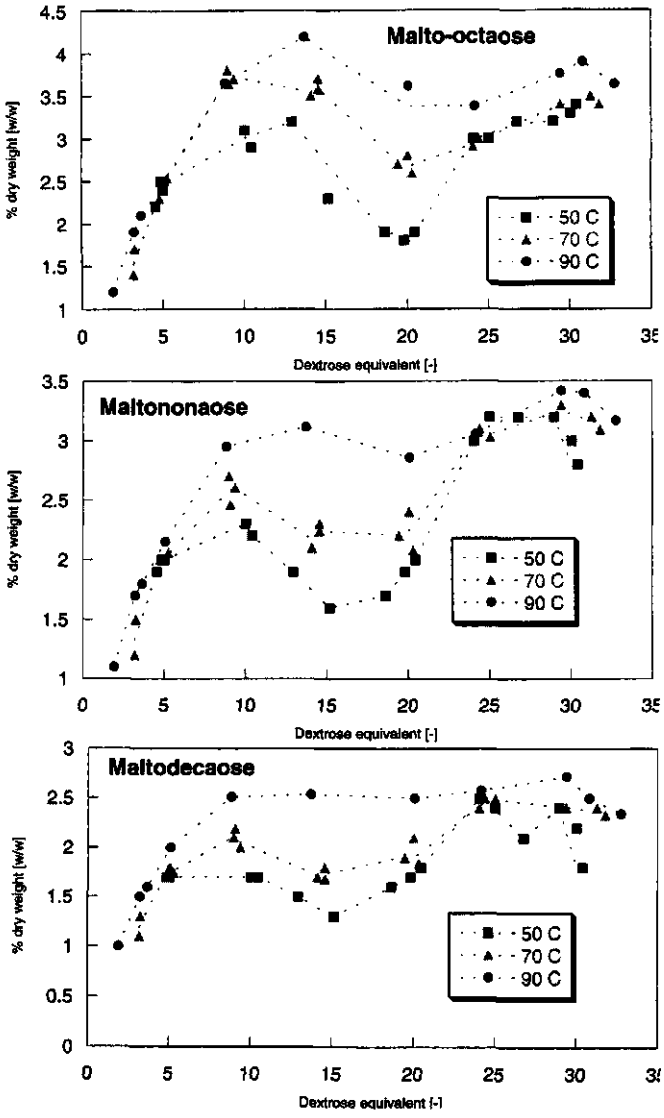

Figure 6: The amount of malto-octaose, maltononaose, and maltodecaose (as weight % of total) as a function of the dextrose equivalent for the hydrolysis of amylopectin potato starch (10% w/w) with *B. licheniformis* α-amylase at 50, 70, and 90°C. The data points are connected for ease of comparison only.

Overall molecular weight distribution during the initial hydrolysis

The ratio of weight-average molecular mass (M_w) and number-average molecular mass (M_n) can be used to express the homogeneity of a system. A monodisperse system has a M_w/M_n ratio of one, a polydisperse system has a ratio >1 (Chang, 1981). Figure 7 gives the weight fraction versus the logarithm of the apparent molecular weight for the hydrolysis of 10% amylopectin potato starch with *B. licheniformis* α-amylase at a dextrose equivalent of 1, 3, and 5. The temperatures of hydrolysis are 50, 70, and 90°C. Apparent molecular weight distributions are compared since the dextran calibrated gel permeation chromatography system used does not allow conclusions to be drawn on absolute molecular weights. These graphs should be used to compare the molecular weight distributions at different temperatures. At all the three temperatures of hydrolysis, the heterogeneity of the initial starch hydrolysate decreases with increasing dextrose equivalent (in the range 1-5). This is also expressed by decreasing values of M_w/M_n with increasing dextrose equivalent. Also, the overall heterogeneity increases with decreasing temperature of hydrolysis (resulting in a higher M_w/M_n ratio). At a lower temperature of hydrolysis (50°C) a much more pronounced bimodal molecular weight distribution is observed than at a higher temperature of hydrolysis (90°C). A bimodal molecular weight distribution has previously been reported for hydrolysis (at 60°C) of potato starch with *B. subtilis* α-amylase by Heitmann et al. (1997). A temperature of hydrolysis of 50°C gives a lower mass fraction between the two molecular weight peaks (at DE 3 and 5) as compared to hydrolysis at 70°C. At a temperature of hydrolysis of 90°C the two molecular weight peaks even merge into each other. The peak of the higher molecular weight fraction lies structurally at a higher molecular weight with a lower temperature of hydrolysis. Although speculative, a possible explanation would be that the amylopectin clusters behave more rigid at lower temperature and are therefore less accessible to the α-amylase.

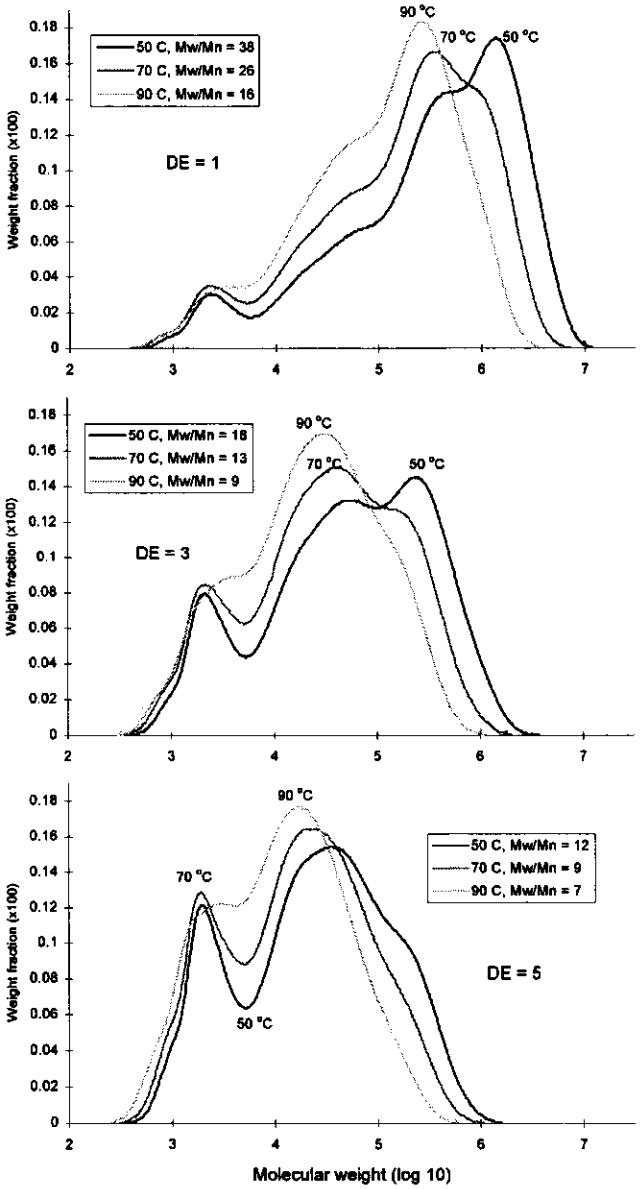

Figure 7: The weight fraction versus the logarithm of the apparent molecular weight for the hydrolysis of amylopectin potato starch (10% w/w, pH 6) with *B. licheniformis* α-amylase at a dextrose equivalent of 1, 3, and 5. The temperatures of hydrolysis are 50, 70, and 90°C.

Temperature sensitivity of the hydrolysis reaction

In literature there are some contradictory reports on the capability of *B. licheniformis* α-amylase to hydrolyse linear oligosaccharides. Morgan and Priest (1981) and Nakakuki et al. (1985) reported that *B. licheniformis* α-amylase was capable of cleaving oligosaccharides with a minimum degree of polymerization of 6 (maltohexaose). Saito (1973) on the other hand reported that *B. licheniformis* α-amylase was capable of cleaving oligosaccharides with a minimum degree of polymerization of 4 (maltotriose). The most obvious difference between these experiments was the temperature of hydrolysis, 50°C (Saito, 1973), 40°C (Nakakuki et al., 1985), and 37°C (Morgan and Priest, 1981). One of the mechanisms involved in the temperature influence could be a temperature dependent change in the capability of *B. licheniformis* α-amylase to hydrolyze different oligosaccharides. To study this, the rate of hydrolysis of maltotetraose (DP4) to maltoheptaose (DP7) was studied at temperatures normally used in industrial starch hydrolysis (60-90°C). Figure 8 gives the rate of hydrolysis for the linear oligosaccharides maltotetraose (DP4) to maltoheptaose (DP7) with *B. licheniformis* α-amylase. The rate of hydrolysis of maltotetraose is very low. This rate is equal to the overall rate of hydrolysis of amylopectin potato starch at a dextrose equivalent of around 30 (at the end of the starch hydrolysis reaction). Starch hydrolysates, which are industrially produced using α-amylases, normally have a dextrose equivalent (Luff-Schoorl or Lane-Eynon titration) of ≤ 20 (Schenck and Hebeda, 1992). This implies that hydrolysis of maltotetraose only plays a minor role in industrial starch hydrolysis. The rate of hydrolysis increases rapidly going from degree of polymerization 5 to degree of polymerization 6, especially at low (60°C) temperatures. At a high temperature (90°C) the differences between the rates of hydrolysis of the individual oligosaccharides, especially maltopentaose and maltoheptaose, diminishes. This means that at an elevated temperature the hydrolysis of maltopentaose is relatively less unfavorable (compared to the rates of hydrolysis of the higher oligosaccharides). Besides this, also other mechanisms must underlay the influence of the temperature of hydrolysis on the saccharide composition.

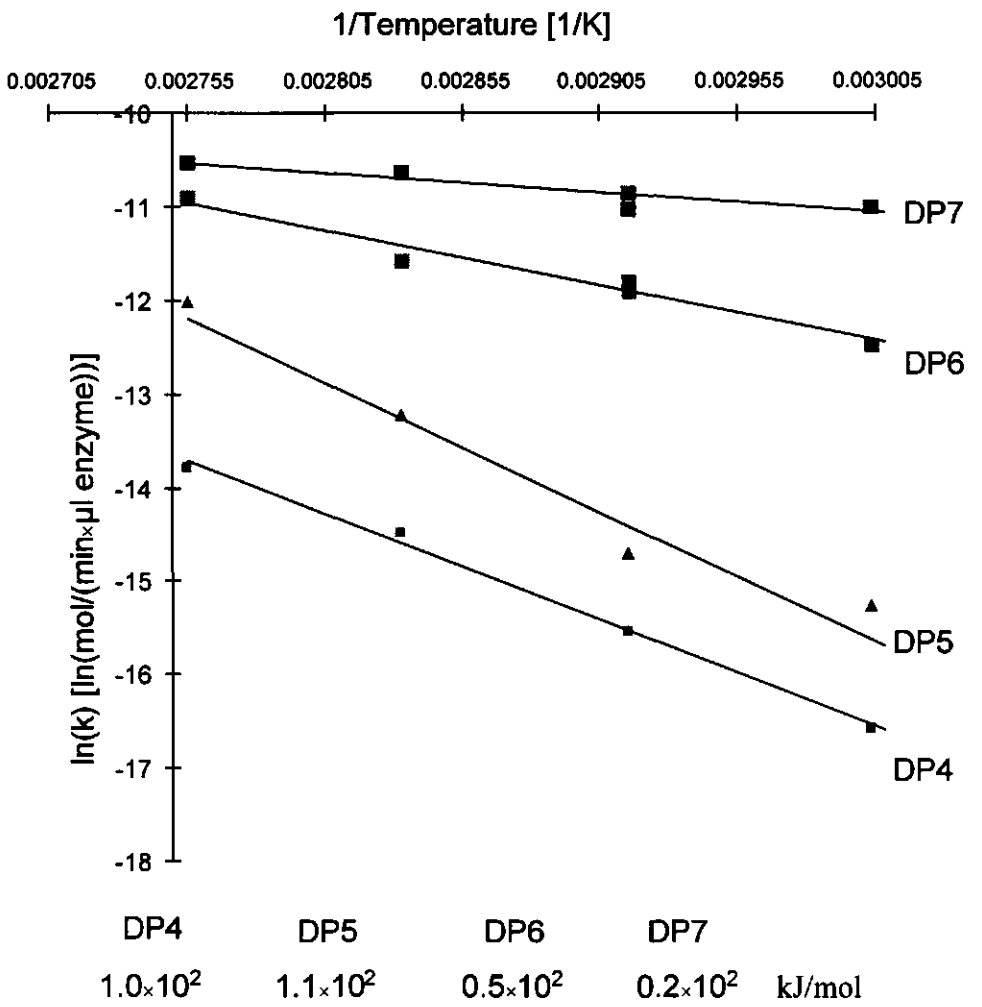

Figure 8: The Arrhenius plots for the hydrolysis of the linear oligosaccharides maltotetraose (DP4) to maltoheptaose (DP7) with *B. licheniformis* α-amylase. The rate of hydrolysis (k) is expressed as mol of the given saccharide converted per minute per µl enzyme.

This can be illustrated as follows: the difference between the amount of maltopentaose at 50 and 90°C at a dextrose equivalent of 20 (see Figure 3) is 9.1% (w/w) whereas the difference (between 50 and 90°C) in the amount of the smaller oligosaccharides (glucose to maltotetraose combined) is -3.9% (w/w). This means that, a decrease of 9.1% (w/w) in the amount of maltopentaose only is "compensated" with an increase of 3.9% (w/w) in the total amount of the smaller oligosaccharides (DP1-DP4). So, a temperature dependent hydrolysis rate of malto-pentaose, thus cannot fully explain the temperature effects observed upon starch hydrolysis. Two other factors which are involved with the influence of the temperature of hydrolysis on the saccharide composition are discussed in the paragraphs on product specificity and transglycosylation. At least two phenomena are involved in the increased temperature sensitivity at a lower degree of polymerization of the linear oligosaccharides. One is the contribution of transglycosylation reaction, which increases with decreasing degree of polymerization and with increasing temperature (see paragraph on transglycosylation). Since the smaller oligosaccharides favor most from this temperature-dependent increase in transglycosylation, their conversion rates are more temperature sensitive. The other phenomenon is the influence of temperature on the fraction of productive substrate enzyme complexes (see paragraph: "Temperature sensitivity of the rate of hydrolysis of linear oligosaccharides" in Appendix I). The specificity to bind an oligosaccharide in a given way decreases with increasing temperature. Calculations demonstrate (Appendix I) that the fraction of productive complexes show the highest temperature sensitivity for maltotetraose and maltopentaose (Table I.2). Assuming that the hydrolysis reaction does not proceed according to complex kinetics, the temperature sensitivity of the rate of hydrolysis of these oligosaccharides (Figure 8) can be expressed as activation energies (Cornish-Bowden, 1995). The temperature sensitivity (activation energy) increases with decreasing degree of polymerization. An increase in the activation energy at decreasing number of glycosyl units in the substrate (range 7 to 4 glycosyl units) has been reported previously for human serum α-amylase by Hafkenscheid and Hessels (1988). Maltoheptaose had a very low activation

energy, usually seen for diffusion limited reactions. The turnover number (k_{cat}) calculated for the fastest reaction here (maltoheptaose at 90°C) is 1125 s^{-1}, which is about the same as the value of 1250 s^{-1} given for the hydrolysis of maltoheptaose with porcine pancreatic α-amylase by Seigner et al. (1987). Calculations based on the method given by Furusaki (1989) showed that diffusion limitation for the reaction of maltoheptaose is very unlikely. Since α-amylase activity is far from simple kinetics, care should be taken to interpret obtained activation energies as they were simple chemical reactions. The activation energy of *B. licheniformis* α-amylase for the hydrolysis of amylopectin potato starch was 12 kJ/mol (temperature range 35-90°C, pH 6, and 10% w/w starch). This is at the lower side for the range of activation energies known from literature (see Table I).

Table I: Some literature values for activation energies (E_a) of *Bacillus* α-amylases. BLA = *B. licheniformis* α-amylase, BAA = *B. amyloliquefaciens* α-amylase. Termamyl is industrial *B. licheniformis* α-amylase as sold by Novo Nordisk (Bagsvaerd, Denmark).

E_a [kJ/mol]	Enzyme	pH	T [°C]	Substrate	Reference
32.75	Termamyl	6.9	37-90	1% NaBH4 potato starch	Gorinstein, 1993
28.65	Termamyl	6.9	37-90	1% NaBH4 cassava starch	Gorinstein, 1993
25	BLA M27	7	52-85	0.5% soluble starch	Ramesh and Lonsane, 1990
12	BLA BLM 1777	6	30-60	1% lintner soluble starch	Chiang et al., 1979
30	BLA	8.2	55-85	1% starch	Violet and Meunier, 1989
42	BLA MY10	6	50-75	1% soluble starch	Kumar et al., 1990
11.4	BAA K	5.8	26-90	1% starch	Kennedy and White, 1979

Product specificity

The hydrolysis of a saccharide (with a degree of polymerization exceeding two) can occur in more than one way, leading to different products. Figure 9 gives the initial measured molar ratio between the products formed from maltoheptaose at four different temperatures

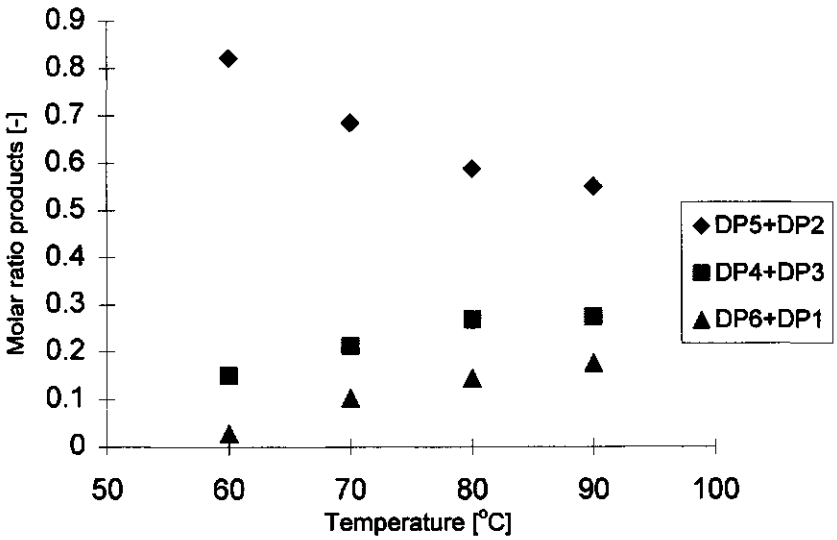

Figure 9: The initial molar ratio [mol/mol] between the hydrolysis products formed from pure linear maltoheptaose (0.08 M) during hydrolysis with *B. licheniformis* α-amylase at 4 different temperatures.

of hydrolysis with *B. licheniformis* α-amylase. A higher temperature of hydrolysis leads to a more uniform distribution between the potential products formed from maltoheptaose. This finding is supported by calculations with the subsite map of *B. amyloliquefaciens* α-amylase (see Appendix I). Table I.1 gives the calculated bond-cleavage frequencies for maltotetraose (n=4) to maltodecaose (n=10) at 30, 60, and 90°C. A higher temperature of hydrolysis leads to a more equal distribution between the possible products formed from a saccharide. From two reports in literature on the action pattern of *B. licheniformis* α-amylase on linear oligosaccharides it is striking that the experiments with a higher temperature of hydrolysis (Saito, 1973) gave a more equal distribution between the products formed as compared to the lower temperature of hydrolysis (Nakakuki et al., 1985). However, it must also be recognized that this difference could result from variations between the α-amylases, since they originate from different isolations of *B. licheniformis*.

Transglycosylation

During the hydrolysis of pure linear oligosaccharides, products were observed with a degree of polymerization higher than that of the starting material. Products with a degree of polymerization higher than that of the starting material, have previously been reported for α-amylase reactions (Ajandouz et al., 1992; Allen and Thoma, 1978a,b; Graber and Combes, 1990; Kimura and Horikoshi, 1990; Monma et al., 1983; Omichi and Ikenaka, 1988; Robyt and French, 1970; Suganuma et al., 1978,1996). This phenomenon is related to transglycosylation and/or a condensation reaction of the α-amylase and increases with the saccharide concentration.

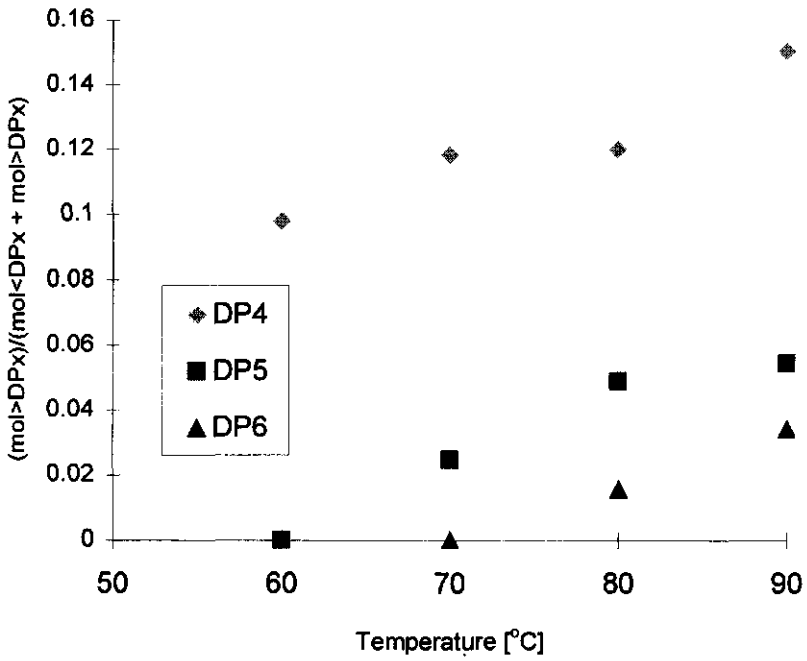

Figure 10: The mol fraction of products with a higher degree of polymerization than that of the starting material as a fraction of the total amount of products formed for the hydrolysis with *B. licheniformis* α-amylase at 60, 70, 80, and 90°C.

In general, condensation plays only a minor part, and the production of saccharides with a higher degree of polymerization than that of the starting material is mainly through transglycosylation (Allen and Thoma, 1978a,b; Suganuma et al., 1978). Furthermore, transglycosylation reactions of α-amylases with other acceptors than linear oligosaccharides have been reported by Brumm et al. (1991) and Nishimura et al. (1994). Figure 10 gives the mol fraction of products with a higher degree of polymerization than that of the starting material as a fraction of the total amount of products formed. This mole fraction increases with temperature, indicating that the contribution of transglycosylation to the total conversion increases with temperature. Also the contribution of the transglycosylation reactions to the total conversion increases with decreasing degree of polymerization of the oligosaccharide (Figure 10), which is in agreement with the findings of Allen and Thoma (1978a).

B. amyloliquefaciens and *B. stearothermophilus* α-amylases

The temperature of hydrolysis also had a significant effect on the saccharide composition upon the hydrolysis of amylopectin potato starch with both *B. amyloliquefaciens* and *B. stearothermophilus* α-amylases. Figure 11 gives the influence of temperature on the hydrolysis of amylopectin potato starch with *B. amyloliquefaciens* α-amylase with the amount of maltohexaose as an example. The overall picture for the influence of the temperature of hydrolysis on the oligosaccharide composition upon hydrolysis with *B. amyloliquefaciens* α-amylase was the same as for the hydrolysis with *B. licheniformis* α-amylase, with a few small differences: glucose started to rise at a dextrose equivalent of 15 (compared to a dextrose equivalent of 20 for *B. licheniformis* α-amylase), there was no significant influence on the amount of maltotriose, and the experimental scatter for saccharides with a degree of polymerization of 10 and 11 was higher as compared to the hydrolysis with *B. licheniformis* α-amylase. The influence of temperature on the oligosaccharide composition upon hydrolysis with *B. stearothermophilus* α-amylase was

somewhat different as compared to the other two *Bacillus* α-amylases. The amount of maltotetraose was higher and the amount of maltopentaose was lower at a lower temperature of hydrolysis, which is the opposite effect as seen with *B. licheniformis* and *B. amyloliquefaciens* α-amylase. More research will be required in order to understand the differences in mode of reaction.

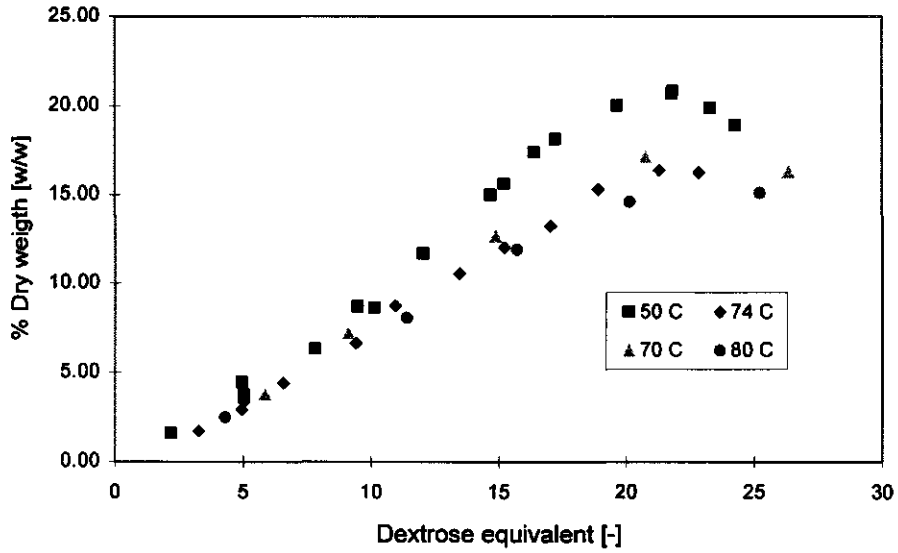

Figure 11: The amount of maltohexaose (as weight % of total) as a function of the dextrose equivalent for the hydrolysis of amylopectin potato starch (10% w/w, pH 6) with *B. amyloliquefaciens* α-amylase at 50, 70, 74, and 80°C.

Conclusion

The temperature was found to have a distinct influence on the oligosaccharide composition during the hydrolysis of amylopectin potato starch with three different *Bacillus* α-amylases. A higher temperature led to a less heterogeneous molecular weight distribution

during the initial phase of the hydrolysis with *B. licheniformis* α-amylase. Experiments with *B. licheniformis* α-amylase on linear oligosaccharides showed that hydrolysis at a higher temperature led to an increased contribution of transglycosylation reactions and a reduced product specificity. At a high temperature of hydrolysis (90°C) the difference between the rate of hydrolysis of the individual oligosaccharides, especially maltopentaose and maltoheptaose, was less as compared to a lower temperature (60°C). Calculations with the subsite map of *B. amyloliquefaciens* α-amylase supported the experimental findings with regard to product specificity and relative rates of hydrolysis. The influence of the temperature of hydrolysis on the saccharide composition can not be explained by one simple mechanism. The observed influence of temperature on the rate of hydrolysis is at least combination of the following aspects:

1) A decrease in product specificity of the α-amylase with increasing temperature.
2) An increase in amount of transglycosylation products with increasing temperature.
3) A change, with the temperature of hydrolysis, between the ratio of the rate of hydrolysis of different linear oligosaccharides with a different degree of polymerization.

The influence of temperature on the action of hydrolysis (shown here for three different α-amylases) is likely to be a more general phenomenon. Starches from various botanical origin (i.e. potato, corn, wheat, tapioca) differ slightly in for example: amylose content, chain length distribution, molecular weight, and the number of chains per cluster. But, the overall molecular features of these starches are more or less the same. The way in which temperature effects the saccharide composition will also hold for other starches, although differences in molecular structure will affect the exact composition of the hydrolysate. The influence of temperature on the saccharide composition, as well as the application of various α-amylases and starches, can be used as new tools to influence the composition of a starch hydrolysate. Thus offering good prospects for development of tailor-made starch hydrolysates using (commercially available) α-amylases.

Acknowledgments

The authors thank Stoffer Rustebiel and Carla Kuiper-Boorsma (Avebe) for performing the HPLC and GPC analysis respectively, Kees de Gooijer (WAU), and Bert Franke (Avebe) for careful reading of the manuscript and their useful comments. Avebe and the Dutch Ministry of Economic Affairs (PBTS Biotechnology Project No. BIO94043) funded this research.

Appendix I: Subsites calculations

The active site of an α-amylase is assumed to consist of a definite number of subsites (the so-called subsite theory; Ajandouz et al., 1992; Allen and Thoma, 1976a,b; Hiromi, 1970; Iwasa et al., 1974; MacGregor et al., 1992,1994; Matsui et al., 1991; Prodanov et al., 1984; Robyt, 1989; Robyt and French, 1963,1970; Sano et al., 1985; Seigner et al., 1987; Suganuma et al., 1978,1996; Thoma et al., 1970,1971; Thoma and Allen, 1976; Torgerson et al., 1979). A short synopsis of the theory is given here. The theoretical calculations are based on the following reaction scheme:

$$E + S_n \begin{array}{l} \xrightleftharpoons{K_{n,p,r}} ES_{n,p,r} \xrightarrow{k_{int}} E + P_i + P_{(n-i)} \\ \xrightleftharpoons{K_{n,x,r}} ES_{n,x,r} \end{array} , \qquad \text{(I.1)}$$

in which S_n represents a saccharide consisting of n glucose units. $ES_{n,p,r}$ represents the productive complexes and $ES_{n,x,r}$ represents the non-productive complexes with respect to the possibility of the α-amylase to hydrolyse a glucose linkage in the saccharide. The r represents the position of the reducing end of the saccharide in the subsite of the enzyme. For saccharides with a degree of polymerization exceeding two, there is always more then one possible productive complex. $K_{n,p,r}$ and $K_{n,x,r}$ are the association constants of the productive (p) or non-productive (x) complexes. In these calculations k_{int} (hydrolytic rate constant) is considered to be independent of n. So, the maximum velocity k_0 (for a saccharide with length n) depends only on the relation between the ratio of the productive

enzyme-substrate complexes to the sum of all possible (productive and non-productive) complexes (Heymann and Guenther, 1994):

$$k_0(n) = k_{int} \frac{K_{n,p}}{K_{n,p} + K_{n,x}}. \qquad (I.2)$$

All possible binding modes are assigned an individual binding constant $K_{n,r}$ (with the reducing end at subsite position number r). The association constant $K_{n,r}$ for a complex can be related to free-energies of interaction of the occupied subsites with glucose residues by Allen and Thoma (1976a):

$$-RT \ln K_{n,r} = \sum_{i=r-n+1}^{r} \Delta G_i + \Delta G_{mix}, \qquad (I.3)$$

where R is the gas constant, T the absolute temperature in Kelvin, ΔG_i is the free energy of binding of a glucose residue at subsite i, and ΔG_{mix} is the free-energy contribution to binding , which is common for bimolecular association processes (Chipman and Sharon, 1970; Hiromi, 1970). ΔG_{mix} in aqueous solution is equal to $\kappa T \ln(55.5)$ (Gurney, 1953). For a bimolecular processes (κ=2) this gives a value of 2.4 kcal (at 298 Kelvin). Since the association constants ($K_{n,r}$) depend on temperature, an influence of temperature on the enzyme-substrate complexes is anticipated. Calculation (based on the generally accepted subsite theory) of the influence of temperature on the amount of productive enzyme-substrate complexes and the ratio between the possible products formed from a given saccharide, would help to understand the observed temperature influence on the saccharide composition. Unfortunately no subsite map has been determined for *B. licheniformis* α-amylase until now. However, the bacterial α-amylases are highly conserved and closely related (Conrad et al., 1995; Svensson, 1994). Therefore, calculations are made here with the subsite map for *B. amyloliquefaciens* α-amylase as determined by Allen and Thoma (1976b). It is stressed that these calculations are meant to demonstrate the implications of

the subsite theory with respect to the influence of temperature on the reaction mode of hydrolysis. These calculations are not considered as proof for the mechanisms behind the temperature influence on the α-amylolytic activity, but merely as a support. Figure I.1 gives the used subsite map of *B. amyloliquefaciens* α-amylase. The point of hydrolysis is situated between subsite number 6 and 7. The reducing end of a saccharide is always situated at the right-hand of the subsite map.

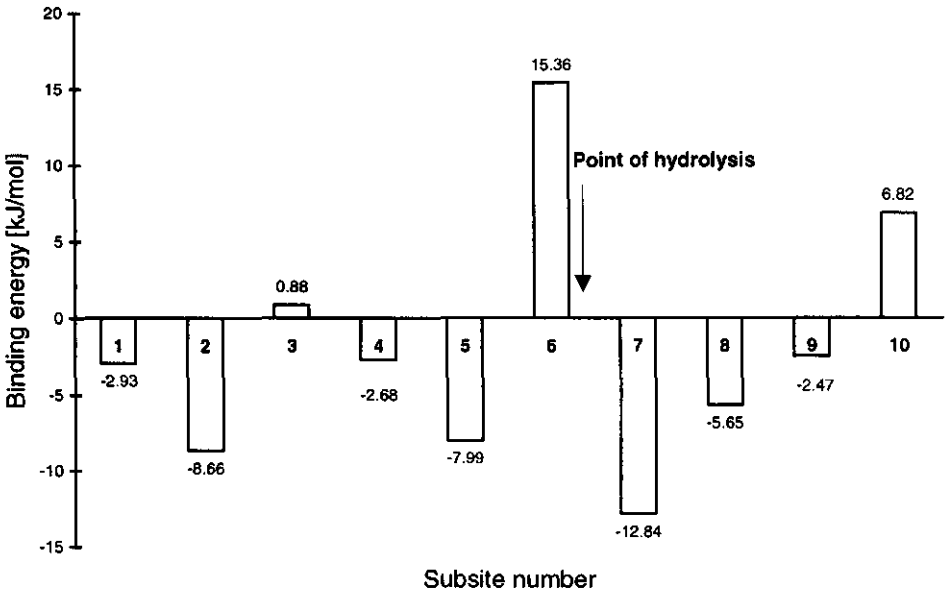

Figure I.1: Subsites energy map (in kJ per mol) for *B. amyloliquefaciens* α-amylase as given by Allen and Thoma (1976b). See text for details.

Calculations of bond-cleavage frequencies

The frequency to hydrolyse an oligosaccharide at a given position (with the reducing end at position r) is the ratio between this particular association constant $K_{n,p,r}$ and the sum of all

the possible productive constants $K_{n,p}$ for this saccharide with length n. By determining the fraction of all the possible productive complexes ($K_{n,p,r}$) of a saccharide in this way, the bond-cleavage frequency for this saccharide (with length n) is determined. Table I.1 gives the calculated bond-cleavage frequencies at 3 different temperatures for maltotetraose (n=4) to maltodecaose (n=10).

Temperature sensitivity of the rate of hydrolysis of linear oligosaccharides

With equation I.3 and I.2 the maximum rate of hydrolysis of a saccharide (with length n) can be calculated at different temperatures. The fraction of productive complexes for a saccharide ($K_{n,p}/(K_{n,p}+ K_{n,x})$) changes with temperature. This change in the fraction of productive complexes of different saccharides is a measure for the temperature sensitivity of the rate of hydrolysis. It is important to notice that, since k_{int} is set to unity and considered independent of temperature, these changes only express the relative temperature sensitivity (based on the fraction of productive enzyme-substrate complexes) for the hydrolysis of a saccharide and not the actual change in the rate of hydrolysis with temperature. Table I.2 gives the change in the fraction of productive complexes at different temperatures compared to 30°C for maltotetraose (n=4) to maltodecaose (n=10).

Table I.2: Calculated relatively change (with temperature) in the fraction of productive complexes at different temperatures (compared to 30°C) for the *B. amyloliquefaciens* α-amylase subsite map as given by Allen and Thoma (1976b). (($K_{n,p}/(K_{n,p}+ K_{n,x})$) at x°C)/(($K_{n,p}/(K_{n,p}+ K_{n,x})$) at 30°C).

DP	10	9	8	7	6	5	4
30°C	1	1	1	1	1	1	1
60°C	0.98	0.98	0.99	1	1.14	1.25	1.25
90°C	0.97	0.97	0.96	0.99	1.26	1.49	1.50

Table I.1: Calculated bond-cleavage frequencies for maltotetraose (n=4) to maltodecaose (n=10) at 30, 60, and 90°C for *B. amyloliquefaciens* α-amylase subsite map as given by Allen and Thoma (1976b). R denotes the reducing end of the oligosaccharide.

10	9	8	7	6	5	4	3	2	R	Temperature [C]
0.000	0.000	0.001	0.000	0.014	0.044	0.685	0.249	0.026		30
0.000	0.000	0.001	0.001	0.019	0.054	0.632	0.259	0.034		60
0.000	0.001	0.002	0.001	0.024	0.063	0.603	0.266	0.041		90
	9	8	7	6	5	4	3	2	R	
	0.000	0.000	0.001	0.000	0.015	0.696	0.261	0.028		30
	0.000	0.000	0.001	0.001	0.020	0.668	0.274	0.036		60
	0.000	0.001	0.002	0.001	0.025	0.643	0.284	0.044		90
		8	7	6	5	4	3	2	R	
		0.000	0.000	0.001	0.001	0.428	0.514	0.055		30
		0.000	0.001	0.002	0.002	0.426	0.503	0.065		60
		0.000	0.001	0.003	0.003	0.424	0.493	0.076		90
			7	6	5	4	3	2	R	
			0.000	0.002	0.008	0.060	0.696	0.236		30
			0.000	0.003	0.008	0.071	0.667	0.250		60
			0.000	0.005	0.012	0.082	0.641	0.260		90
				6	5	4	3	2	R	
				0.000	0.011	0.462	0.122	0.404		30
				0.001	0.015	0.451	0.135	0.399		60
				0.001	0.019	0.441	0.145	0.394		90
					5	4	3	2	R	
					0.001	0.461	0.501	0.037		30
					0.002	0.458	0.494	0.047		60
					0.003	0.454	0.487	0.056		90
						4	3	2	R	
						0.079	0.705	0.217		30
						0.092	0.676	0.231		60
						0.105	0.652	0.244		90

References

Ajandouz, E.H., Abe, J., Svensson, B., Mouren, G.M. 1992. Barley malt-α-amylase. Purification, action patern and subsite mapping of isozyme 1 and two members of the isozyme 2 subfamily using p-nitrophenylated maltooligosaccharide substrates. Biochim. Biophys. Acta. **1159:** 193-202.

Allen, J.D., Thoma, J.A. 1976a. Subsite mapping of enzymes. Application of the depolymerase computer model to two α-amylases. Biochem. J. **159:** 121-132.

Allen, J.D., Thoma, J.A. 1976b. Subsite mapping of Enzymes. Depolymerase computer modelling. Biochem. J. **159:** 105-120.

Allen, J.D., Thoma, J.A. 1978a. Model for Carbohydrate action. *Aspergillus oryzae* α-amylase degradation of maltotriose. Biochemistry. **17:** 2345-2350.

Allen, J.D., Thoma, J.A. 1978b. Multimolecular substrate reaction Catalyzed by Carbohydrates. *Aspergillus oryzae* α-amylase degradation of Maltooligo-saccharides. Biochemistry. **17:** 2338-2344.

Brumm, P.J., Hebeda, R.E., Teague, W.M. 1991. Purification and characterization of the commercialized, cloned *Bacillus megaterium* alpha-amylase. Part II: transferase properties. Starch. **43:** 319-323.

Chang, R.C. 1981. Physical Chemistry with applications to biological systems. 2: MacMillan Publishing Co., New York.

Chiang, J.P., Alter, J.E., Stemberg, M. 1979. Purification and characterization of a thermostable alpha-amylase from *Bacillus licheniformis*. Starch. **31:** 86-92.

Chipman, D.M., Sharon, N. 1970. Mechanism of Lysozyme action. Science. **165:** 454-465.

Conrad, B., Hoang, V., Polley, A., Hofemeister, J. 1995. Hybrid *Bacillus amyloliquefaciens* X *Bacillus licheniformis* alpha-amylases: Construction, properties and sequence determinants. European Journal of Biochemistry. **230:** 481-490.

Cornish-Bowden, A. 1995. Fundementals of Enzyme Kinetics. revised: Portland Press, London.

French, D., Smith, E.E., Whelan, W.J. 1972. The structural analysis and enzymatic synthesis of a pentasaccharide alpha-limit dextrin formed from amylopectin by *Bacillus substilis* alpha-amylase. Carbohydr. Res. **22:** 123-134.

Furusaki, S. 1989. Intradiffusion effect on reactivity of Immobilized microorganisms, pp.71-85.In: Fiechter, Okada, and Tanner (eds.), Bioproducts and Bioprocesses, Springer-Verlag, Berlin.

Gorinstein, S. 1993. Kinetic studies during enzyme hydrolysis of potato and cassava

starches. Starch. **45:** 91-95.

Graber, M., Combes, D. 1990. Action pattern of alpha-amylase from *Aspergillus oryzae* in concentrated media. Biotechnol. Bioeng. **36:** 12-18.

Gurney, R.W. 1953. Ionic processes in solution. McGraw-Hill Publishing company, Ltd, London.

Hafkenscheid, J.C.M., Hessels, M. 1988. Some thermodynamic parameters and temperature-conversion factors for determinig α-amylase concentration in serum. Clin. Chem. **34:** 2016-2018.

Heitmann, T., Wenzig, E., Mersmann, A. 1997. Characterization of three different potato starches and kinetics of their enzymatic hydrolysis by an α-amylase. Enzyme Microb. Technol. **20:** 259-267.

Heymann, H., Guenther, S. 1994. Calculation of subsite affinities of human small intestinal glucoamylase-maltase. Biol. Chem. Hoppe-Seyler. **375:** 451-455.

Hiromi, K. 1970. Interpreatation of dependency of rate parameters of the degree of polymerization of substrate in enzyme-catalysed reactions. Evaluation of subsite affinities of exo-enzyme. Biochem. Biophys. Res. Commun. **40:** 1-6.

Hizukuri, S. 1996. Starch:Analytical Aspects, pp.347-429.In: Eliasson AC (eds.), Carbohydrates in food, Marcel Dekker, inc., New York.

Hughes, R.C., Smith, E.E., Whelan, W.J. 1963. Structure of a pentasaccharide of α-limit dextrin formed from amylopectin by *Bacillus subtilis* α-amylase. Biochem. J. **88:** 63P-64P.

Ishikawa, K., Matsui, I., Honda, K., Kobayashi, S., Nakatani, H. 1991. The pH dependance of the action pattern in porcine pancreatic α-amylase-catalysed reaction for maltooligosaccharide substrates. Archs. Biochem. Biophys. **298:** 124-129.

ISO, 1978 Determination of water - Karl Fischer method. International organization for standarization, ISO 760.

Ivanova, V., Emanuilova, E., Sedlak, M., Pazlarova, J. 1991. HPLC study of starch hydrolysis products obtained with alpha-amylase from *B. amyloliquefaciens* and *B. licheniformis*. Applied Biochemistry and Biotechnology. **30:** 193-202.

Iwasa, S., Aoshima, H., Hiromi, K., Hatano, H. 1974. Subsite affinities of bacterial liquefying α-amylase evaluated from the rate parameters of linear substrates. J. Biochem. **75:** 969-978.

Kennedy, J.F., White, C.A. 1979. Characteristics of alpha-amylase K, a novel amylase from a strain of *Bacillus subtilis*. Starch. **31:** 93-99.

Kimura, T., Horikoshi, K. 1990. Characterization of pullulan-hydrolyzing enzyme from an

alkalopsychrotrophic *Micrococcus sp.* Appl. Microbiol. Biotechnol. **34:** 52-56.

Kumar, S.U., Rehana, F., Nand, K. 1990. Production of an extracellular thermostable calcium-inhibited alpha-amylase by *Bacillus licheniformis* MY 10. Enzyme Microb. Technol. **12:** 714-716.

MacGregor, A.W., Morgan, J.E., MacGregor, E.A. 1992. The action of germinated barley alpha-amylase on linear maltodextrins. Carbohydr. Res. **227:** 301-313.

MacGregor, E.A., MacGregor, A.W., Macri, L.J., Morgan, J.E. 1994. Models for the action of barley alpha-amylase isozymes on linear substrates. Carbohydr. Res. **257:** 249-268.

Marchal, L.M., Jonkers, J., Tramper, J. 1996. The use of freezing point depression to determine the theoretical dextrose equivalent. Starch. **48:** 220-224.

Marchal, L.M., Jonkers, J., Franke, G.Th., de Gooijer, C.D., Tramper, J. 1999. The effect of process conditions on the α-amylolytic hydrolysis of amylopectin potato starch. an experimental-design approach. Biotechnol. Bioeng. **62:** 348-357.

Matsui, I., Ishikawa, K., Matsiu, E., Miyairi, S., Fukai, S., Honda, K. 1991. Subsite structure of saccharomycopsis α-amylase secreted from *Saccharomyces cerevisiae*. J. Biochem. **109:** 566-569.

Monma, M., Nakakuki, T., Kainuma, K. 1983. Formation and hydrolysis of maltohexaose by an extracellular exo-maltohexaohydrolase. Agric. Biol. Chem. **47:** 1769-1774.

Morgan, F.J., Priest, F.G. 1981. Characterization of a thermostable alpha-amylase from *Bacillus licheniformis* NCIB 6346. J. Appl. Bacteriol. **50:** 107-114.

Nakakuki, T., Azuma, K., Kainuma, K. 1984. Action patterns of various exo-amylases and the anomeric configuration of their products. Carbohydr. Res. **128:** 297-310.

Nishimura, T., Kometani, T., Takii, H., Terada, Y., Okada, S. 1994. Acceptor specificity in the glucosylation reaction of *Bacillus subtilis* X-23 alpha-amylase towards various phenolic compounds and the structure of kojic acid glucoside. J. Ferment. Bioeng. **78:** 37-41.

Omichi, K., Ikenaka, T. 1988. Inspection of Human Salvivary α-amylase Action by Its Transglycosylation Action. J. Biochem. **104:** 881-883.

Prodanov, E., Seigner, C., Marchis-Mouren, G. 1984. Subsite profile of the active center of porcine pancreatic α-amylase. Kinetic studies using maltooligosaccharides as substrates. Biochem. Biophys. Res. Commun. **122:** 75-81.

Ramesh, M.V., Lonsane, B.K. 1990. Characteristics and novel features of thermostable alpha-amylase produced by *Bacillus licheniformis* M27 under solid-state fermentation. Starch. **42:** 233-238.

Robyt, J.F. 1989. Mechanism and Product Specificity of Alpha-Amylases. DEnpun Kagaku. **36:** 287-301.

Robyt, J.F., French, D. 1963. Action Pattern and Specificity of an Amylase from *Bacillus subtilis*. Archs. Biochem. Biophys. **100:** 451-467.

Robyt, J.F., French, D. 1970. The action pattern of porcine pancreatic α-amylase in relation to the substrate binding site of the enzyme. J. Biol. Chem. **245:** 3917-3927.

Saito, N. 1973. A Thermophilic Extracellular α-Amylase from *Bacillus licheniformis*. Archs. Biochem. Biophys. **155:** 290-298.

Sano, M., Sakano, Y., Kobayashi, T. 1985. Subsite structure and action mode of the α-amylase from *Thermoactinomyces vulgaris*. Agric. Biol. Chem. **49:** 2843-2846.

Schenck, F.W., Hebeda, R.E. 1992. Starch hydrolysis products. VCH, New York.

Seigner, C., Prodanov, E., Mouren, G.M. 1987. The determination of subsite binding energies of porcine pancreatic α-amylase by comparing hydrolytic activity towards substrates. Biochim. Biophys. Acta. **913:** 200-209.

Suganuma, T., Matsuno, R., Ohnishi, M., Hiromi, K. 1978. A study of the mechanism of action of Taka-amylase on linear oligosaccharides by product analysis and computer simulation. J. Biochem. **84:** 293-216.

Suganuma, T., Ohnishi, M., Hiromi, K., Nagahama, T. 1996. Elucidation of the subsite structure of bacterial saccharifying alpha-amylase and its mode of degradation of maltose. Carbohydr. Res. **282:** 171-180.

Svensson, B. 1994. Protein engineering in the alpha-amylase family: catalytic mechanism, substrate specificity, and stability. Plant. Mol. Biol. **25:** 151-157.

Thoma, J.A., Brothers, C.E., Spradlin, J.E. 1970. Subsite mapping of Enzymes. Studies on *Bacillus subtilis* Amylase. Biochemistry. **9:** 1768-1775.

Thoma, J.A., Rao, C.V., Brothers, C.E., Spradlin, J.E. 1971. Subsite mapping of Enzymes. Biochem. J. **246:** 5621-5635.

Thoma, J.A., Allen, J.D. 1976. Subsite mapping of enzymes: collecting and processing experimental data: a case study of an amylase-malto-oligosaccharide system. Carbohydr. Res. **48:** 105-124.

Torgerson, E.M., Brewer, L.C., Thoma, J.A. 1979. Subsite mapping of enzymes. Use of subsite map to simulate complete time course of hydrolysis of a polymer substrate. Archs. Biochem. Biophys. **196:** 13-22.

Violet, M., Meunier, J.C. 1989. Kinetic study of the irreversible thermal denaturation of *Bacillus licheniformis* alpha-amylase. Biochem. J. **263:** 665-670.

Chapter 5

Monte Carlo Simulation of the α-Amylolysis of Amylopectin Potato Starch

Part I: Modeling of the Structure of Amylopectin

L.M. Marchal, J. Zondervan, J. Bergsma, H.H. Beeftink, J. Tramper

submitted to Biotechnology & Bioengineering

Abstract

The branched structure of potato amylopectin (degree of polymerization ~ 200,000) was modeled in a computer matrix. The chain-length distribution, and the length and width of a cluster of the amylopectin molecule were used as input variables in the model. Independent literature values related to the structure of amylopectin (% β-hydrolysis and ratio of A to B chains) were used for evaluation of the branching characteristics (length of branch area and chance of branching) of the modeled amylopectin. The structural parameters predicted by the model agreed very well with data from literature. The chain-length distribution and values for the % of β-hydrolysis were the two most important parameters required to model the structure of amylopectin. This computer-generated model of potato amylopectin in solution can be used to simulate various enzymatic (i.e. α-amylase, β-amylase, glucoamylase, pullunanase) or chemical reactions (i.e. acid hydrolysis, hypochlorite oxidation). The modeling approach described in this paper is also suitable for starches from other botanical sources (i.e. corn, wheat, tapioca).

Introduction

One of the most occurring commercial enzyme processes is the (partial) hydrolysis of starch. The highly polymeric and heterogeneous nature of starch and products obtained after partial hydrolysis has restricted studies on hydrolysis severely. Most kinetic studies only express the decrease in number-averaged molecular weight during hydrolysis (Henderson and Teague, 1988; Rosendal et al., 1979; Yankov et al., 1986). However, during the hydrolysis of starch with an α-amylase for example, several hundreds to thousands of different saccharides (both branched and linear) make up this number-average mass. This saccharide composition depends on the botanical source of the starch, the type of α-amylase used, as well as on the process conditions. Since there is an increasing interest in the development of more tailor-made starch hydrolysis products with a defined saccharide composition, models are required that describe the complex kinetics of starch hydrolysis in more detail.

The hydrolysis of short-chain linear oligosaccharides with an α-amylase to all the possible products, using kinetic equations, has been described previously (Torgerson et al., 1979). However, the problem with this approach is the dramatic increase of the number of kinetic equations needed as the degree of polymerization of the substrate increases (see also Chapter 7). This originates from the fact that (above a degree of polymerization of 3) an α-amylase can hydrolyze a substrate to more then one product, each of which in turn is substrate for subsequent hydrolysis. Therefore, in this work an approach according to the Monte Carlo method was chosen to model the mixture of saccharides produced during the hydrolysis of starch. Previously reported studies using a Monte Carlo type of simulation to describe the hydrolysis of starch components used highly simplified amylopectin structures, which permitted the prediction of very short linear oligosaccharides only (Nakatani, 1996; Nakatani, 1997; Toner and Potter, 1977). The first step taken here is to model the substrate as best as one can within the framework of the actual knowledge of the structure of starch (this chapter). The structure of potato amylopectin is modeled in a computer matrix according to the generally accepted cluster model. Variable chain lengths

and α(1→6)-branchpoints are incorporated and the model is evaluated with other literature values for the structure of amylopectin. The resulting computer model of amylopectin in solution can then be used to simulate hydrolysis by α-amylase, or other enzymatic or chemical reactions (Chapter 7).

Theory

Good reviews on the structure of amylopectin, and the various analytical methods used to determine its structure, have recently been given by (Buleon et al., 1998; Hizukuri, 1996). Therefore, only a synopsis of structural aspects, relevant to this study, is given here.

General structure

Amylopectin is a branched macromolecule in which linear chains of (1→4)-α-linked D-glucose residues are linked by (1→6)-α-D-glucosidic linkages to form a branched structure, as schematically illustrated in Figure 1.

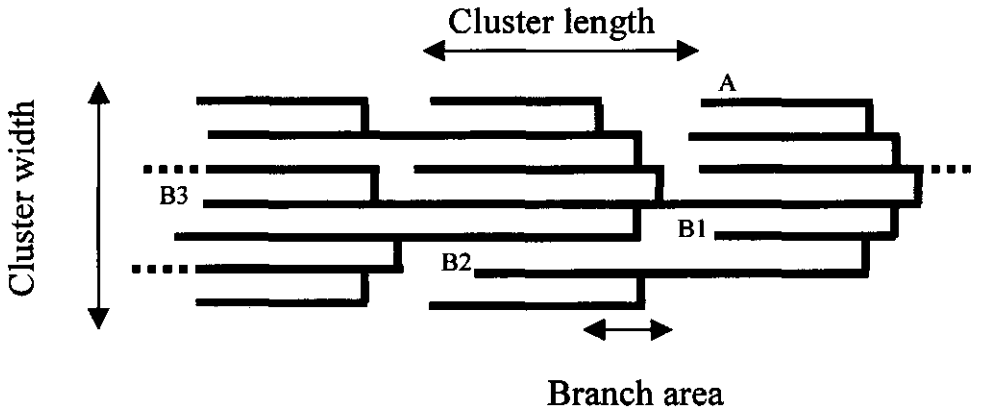

Figure 1: A schematic representation of a small part of the amylopectin structure. A = unsubstituted chain; B = chain substituted by at least one other chain. The reducing end of the amylopectin is situated to the far right hand side of the polymer. See text for further details.

Potato amylopectin is modeled according to the generally accepted cluster model (Buleon et al., 1998; Hizukuri, 1996; Manners, 1989; Manners and Matheson, 1981; Zhu and Bertoft, 1996), in which clusters of chains constitute the basic unit of the macromolecule. Two main groups of chains have been defined, namely A-chains (unsubstituted) and B-chains (substituted by other chains). The B-chains show a high variation with respect to the degree of polymerization, spanning on average one cluster (B1), two clusters (B2), three clusters (B3), etc. In this model a tetramodal distribution of the B chains B1-B4 as determined by Hizukuri (1986) is assumed.

Chain-length distribution

The chain-length distribution of amylopectins can be established after enzymatic debranching. Hizukuri (1986) used gel chromatography with a combined low-angle laser-light-scattering photometer and a differential refractometer detection system to determine the total amount of chains in the clusters. However, the exact number of each chain, with a certain degree of polymerization (DP), is not established with this method. Individual chains up to a degree of polymerization of around 80 can be identified on a molar basis using a high-performance anion-exchange chromatography with a pulsed amperometric detector (HPAEC-PAD) (Hanashiro et al., 1996). The problem with this method is however that the detector response is not constant for individual chains, so that only qualitative results are obtained. Koizumi et al. (1991) determined the quantitative amount of the individual chains using adequate calibration standards, but only up to a degree of polymerization of 17. Oshea and Morell (1996) determined the chain-length distribution of potato amylopectin on a molar basis up to a DP of 62, using a DNA sequencer with tagged oligosaccharides. The number-average chain length (CL_n) of amylopectin calculated from this distribution is 20, which is lower than the CL_n of around 24 established by various other techniques (Hizukuri, 1996; Hizukuri and Abe, 1993; Nilsson et al., 1996). There are two reasons for this lower CL_n, making a correction possible:

1) Debranched potato starch consists of neutral chains and chains containing an esterified phosphate group (P-chains) (Hizukuri and Abe, 1993). Since Oshea and Morell (1996) used a mixed-bed ion-exchange resin to desalt debranched potato amylopectin, most likely only the distribution of the neutral chains was determined (Hanashiro et al., 1996; Takeda and Hizukuri, 1981). Although the amount of the P-chains is low, the average chain-length of these P-chains (42.2) is higher than the average chain-length of the neutral chains (22.7) (Hizukuri and Abe, 1993). This leads to an underestimation of the longer B2 chains as compared to the shorter A and B1 chains.
2) The chains analyzed (up to DP 62) are the A, B1, and B2 chains in potato amylopectin. The longer B3 and B4 chains are excluded from the analysis. This leads to an underestimation of the average chain length.

The data provided by Oshea and Morell (1996) is corrected for these two phenomena described above with the data on P-chains (Hizukuri and Abe, 1993) and the ratios between the different B-chains (Hizukuri, 1986). Figure 2 gives the resulting chain-length distribution. The chain-length distribution used in the present model thus is a combination of the information available in literature on the distribution of the individual chains with a degree of polymerization up to around 60 combined with the more overall distribution over a wider degree of polymerization. A minimum chain length of 6 and the characteristic "dip" for potato amylopectin with degree of polymerization of 8 has been observed by several authors (Hanashiro et al., 1996; Koch et al., 1998; Koizumi et al., 1991; OShea and Morell, 1996).

It should be noted that the chain-length distribution as determined by various authors gives an average value for starches from one botanical source (i.e. potato starch). Starches are harvested as solid granules with a range of diameters. For potato starch the diameter range of starch granules normally lies between 5 and 100 μm (Snyder, 1984; Swinkels, 1985). Jane and Shen (1993) showed that amylopectin in small granules (<20 μm) has a longer average chain length than amylopectin from larger granules (>52 μm). Furthermore, it was

shown that amylopectin in the core of a starch granule has significantly longer B-chains as compared to the amylopectin at the periphery.

In the studies mentioned above on the chain-length distribution of amylopectin, starch (the complete range of granules) is dissolved, and an average chain-length distribution is thus determined. Besides this, it is known that starches from different potato varieties show somewhat different chain-length distributions (Blennow et al., 1998). It should be noted however, that despite the variations mentioned here, the overall pattern of the chain-length distribution is relatively constant.

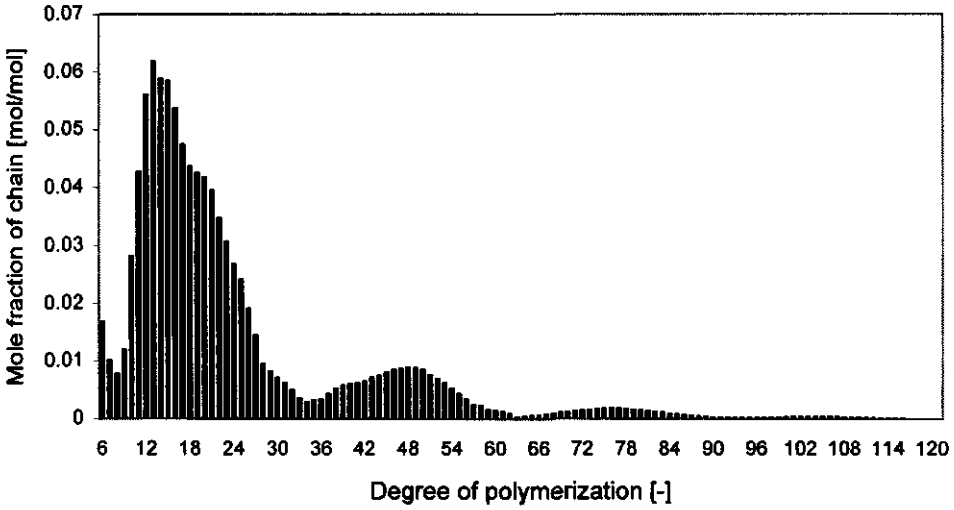

Figure 2: The distribution of the linear chains of amylopectin used in the model. The x-axis gives the degree of polymerization of the individual chains; the y-axis gives the corresponding mol fraction of these chains. The number-average chain length is 23.98.

Clusters

The length of each cluster (see Figure 1), as determined by the chain-length distribution after debranching (Hizukuri, 1986; OShea and Morell, 1996), is 27 glucose units on average. Variations in cluster lengths between 25 and 29 glucose units on the model predictions are also evaluated. The cluster width is estimated to be around 30 glucose units (Gallant et al., 1997; Yamaguchi et al., 1979) and since this value originates from a rather uncertain range, the influence on the model predictions of a width of 20 and 40 glucose units is also evaluated.

Branching characteristics

If a glucose unit is (1→6)-α-branched, then the adjacent glucose units are not capable of branching. The cluster model assumes that the branching occurs in the beginning of each cluster (see Figure 1). There is no direct information on the length or the distribution of these branch points within the branch area. However, literature data on the % of hydrolysis of amylopectin with a β-amylase can be used as follows. A β-amylase releases maltose (DP_2) starting from the non-reducing ends of the amylopectin and is not capable to cleave or bypass the (1→6)-α-D-glucosidic linkages. So the % of hydrolysis of amylopectin with a β-amylase is related to the branching characteristics of the polymer (see Figure 1) and is used to evaluate the influence of the length of the branching area and the chance of branching within this branching area on the predicted amylopectin structure.

Phosphate groups

About one in every 200 to 300 glucose units contains a naturally occurring phosphate group (Hizukuri, 1996), which is esterified for 60-70% to the C-6 position of glucose units, the remaining at the C-3 position. There is some controversy in the literature on the location of these phosphate groups. Radomski and Smith (1963) reported that the phosphate group is located close to the branch points, whereas Takeda and Hizukuri (1982) suggested that the phosphate group is located statistically near the center of the unit chain

and more than nine glucosyl residues separated from a branch point. Since the location of these phosphate groups is not clear and the degree of substitution low, they are not included in this model.

To sum up: literature values for chain-length distribution, cluster length and width are used as input parameters in this model. Other literature values related to the structure of amylopectin (i.e. % β-hydrolysis and A/B chain ratio) are used to evaluate the model predictions.

Modeling

The information on the structure of amylopectin as described above has to be translated into a computer model. The model, which is specifically developed for this purpose, is written in Borland Delphi 3.0 for Microsoft Windows.

Dimensions of the matrix

Information on the three-dimensional structure of amylopectin in solution is scarce. The best approximation of the structure of amylopectin in a concentrated solution seems to be a random coil type (like a plate of spaghetti), enabling interactions between chains far apart in a two-dimensional representation. Hydrolytic enzymes (i.e. α-amylases, β-amylases) are assumed to encounter the individual chains in solution at random. Since a random type of attack does imply no preference for specific chains this means that for modeling purposes amylopectin can be modeled in a two dimensional matrix, like drawing the structure on a piece of paper as in Figure 1.

Buildup procedure

Figure 3 shows the flow sheet of the general buildup procedure used to model the structure of amylopectin, in which issues between [ ] denote processes, < > decisions, and [ ] loops. Several aspects of this flow sheet will be discussed in more detail. The procedure starts

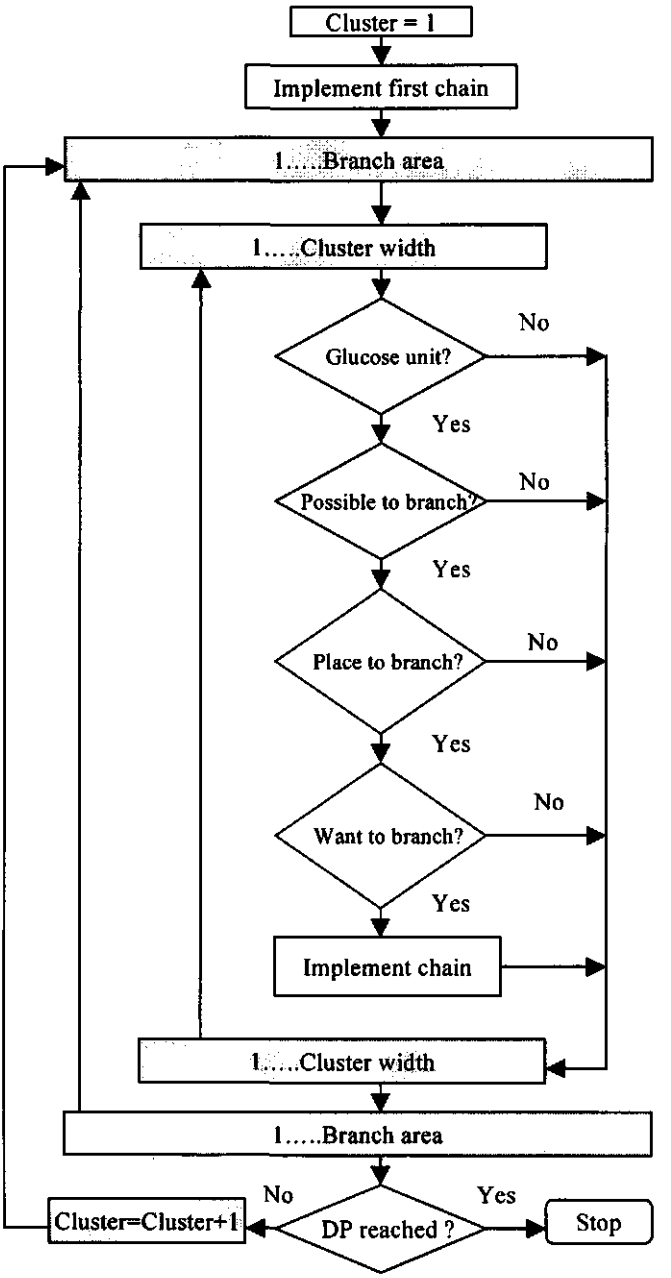

Figure 3: The flow sheet of the general procedure to model the amylopectin structure in a matrix. See text for details.

with implementing a first chain in the matrix [Implement first chain]. Within each new cluster there are two main loops [1 ...Branch area] and [1 ...Cluster width]. The loop starts always at the first position in each new branch area (see Figure 4). If there is a glucose unit at that position in the matrix <glucose unit?>, it is determined if it would be possible to branch this glucose unit <possible to branch ?>. If the glucose unit adjacent to this glucose unit in the chain is already branched, this is not possible (Hizukuri, 1996). If it is possible to branch this glucose unit, it is checked whether there is still space <Place to branch?> to place an additional chain in the cluster, or that the total cluster width is already occupied with other chains. Whether this glucose unit is now actually branched <Want to branch?> depends on the chance of branching set in the model. If the chance of branching is set to 1, every time when it is possible to branch, the glucose unit is branched. If the chance of branching is set to for example 0.5, only 50% of the time, the glucose unit is actually branched. If it is decided to branch the chain at this glucose position, a new chain (with a certain degree of polymerization) is selected at random. The chance of selection is proportional to its molar fraction as given in Figure 2. This chain is added to the amylopectin molecule and the matrix is adjusted accordingly [Implement chain]. The inner loop [1 ...Cluster width] repeats until the width of the cluster is reached (30 in the example in Figure 4). After completion of all the first positions of the branch area, the loop moves to the next position of the branch area. The inner loop [1 ...Cluster width] is again repeated etc, until the end of the branch area is reached (8 positions in the example in Figure 4).

Upon completion of each cluster (thus after checking all the positions within the branch area), the model moves to the next cluster in the matrix [cluster = cluster+1] until the desired degree of polymerization is reached <DP reached?>, which was set here to ≈ 200,000 (Aberle et al., 1994; Hizukuri, 1996; Manners and Matheson, 1981). Since the buildup procedure is a random phenomenon, it is possible that there is no chain in the next cluster considered. The buildup procedure of amylopectin then stops before the desired degree of polymerization is reached (auto termination). The probability of auto termination is obviously correlated to the branching characteristics used in the model (i.e. branch area,

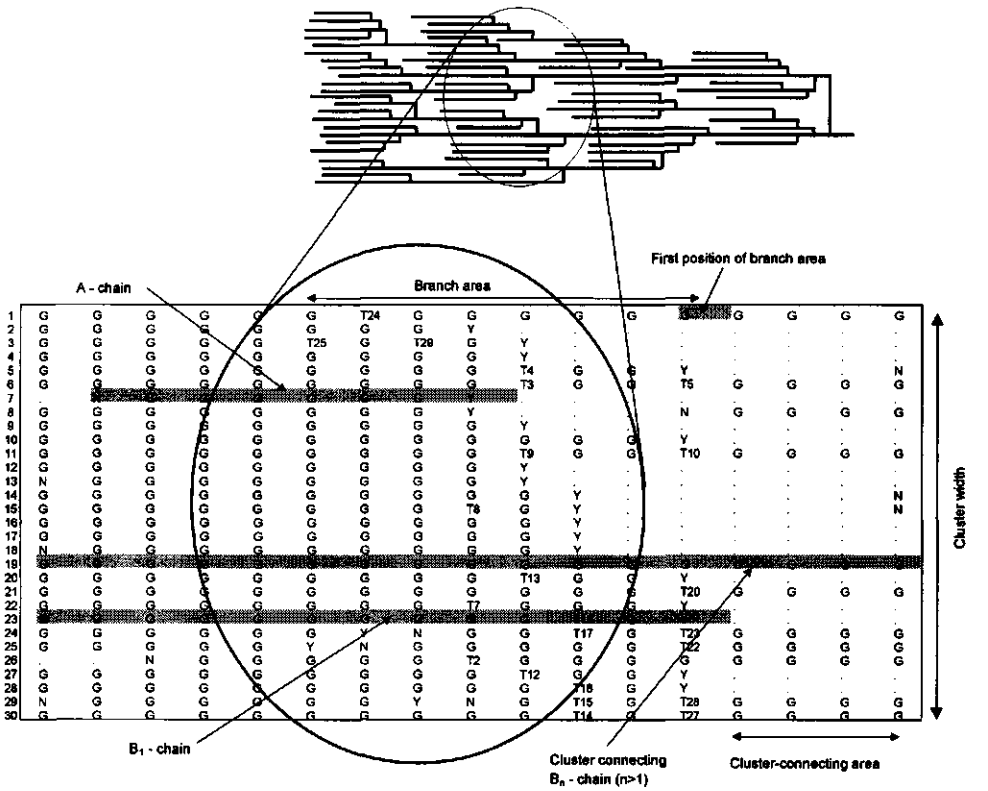

Figure 4: Visual representation of part of the matrix in which the amylopectin is built. Nomenclature of the glucose units: G: α(1→4) linked; N: α(1) linked (non-reducing end); Y: α(1→4) linked to a branch point (6); T: α(1,4,6) linked, the number behind T is the position of the row where the glucose unit lies to which the 6 position is linked; R (not visible in matrix): α(4) linked (reducing end).

chance of branching). When the buildup procedure stops before the desired degree of polymerization is attained, more molecules are build until the total desired degree of polymerization of 200,000 is reached. Of course, it is also possible to repeat the buildup procedure until the desired degree of polymerization is attained with only one molecule.

The necessity of the latter depends on the intended application of the model. If the high-molecular-weight distribution (say above a DP of 10,000) in the initial phase of the hydrolysis has to be simulated this is a prerequisite, since simulation of high-molecular-weight saccharides requires substrates with (much) higher molecular weight. If the simulation focuses on the production of the lower-molecular-weight products (say up a degree of polymerization of 1000), this is not required. After completion of the buildup procedure, the % of β-hydrolysis and the ratio of A to B chains of the amylopectin molecule built are determined. By comparing these with literature values the influence of various model parameters can be investigated.

Results and discussion

General structure

The modeled amylopectin structure was in accordance with the visual representation as given by several authors (Hizukuri, 1996; Manners, 1989; Manners and Matheson, 1981; Zhu and Bertoft, 1996). Figure 4 gives a small fraction of a built amylopectin matrix as an example. The branch area, cluster width, and cluster-connecting area are indicated with arrows. For ease of interpretation one A and one B chain, and one cluster connecting B-chain are highlighted in the matrix. The coding used in the matrix to describe the various glucose units in the amylopectin structure is described in the legend of Figure 4.

Accuracy of the model buildup procedure

Experimentally determined values, for example the chain-length distribution, % β-hydrolysis, or A to B ratio are based on a large number of molecules. Even when a limited amount of a starch (for example a typical 50 µl injection volume of a 1% [w/w] debranched-starch solution with a CL_n of 24) is taken, this analysis sample already consists of a large number of molecules:

$$\text{number of molecules} = \frac{g}{M_n} N_A = \frac{50.10^{-6} \times 10}{(24 \times 162 + 18)} 6.10^{23} \approx 8.10^{16}, \qquad (1)$$

in which N_A is the number of Avogadro [mol^{-1}], M_n is the number-average molecular weight [$g.mol^{-1}$], and g is the weight [g] of the sample considered. Simulating such a tremendous number of molecules is highly impractical. Although this situation can be approximated using a fraction of this number, there will always be a deviation from the actual (average!) value. A good criterion to test whether the size of the population (= size of amylopectin considered times the number of buildup simulations) is large enough to be considered representative is the standard deviation of an input parameter, such as the average chain length. The standard deviation predicted by the model is less then 1% of its actual value (used as an input parameter in this model). When the average of 5 simulations is taken this value decreases below 0.3% and after 10 simulations the standard deviation becomes less then 0.23% of the average value. These standard deviations can be regarded as very low. Similar results are obtained if the size of the modeled amylopectin is increased instead of the number of simulations. In general, the accuracy of a Monte Carlo simulation is proportional to $N^{-½}$, with N the number of simulations considered (Bruns et al., 1981), implying that a ten-fold increase in model accuracy requires a 100-fold increase of the number of simulations. During the structural evaluation of branch area and probability of branching an average of 5 buildups is taken.

Evaluation of branch area and chance of branching

The two model parameters branch area and chance of branching, on which little information is available, are evaluated using the independent output parameters % β-hydrolysis and A/B ratio. Figure 5 gives the influence of branch area and chance of branching on the value of % β-hydrolysis in a contour plot.

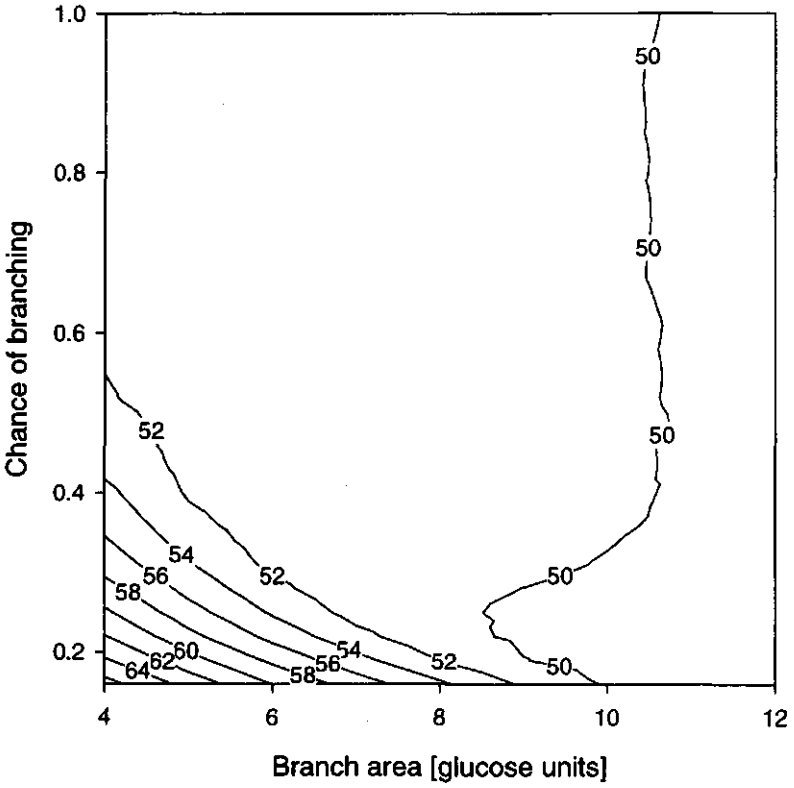

Figure 5: Contour plot describing how the % of β hydrolysis (contour lines) depends on branch area (x-axis) and chance of branching (y-axis). Other model parameters: cluster length 27, cluster width 30.

The branch area is varied between 4 and 12 glucose units long. The chance of branching is varied between 1 (branch always if possible) and 0.15 (branch in 15% of the possible branch positions). Most of the values reported in literature for the % of β-hydrolysis were previously shown to be slightly overestimated due to hydrolytic gain being unaccounted for (chapter 6). Since the % of β-hydrolysis is used here to distinguish between differences in chemical structure of the modeled amylopectin, this non-linear overestimation of the actual

% of β-hydrolysis has to be corrected for. The corrected values for % β-hydrolysis range from 51 to 56 (Table I), with an average of 54 %.

Table I: Literature values for the % of hydrolysis of potato amylopectin with a β-amylase. If available; also the botanical source of the amylopectin is given. The corrected values for the % of β-hydrolysis (Marchal and Tramper, 1999) are given with one additional decimal to minimize further deviations.

Botanical Source	β-hydrolysis	Corrected β-hydrolysis	Reference
Epicure	57	55.7	Banks and Greenwood, 1959
Redskin	57	55.7	Banks and Greenwood, 1959
Golden wonder	56	54.7	Peat et al., 1956
	51.5	50.15	Peat et al., 1956
Red Star	55	53.7	Bathgate and Manners, 1966
	56	54.7	Hizukuri and Abe, 1993
	56	54.7	Hizukuri, 1996
Pentland Crown	53	51.7	Geddes et al., 1965
	56	54.7	Bender et al., 1982
Bintje	52.5	51.15	Thorn and Mohazzeb, 1990

As can be seen from Figure 5, all values for the % of β-hydrolysis reported in literature can be constructed using various combinations of branch area and chance of branching. The reported values in literature for the ratio of A to B chains for potato starch are in the range 0.8-1.3 (Bender et al., 1982; Hizukuri, 1986; Manners, 1989). For all the combinations of branch area and chance of branching investigated, the predicted A to B chain ratio (contour plot Figure 6) is in accordance with the range cited in literature. Hizukuri (1996), however, showed that actually, due to inaccuracies in the methods used to determine the ratio of A to B chains, these ratios should only be interpreted as around 1. All combinations of branch area and chance of branching in this model gave an A/B ratio of around 1.

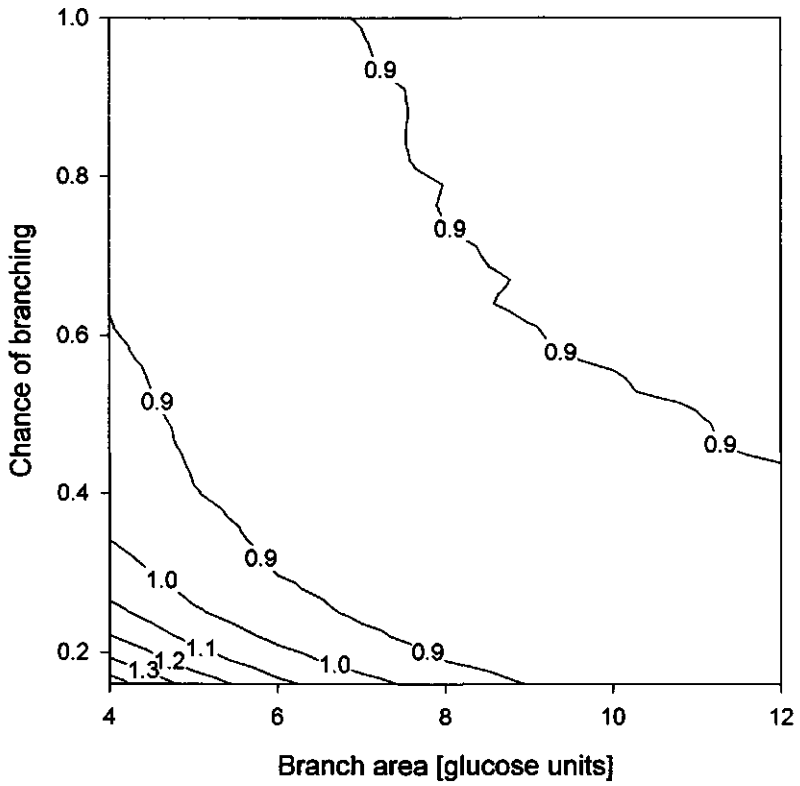

Figure 6: Contour plot describing how the ratio of A to B chains (contour lines) depends on branch area (x-axis) and chance of branching (y-axis). Other model parameters: cluster length 27, cluster width 30.

This means that the A to B chain ratio does not impose additional restrictions (other then already enforced by the % of β-hydrolysis) to the branch area and chance of branching. Since amylopectin is known to consist of heavily and sparsely branched regions (Bender et al., 1982; Bertoft, 1991; Geddes et al., 1965; Hizukuri, 1996; Hizukuri and Maehara, 1991; Jane and Shen, 1993; Zhu and Bertoft, 1996) the values for the % of β-hydrolysis in Table I should be interpreted as averages. So the best approximation of actual amylopectin is obtained by varying the branching characteristics of the modeled amylopectin. By varying

the branching characteristics for different clusters within the amylopectin molecule built, a molecule with the desired branch distribution can be constructed.

Cluster length and width

The sensitivity of the model predictions towards the two literature parameters (length and width of an individual cluster) was evaluated. The length of a cluster (literature value 27) was varied between 25 and 29 glucose units (in steps of 1). This did not lead to dramatic changes in predicted values for % β-hydrolysis and ratio of A to B chains. The overall shape of the contour plots of the chance of branching and branch area on the model-predicted % of β-hydrolysis and A to B ratio remains unchanged. Table II summarizes these 8 contour plots and gives for these cluster lengths (25-29) the average deviation in % of β hydrolysis and ratio A to B chains from the values for a cluster length of 27 glucose units.

Table II: Deviation (from a cluster length of 27) in the model-predicted % of β-hydrolysis and ratio of A to B chains for other lengths of a cluster (25 to 29 glucose units). The chance of branching was varied between 0.15 and 1 (steps of 0.01), and the branch area between 4 and 12 glucose units. The width of the cluster was set to 30 glucose units. The value –1.68 for example means that the model-predicted % of β-hydrolysis, for a certain combination of branch area and chance of branching, is on average 1.68 lower as compared to the value predicted for the same branch characteristics at a cluster length of 27 glucose units.

Cluster length	25	26	28	29
Deviation in %β-hydrolysis	-3.49	-1.68	1.29	2.17
Deviation in A/B ratio	4.08×10^{-4}	-1.38×10^{-3}	6.43×10^{-3}	1.16×10^{-2}

In general, with the same branching characteristics (chance of branching and branch area), a higher cluster length leads to a small increase in the % of β-hydrolysis and a lower cluster length leads to a small decrease. The influence of cluster length on the ratio of A to B chains is very small. The influence of the width of a cluster (varying between 20 and 40 glucose units) on the % of β-hydrolysis and ratio A to B chains is even smaller then that of

the length of a cluster (results not shown). So the model predictions are not very sensitive to the relative inaccuracy of the value for the width of an individual cluster (around 30 glucose units).

The chain-length distribution and values for the % of β-hydrolysis are therefore the most important parameters required in modeling the structure of an amylopectin molecule.

Conclusion

For the first time in literature the complete branched structure of amylopectin was modeled in a computer matrix. The structural parameters predicted from the model (% β-hydrolysis and A/B ratio) agree well with values from literature, thus indicating the validity of the model within the framework of the actual scarce knowledge of the amylopectin structure. Since chain-length distributions and % of β-hydrolysis of starches of other crops (i.e. corn, wheat, and tapioca) are also available, it is relatively simple to model their structure in a similar way. Incorporation of the slightly branched long amylose chains alongside the amylopectin in the matrix would make it feasible to simulate also regular starch (which consists for about 80% of amylopectin and the remainder of amylose). This computer model of amylopectin in solution can be used to simulate all kinds of enzymatic (i.e. α-amylase, β-amylase, glucoamylase, pullulanase) or chemical reactions (i.e. acid hydrolysis, hypochlorite oxidation). In part II of this article this is demonstrated by evaluation of the saccharides produced upon α-amylolysis of potato amylopectin.

Acknowledgements

The authors thank Avebe and the Dutch Ministry of Economic Affairs (PBTS-Biotechnology Project No. BIO94043) for funding of this research.

References

Aberle, T., Burchard, W., Vorwerg, W., Radosta, S. 1994. Conformational Contributions of Amylose and Amylopectin to the Structural Properties of Starches from Various Sources. Starch. **46:** 329-335.

Banks, W., Greenwood, C.T. 1959. Physicochemical studies on starches. Part XX. The existence of an anomalous amylopectin in starch. J. Chem. Soc. 3436-3439.

Bathgate, G.N., Manners, D.J. 1966. Mutiple Branching in Glycogens. Biochem. J. **101:** 3c-5c.

Bender, H., Siebert, R., Stadler-Szöke, A. 1982. Can cyclodextrin glycosyltransferase be useful for the investigation of the fine structure of amylopectins?: characterisation of highly branched clusters isolated from digests with potato and maize starches. Carbohydr. Res. **110:** 245-259.

Bertoft, E. 1991. Investigation of the fine structure of alpha-dextrins derived from amylopectin and their relation to the strcuture of waxy-maize starch. Carbohydr. Res. **212:** 229-244.

Blennow, A., Bay-Smidt, A.M., Wischmann, B., Olsen, C.E., Moller, B.L. 1998. The degree of starch phosphorylation is related to the chain length distribution of the neutral and the phosphorylated chains of amylopectin. Carbohydr. Res. **307:** 45-54.

Bruns, W., Motoc, I., and O'Shea, G.K. 1981. Monte Carlo applications in polymer science. Springer-Verlag, Berlin.

Buleon, A., Colonna, P., Planchot, V., Ball, S. 1998. Starch granules: structure and biosynthesis. International Journal of Biological Macromolecules. **23:** 85-112.

Gallant, D.J., Bouchet, B., Baldwin, P.M. 1997. Microscopy of starch: evidence of a new level of granule organization. Carbohydrate Polymers. **32:** 177-191.

Geddes, R., Greenwood, C.T., Mackenzie, S.L. 1965. Studies on the biosynthesis of starch granules.Part III: The properties of the components of starches from the growing potato tuber. Carbohydr. Res. **1:** 71-82.

Hanashiro, I., Abe, J., Hizukuri, S. 1996. A periodic distribution of the chain length of amylopectin as revealed by high performance anion-exchange chromotography. Carbohydr. Res. **283:** 151-159.

Henderson, W.E., Teague, W.M. 1988. A kinetic model of *Bacillus stearothermophilus* alpha-amylase under process conditions. Starch. **40:** 412-418.

Hizukuri, S. 1986. Polymodal distribution of the chain lengths of amylopectins, and its significance. Carbohydr. Res. **147:** 342-347.

Hizukuri, S. 1996. Starch:Analytical Aspects, pp.347-429.In: Eliasson AC (eds.), Carbohydrates in food, Marcel Dekker, inc., New York.

Hizukuri, S., Abe, J. 1993. A new method of enzyme analysis of amylopectin structure, pp.16-25.In: Meuser F, Manner DJ, and Seibel W (eds.), Plant Polymeric Carbohydrates, Royal Society of Chemistry, Cambridge.

Hizukuri, S. and Maehara, Y.1991 Distribution of the Binding of A chains to a B chain in Amylopectins. pp.212-218.In: Friedman, R.B., editor. ACS symposium **458** American Chemical Society, Washington.

Jane, J.L., Shen, J.J. 1993. Internal structure of the potato starch granule revealed by chemical gelatinization. Carbohydr. Res. **247:** 279-290.

Koch, K., Andersson, R., Aman, P. 1998. Quantitative analysis of amylopectin unit chains by means if high performance anion-exchange chromatography with pulsed amperometric detection. Journal of Chromatography A. **800:** 199-206.

Koizumi, K., Fukada, M., Hizukuri, S. 1991. Estimation of the distribution of chain length of amylopectin by high-performance liquid chromatography with pulsed amperometric detection. J. Chromatogr. **585:** 233-238.

Manners, D.J. 1989. Recent Developments in Our Understanding of Amylopectin Structure. Carbohydrate Polymers. **11:** 87-112.

Manners, D.J., Matheson, N.K. 1981. The fine structure of amylopectin. Carbohydr. Res. **90:** 99-110.

Marchal, L.M., Tramper, J. 1999. Hydrolytic gain during hydrolysis reactions; implications and correction procedures. Biotechnol. Tech. **13:** 325-328

Nakatani, H. 1996. Monte Carlo simulation of multiple attack mechanism of α-amylase. Biopolymers. **39:** 665-669.

Nakatani, H. 1997. Monte carlo simulation of multiple attack mechanism of beta-amylase-catalyzed reaction. Biopolymers. **42:** 831-836.

Nilsson, G.S., Bergquist, K.E., Nilsson, U., Gorton, L. 1996. Determination of the degree of branching in normal and amylopectin type potato starch with 1H-NMR spectroscopy. Starch. **48:** 352-357.

OShea, M.G., Morell, M.K. 1996. High resolution slab gel electrophoresis of 8-amino-1,3,6- pyrenetrisulfonic acid (apts) tagged oligosaccharides using a dna sequencer. Electrophoresis. **17:** 681-686.

Peat, S., Whelan, W.J., Thomas, G.J. 1956. The enzymatic synthesis and degradation of starch. Part XXII. Evidence of multiple branching in waxy-maize starch. A correction. J. Chem. Soc. 3025-3030.

Radomski, M.W., Smith, M.D. 1963. Location and possible role of esterified phosphorus in starch fractions. Cereal. Chem. **40:** 31-38.

Rosendal, P., Nielsen, B.H., Lange, N.K. 1979. Stability of bacterial alpha-amylase in the starch liquefaction process. Starch. **31:** 368-372.

Snyder, E.M. 1984. Industrial microscopy of starches, pp.661-673.In: Whistler RL, Bemiller JN, and Paschall EF (eds.), Starch chemistry and technology, 2nd: Academic press, Orlando.

Swinkels, J.J.M. 1985. Composition and properties of commercial native starches. Starch. **37:** 1-5.

Takeda, Y., Hizukuri, S. 1981. Re-examination of the action of sweet potato beta-amylase on phosphorylated (1-4)-α-D-glucan. Carbohydr. Res. **89:** 174-178.

Takeda, Y., Hizukuri, S. 1982. Location of phosphate groups in potato amylopectin. Carbohydr. Res. **102:** 321-327.

Thorn, W., Mohazzeb, S. 1990. Molecular weights, lengths, and distribution of side-chains in alpha-D-polyglucanes. Starch. **42:** 373-376.

Toner, M.C., Potter, O.E. 1977. Computer simulation of the beta-amylolysis of starch components. Journal of the Institute of Brewing. **83:** 78-81.

Torgerson, E.M., Brewer, L.C., Thoma, J.A. 1979. Subsite mapping of enzymes. Use of subsite map to simulate complete time course of hydrolysis of a polymer substrate. Archs. Biochem. Biophys. **196:** 13-22.

Yamaguchi, M., Kainuma, K., French, D. 1979. Electron Microscopic observations of waxy maize starch. Ultrastruct. Res. **69:** 249-261.

Yankov, D., Dobreva, E., Beschkov, V., Emanuilova, E. 1986. Study of optimum conditions and kinetics of starch hydrolysis by means of thermostable alpha-amylase. Enzyme Microb. Technol. **8:** 665-667.

Zhu, Q., Bertoft, E. 1996. Composition and structural analysis of alpha-dextrins from potato amylopectin. Carbohydr. Res. **288:** 155-174.

Chapter 6

Hydrolytic Gain during Hydrolysis Reactions: Implications and Correction Procedures

L.M. Marchal and J. Tramper

Biotechnology Techniques (1999), **13**, 325-328

Abstract

Some of the structural parameters of starch (i.e. % beta- or gluco-hydrolysis) were influenced by the increase in mass during the hydrolysis reactions (hydrolytic gain). Procedures were derived to correct this apparent % of hydrolysis to actual % of hydrolysis. These analytically derived equations are not only valid for the hydrolysis of starch but also for the hydrolysis of lower molecular weight saccharides (e.g. α-limit dextrin). With a small modification, these equations can be used to correct for hydrolytic gain which occurs during the hydrolysis of other (bio)polymers.

Introduction

During the hydrolysis of starch the cleavage of each glycosidic linkage results in the net addition of one molecule of water, thus increasing the mass of the solute (hydrolytic gain). This addition is not negligible. When, for example 162 g starch is totally converted to its monomers (dextrose), the dry mass of the solute increases by some 11% to 180 g. The partial hydrolysis of amylopectin and amylose (both components of starch), using various enzymes (i.e. β-amylase, glucoamylase), is widely used to determine structural parameters of these molecules. It is shown that the hydrolytic gain influences these values. Previously relations were derived which describe the dry-weight increase during hydrolysis as a function of dextrose equivalent, degree of polymerization, or mean-average molecular

weight (Marchal et al., 1996). In this paper, relations are derived for the hydrolytic gain as a function of both the % of glycosidic linkages hydrolyzed and the % of monomers liberated from the starting material. Furthermore a correction equation to convert the reported apparent % of hydrolysis to the actual % of hydrolysis is presented.

Method

In this article no materials but analytically derived equations are used. The following abbreviations, which definitions are explained in the text for reasons of clarity, are used in these calculations.

CL	=	chain length	[-]
DE	=	dextrose equivalent	[-]
DP_n	=	degree of polymerization (n)	[-]
DP_x	=	degree of polymerization liberated oligomer (x)	[-]
HG	=	hydrolytic gain	[g/g]
ICL	=	inner chain length	[-]
M_n	=	number-average molecular weight	[g/mol]
M_x	=	molecular weight of saccharide (x)	[g/mol]
n_x	=	amount of saccharide (x)	[mol]
OCL	=	outer chain length	[-]

Results and discussion

Implications of hydrolytic gain

The implications of hydrolytic gain can be illustrated as follows. Consider the hydrolysis of 162 g of amylopectin (degree of polymerization of 1.10^5) with a β-amylase to the extent where 50% of the glucose units are split off (as maltose). This will yield 81 g branched, high molecular mass carbohydrate and 81x(342/324)=85.5 g of maltose. The number-

average molecular weight (M_n) of the hydrolyzate is now (n_x=amount (moles) of saccharide; M_x= molecular weight of saccharide):

$$M_n \equiv \frac{n_1 M_1 + n_2 M_2}{n_1 + n_2} = \frac{0.25 \times 342 + 1.10^{-5}(162 \times 1.10^{5} \times 0.5)}{0.25 + 1.10^{-5}} = 666. \quad \left[\frac{g}{mol}\right] \qquad (1)$$

In literature several methods are described to determine the % β-amylolysis after complete hydrolysis of starch with a β-amylase. In general, two categories of methods are used:

1) Determination of the weight percentage of maltose in the hydrolyzate by chromatographic methods (Bender et al., 1982; Bertoft, 1989a). The % of β-hydrolysis is calculated by dividing the peak area of maltose by the total amount of carbohydrates [g/g]. In our example this would yield a % β-amylolysis of 85.5/(81+85.5)×100% = 51.35%.
2) Determination of the mean number-average molecular weight by titration methods (dextrose equivalent) or enzymatic methods (Banks and Greenwood, 1959; Bathgate and Manners, 1966; Bertoft, 1989b; Hizukuri and Abe, 1993; Peat et al., 1956; Thorn and Mohazzeb, 1990). The % of β-amylolysis is then given by (DE hydrolysate/DE maltose) or (M_n maltose/M_n hydrolysate). Both expressions are equivalent since the DE is defined as (180/M_n hydrolysate)×100. In our example both expressions yield a % β-amylolysis of 51.35%.

Therefore, in both examples the % of actual hydrolysis is overestimated by 1.35% due to the hydrolytic gain, and a higher apparent % of hydrolysis is determined. This has several implications. The % of β-amylolysis is for example used to calculate several structural parameters of amylopectin. Amylopectin is a branched macromolecule in which linear chains of about 24 (1→4)-α-linked D-glucose residues on average are linked by (1→6)-α-D-glucosidic linkages to form a branched structure as schematically illustrated in Figure 1. Two main groups of chains in amylopectin have been defined, namely A-chains (unsubstituted) and B-chains (substituted by other chains). A β-amylase releases maltose

(DP_2) starting from the non-reducing ends of the amylopectin and is not capable to cleave or bypass the (1→6)-α-D-glucosidic linkages.

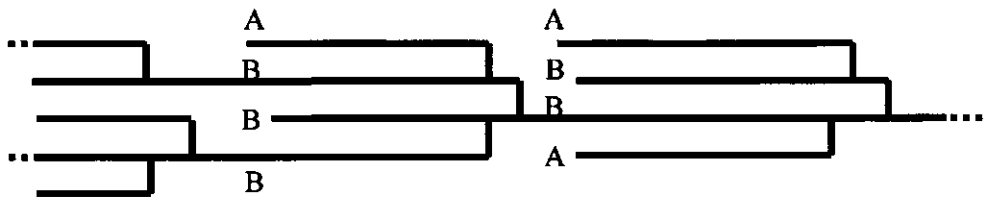

Figure 1: A schematic representation of a small part of the amylopectin structure. A = unsubstituted chain, B = chain substituted by at least one other chain. The reducing end of the amylopectin is situated to the right hand side of the polymer.

The total amount of maltose units released starting from the non-reducing end of a chain depends on the type of chain (A or B) and the number of glucose units (odd or even) in the chain. After hydrolysis with a β-amylase there are one (odd) or two (even) glucose units left connected to an A-chain and two (even) or three (odd) glucose units left connected to a B-chain. The % of β-amylolysis is used to calculate the average chain length of the outer chains (OCL) of the amylopectin according to (Hizukuri, 1996):

$$OCL = (\%\ \beta\text{-hydrolysis}) \times CL + 2\,, \qquad (2)$$

where CL is the average chain length of the amylopectin chains and the number 2 is the average amount of glucose units left connected to a (1→6)-linkages after β-amylolysis (assuming an A/B ratio of 1 and an equal amount of odd and even chains).

An overestimation of the % of β-amylolysis leads thus to an overestimation of the value for the outer chain length. In our example of 50% hydrolysis of amylopectin (taking an average chain length of 24), this leads to an overestimation of the OCL with 0.324 glucose units.

Another parameter related to this is the average inner chain length (ICL), which is defined as (Hizukuri, 1996):

$$ICL \equiv CL - OCL - 1. \qquad (3)$$

The overestimation of the OCL thus leads to an equivalent underestimation of this inner chain length, both caused by an overestimation of the % of β-amylolysis.

The % of β-amylolysis, OCL and ICL are often used to compare different varieties and botanical sources of starches with respect to their chemical structural (Hizukuri, 1996). Since the overestimation of % β-amylolysis is not linear with the % of hydrolysis (see below), the differences in % of β-amylolysis, OCL and ICL are not directly proportional to the differences in branching characteristics of the polymer. Because of these implications, it is important to derive correction procedures to convert the apparent % of hydrolysis to an actual % of hydrolysis.

Hydrolytic gain as a function of % of hydrolysis

One mol of a glucose polymer with degree of polymerization n (DP_n) has a molecular weight of ($162xDP_n+18$) g/mol. One mol of polymer (DP_n) is linked by (DP_n-1) mol glycosidic bonds. The amount (mols) of bonds per g of polymer is thus given by:

$$\frac{DP_n - 1}{DP_n \times 162 + 18}. \qquad \left[\frac{mol}{g}\right] \qquad (4)$$

Per mol of bonds hydrolyzed the total dry weight increases with 18 g. The hydrolytic gain (HG, in g per g starting material) as a function of % of bonds hydrolyzed is then given by:

$$HG = \frac{\%\ actual\ bond\ hydrolysis}{100\%} \times 18 \times \frac{DP_n - 1}{DP_n \times 162 + 18}. \qquad \left[\frac{g}{g}\right] \qquad (5)$$

Since in most cases the % of hydrolysis is defined as % of monomeric units liberated from the starting material, equation 5 has to be converted. In a polymer, the ratio between the amount of monomeric units and amount of linkages is given by:

$$\frac{\text{mol monomeric units}}{\text{mol linkages}} = \frac{DP_n}{DP_n - 1}. \qquad \left[\frac{\text{mol}}{\text{mol}}\right] \qquad (6)$$

When the monomeric units are split off from the polymer as glucose units (DP_1), the ratio between the amount of linkages hydrolyzed and monomeric units liberated is 1. When the monomeric units are split off from the polymers as maltose (DP_2), as in the case with β-amylolyis, the ratio between the amount of linkages hydrolyzed and monomeric units liberated becomes ½. Or, in a general form:

$$\frac{\text{mol linkages hydrolyzed}}{\text{mol monomeric units liberated}} = \frac{1}{DP_x}, \qquad \left[\frac{\text{mol}}{\text{mol}}\right] \qquad (7)$$

in which DP_x is the degree of polymerization of the liberated oligomers. Multiplying equation 5 with equation 6 and 7 gives the hydrolytic gain (in g/g starting material) as a function of % of hydrolysis, now defined as the amount of monomeric units liberated from the starting material :

$$HG = \frac{\%\ \text{actual hydrolysis}}{100\%} \times \frac{18}{DP_x} \times \frac{DP_n}{DP_n \times 162 + 18}. \qquad \left[\frac{\text{g}}{\text{g}}\right] \qquad (8)$$

A higher degree of polymerization of the hydrolysis product (DP_x) leads to a lower amount of hydrolytic gain. Hydrolysis to glucose (DP_1) thus leads to a higher increase in dry weight then hydrolysis to, for example, maltose (DP_2).

Correcting apparent % of hydrolysis to actual % of hydrolysis

As illustrated in the example of β-amylolyis, the overestimation of the % of actual hydrolysis is caused by hydrolytic gain. The determined apparent % of β-amylolysis actually consists of:

$$\frac{\%\,\text{apparent}}{100\%} = \frac{\text{mass of maltose (as monomeric units)} + \text{hydrolytic gain}}{\text{mass starting material} + \text{hydrolytic gain}}. \qquad [-] \qquad (9)$$

Or rewritten in a general form:

$$\frac{\%\,\text{apparent}}{100\%} = \frac{(\%\,\text{actual}/100\%) + HG}{1 + HG}. \qquad [-] \qquad (10)$$

Substituting equation 8 in equation 10 leads to a relation to calculate the actual % of hydrolysis from the apparent % of hydrolysis:

$$\frac{\%\,\text{actual}}{100\%} = \frac{(\%\,\text{apparent}/100\%)}{1 + \frac{18}{DP_x} \times \frac{DP_n}{DP_n \times 162 + 18} \times (1 - \frac{\%\,\text{apparent}}{100\%})}. \qquad [-] \qquad (11)$$

Figure 2 illustrates the (non-linear) overestimation of the actual % of hydrolysis of starch (DP_n = 100000) as a function of the apparent % of hydrolysis for two hydrolysis products maltose (DP_2) and glucose (DP_1).

With equation 11 or Figure 2 values reported in literature can be corrected to the actual % of hydrolysis. If the difference in the chemical structure (e.g. between different starches of botanical origin) is investigated, this non-linear overestimation of the actual % of hydrolysis has to be corrected for. Equation 11 can, with a minor modification, also be used for the hydrolysis of other polymers. The molecular weight of the monomeric units (162 for starch) has to be changed in the molecular weight of the monomeric units of the polymer considered.

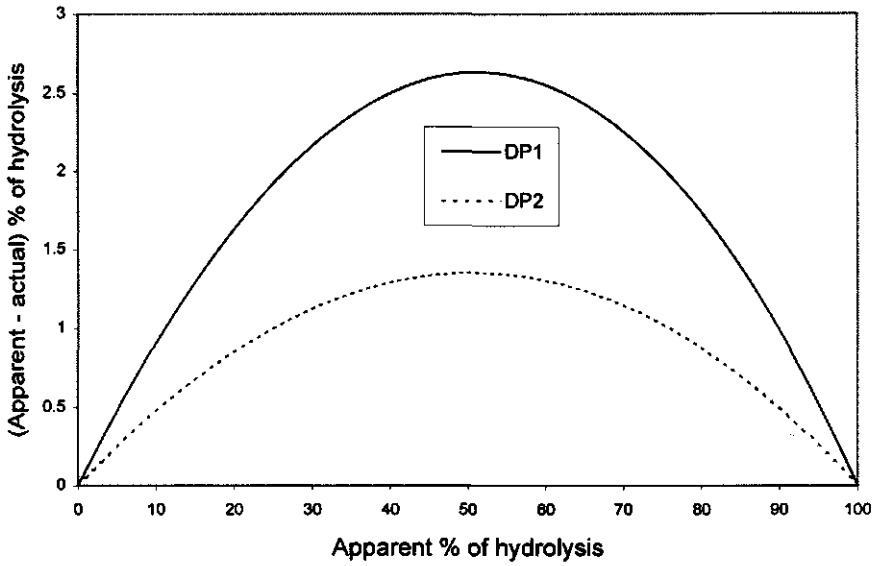

Figure 2: The overestimation of the actual % of hydrolysis of starch (DP_n = 100000) as a function of the apparent % of hydrolysis for two hydrolysis products maltose (DP_2) and glucose (DP_1).

Ackowledgements

The authors thank Avebe and the Dutch Ministry of Economic Affairs (PBTS-Biotechnology Project No. BIO94043) for funding of this research.

References

Banks, W., Greenwood, C.T. 1959. Physicochemical studies on starches. Part XX. The existence of an anomalous amylopectin in starch. J. Chem. Soc. 3436-3439.

Bathgate, G.N., Manners, D.J. 1966. Mutiple Branching in Glycogens. Biochem. J. **101:** 3c-5c.

Bender, H., Siebert, R., Stadler-Szöke, A. 1982. Can cyclodextrin glycosyltransferase be useful for the investigation of the fine structure of amylopectins?: characterisation of highly branched clusters isolated from digests with potato and maize starches. Carbohydr. Res. **110:** 245-259.

Bertoft, E. 1989a. Investigation of the fine structure of amylopectin using alpha- and beta-amylase. Carbohydr. Res. **189:** 195-207.

Bertoft, E. 1989b. Partial characterisation of amylopectin alpha-dextrins. Carbohydr. Res. **189:** 181-193.

Hizukuri, S. 1996. Starch:Analytical Aspects, pp.347-429.In: Eliasson AC (eds.), Carbohydrates in food, Marcel Dekker, inc., New York.

Marchal, L.M., Jonkers, J., Tramper, J. 1996. The use of freezing point depression to determine the theoretical dextrose equivalent. Starch. **48:** 220-224.

Peat, S., Whelan, W.J., Thomas, G.J. 1956. The enzymatic synthesis and degradation of starch. Part XXII. Evidence of multiple branching in waxy-maize starch. A correction. J. Chem. Soc. 3025-3030.

Thorn, W., Mohazzeb, S. 1990. Molecular weights, lengths, and distribution of side-chains in alpha-D-polyglucanes. Starch. **42:** 373-376.

Chapter 7

Monte Carlo Simulation of the α-Amylolysis of Amylopectin Potato Starch

Part II: α-Amylolysis of Amylopectin

L.M. Marchal, R.V. Ulijn, C.D. de Gooijer, G.Th. Franke, J. Tramper

submitted to Biotechnology & Bioengineering

Abstract

A model is presented that describes all the saccharides that are produced during the hydrolysis of starch by an α-amylase. Potato amylopectin, the substrate of the hydrolysis reaction, was modeled in a computer matrix. The four different subsite maps presented in literature for α-amylase originating from *Bacillus amyloliquefaciens* were used to describe the hydrolysis reaction in a Monte Carlo simulation. The saccharide composition predicted by the model was evaluated with experimental values. Overall, the model predictions were acceptable, but no single subsite map gave the best predictions for all saccharides produced. The influence of an α(1→6) linkage on the rate of hydrolysis of nearby α(1→4) linkages by the α-amylase was evaluated using various inhibition constants. For all the subsites considered the use of inhibition constants led to an improvement in the predictions (decrease of residual sum of squares), indicating the validity of inhibition constants as such. As without inhibition constants, no single subsite map gave the best fit for all saccharides. The possibility of generating a hypothetical subsite map by fitting was therefore investigated. With a genetic algorithm it was possible to construct hypothetical subsite maps (with inhibition constants) that gave further improvements in the average prediction for all saccharides. The advantage of this type of modeling over a regular fit is the

additional information about all the saccharides produced during hydrolysis, including the ones that are difficult to measure experimentally.

Introduction

Part I of this article (chapter 5) describes the modeling of the structure of potato amylopectin in solution as a computer matrix. This computer-generated amylopectin can be used to simulate various enzymatic (e.g. α-amylase, β-amylase, glucoamylase, pullulanase) or chemical reactions (e.g. acid hydrolysis, hypochlorite oxidation). This is demonstrated here by evaluation of the modeled saccharides produced after hydrolysis of amylopectin potato starch with an α-amylase, which exhibits the most complex reaction scheme of the examples cited above. The hydrolysis of saccharides by α-amylases can be described using the so-called subsite theory (Allen and Thoma, 1976a). The theory assumes that around the catalytic site a number of independent subsites exist, each of which can accommodate one glucose unit with a certain affinity (Figure 1). The combination of these individual affinities is able to describe the way in which and the rate wherein saccharides are hydrolyzed. This description of the enzyme specificity together with the computer-generated model of amylopectin presented in part I is used here to predict (in a Monte Carlo type of simulation) the production of the saccharides that evolve during hydrolysis. A Monte Carlo simulation is based on chances, in this case the chance that a certain linkage in the polymer is hydrolyzed by the enzyme. In this model, the rate of hydrolysis and the enzyme specificity of the α-amylase thus have to be translated to stochastic events.

The most widely used thermostable bacterial α-amylases in industrial starch hydrolysis are isolated from *Bacillus licheniformis, B. stearothermophilus,* and *B. amyloliquefaciens*. Only for the α-amylase from *B. amyloliquefaciens* a subsite map is described in literature. Two independent research groups, both defining two different isolations, presented in total 4 different subsite maps for an α-amylase originating from *B. amyloliquefaciens* (Allen and Thoma, 1976a; Iwasa et al., 1974; Torgerson et al., 1979). Since both groups used different

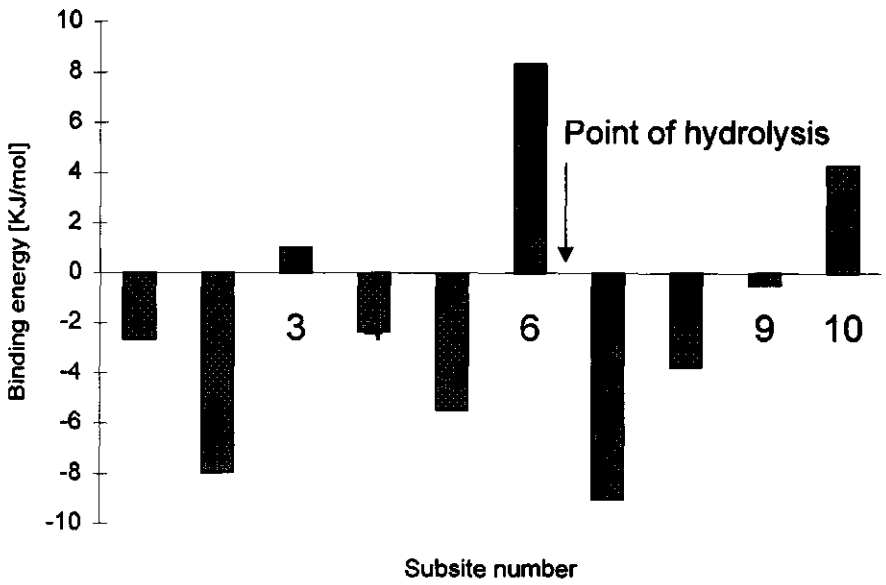

Figure 1: The subsite map as determined by Torgerson et al. (1979) for α-amylase from *Bacillus amyloliquefaciens*. The point of hydrolysis is situated between subsite number 6 and 7. The reducing end of a saccharide is always situated at the right-hand side of the subsite map.

isolations and methods for determination of the subsite map, at least two different *B. amyloliquefaciens* α-amylases exist. The product profiles predicted on the bases of these four subsite maps are evaluated with experimental values for the hydrolysis of amylopectin potato starch.

All subsite maps described in literature are based solely on the hydrolysis of linear α(1→4) linked oligosaccharides. Slightly over 4% of the glucose units in amylopectin are also α(1→6)-linked (branch points). An α-amylase is not able to hydrolyze these α(1→6) links nor the directly adjacent α(1→4) links. Unfortunately there are no kinetic data available describing the influence of α(1→6) linkages on the rate of hydrolysis of α(1→4) linkages at some distance from this branch point. The influence of various inhibition constants on

the model predictions are therefore evaluated with experimental data from the hydrolysis of amylopectin potato starch.

Materials and methods

The model, specifically developed for this purpose, was written in Borland Delphi 3.0 for Microsoft Windows. The materials and methods for the evaluation experiments were similar to those described previously (Marchal et al., 1999b). Amylopectin potato starch (Avebe, Veendam, the Netherlands) was obtained from transgenic potatoes (amylose content of starch < 1%, calcium content 481 [μg/g]). The *B. amyloliquefaciens* α-amylase (BAN 240L) was obtained from Novo Nordisk (Bagsvaerd, Denmark). The enzyme preparation gave a single band on a gradient gel, so further purification was omitted.

Theory & Modeling

The subsite theory

According to the so-called subsite theory a defined number of subsites can be defined close to the active site of an α-amylase. These subsites, each with a different affinity to bind a glucose unit, together form the subsite map of the α-amylase. A subsite map describes the specificity of an α-amylase (i.e. the products wherein and the rate with which a specific saccharide is hydrolyzed). This subsite map is used for modeling the α-amylolysis of amylopectin potato starch. Table I gives the reported subsite maps for α-amylase from *B.amyloliquefaciens* (Allen and Thoma, 1976a; Iwasa et al., 1974; Torgerson et al., 1979). Here, only a synopsis of the subsite theory is given; for more information we refer to the pertinent literature (MacGregor et al., 1994; Thoma et al., 1970; Thoma et al., 1971; Torgerson et al., 1979).

Table I: The subsite energy maps (in kJ per mol) for 4 different isolations of α-amylase from *Bacillus amyloliquefaciens*, as given by Allen and Thoma (1976a), Iwasa et al. (1974), and Torgerson et al. (1979). Hydrolysis takes place between subsite number 6 and 7. The subsite maps as determined by Iwasa et al. (1974) give a combined value for the energy of binding of subsite 6 and 7. ΔG_a is the acceleration factor (see text for details) as determined for the subsite maps BLA-N, and B. The reducing end of the saccharide is always located at the right-hand site of the subsite map. The same abbreviation for each subsite map, as given by their authors, is used: BLA-N (Allen and Thoma, 1976a), BLA-B (Torgerson et al., 1979), BLA-F and BLA-D (Iwasa et al., 1974).

Abr.	1	2	3	4	5	6	7	8	9	10	ΔG_a
BLA-N	-2.93	-8.66	0.88	-2.68	-7.99	15.36	-12.84	-5.65	-2.47	6.82	1.55
BLA-B	-2.66	-7.95	1.00	-2.34	-5.46	8.32	-9.00	-3.74	-0.46	4.29	2.22
BLA-F	-4.60	-10.04	0	-2.51	-10.04	12.97		-5.02			0
BLA-D	-5.44	-11.72	-0.42	-5.02	-11.30	15.90		-4.184			0

Consider the hydrolysis of a saccharide S_n (composed of n glucose units) by the enzyme E into two products (P) composed of m and n-m glucose units respectively:

$$E + S_n \underset{k-1,i,n}{\overset{k+1,i,n}{\rightleftarrows}} ES_{i,n} \xrightarrow{k+2,i,n} E + P_{n-m} + P_m , \qquad (1)$$

where n refers to the number of glucose units of the oligosaccharide, and i to the position of the reducing end of the saccharide (S_n) in the subsite map. Since the subsite theory assumes that $k_{+2,i,n} \ll k_{-1,i,n}$, the association constant for the $ES_{i,n}$ complex ($K_{i,n}$) becomes equal to $k_{+1,i,n}/k_{-1,i,n}$. Figure 2 gives, as an example, some of the modes of binding of maltopentaose (n=5) to a subsite map consisting of 10 independent subsites. Two main groups of binding can be distinguished in Figure 2; productive and non-productive complexes. Complexes are productive if subsite 6 and 7 are occupied with substrate, enabling hydrolysis of the α(1→4) linkage in-between. Complexes are non-productive if part of the subsite map of the enzyme is occupied but not the catalytic site.

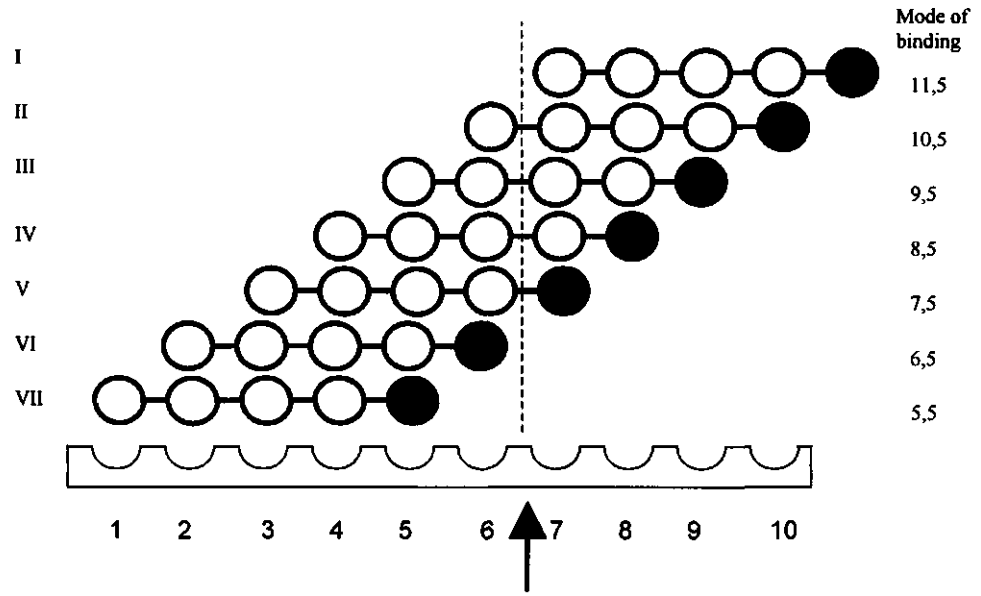

Figure 2: Modes of binding for maltopentaose (n=5) on an enzyme with 10 subsites. All the productive (II to V) and some non-productive complexes are given. When the substrate extends beyond the right of the binding region (I) virtual subsites are used to designate the binding mode index. The mode of binding is coded as: position of the reducing end, length of the saccharide. ↑ Position of the catalytic site, ○ glucose unit, ● reducing glucose unit. – α(1→4) linkage.

In a polymer mixture, with a maximum degree of polymerization of x, the rate of formation of products (P_m and P_{n-m}) is given by (Torgerson et al., 1979):

$$\frac{d[P_m]}{[E_0]dt} = \frac{d[P_{n-m}]}{[E_0]dt} = \frac{k_{+2,i,n}[S_n]K_{i,n}}{1 + \sum_{n=1}^{x}[S_n]\sum_{i=1}^{z+n-1}K_{i,n}}, \qquad (2)$$

in which z is the number of subsites of the enzyme, and E_0 the total amount of enzyme. Note that the denominator of equation 2 is a constant for all products of the reaction since it represents the sum of all substrates present times all their possible association constants.

The number of productive complexes for a linear substrate (with degree of polymerization n) is equal to n-1. The number of non-productive enzyme-substrate complexes is independent on the degree of polymerization of the saccharide and equal to the number of subsites of the enzyme (z). The association constant $K_{i,n}$ for an enzyme substrate complex can be related to free energies of interaction of the occupied subsites with glucose residues by (Allen and Thoma, 1976b; MacGregor et al., 1994; Thoma et al., 1971):

$$-RT \ln K_{i,n} = \sum_{b=i-n+1}^{i} \Delta G_b + \Delta G_{mix} \quad , \qquad (3)$$

where R is the gas constant, T the absolute temperature in Kelvin, ΔG_b is the free energy of binding of a glucose residue at subsite i, and ΔG_{mix} is the free-energy contribution to binding, which is common for bimolecular association processes (Chipman and Sharon, 1970; Hiromi, 1970). ΔG_{mix} in aqueous solution is equal to $\kappa T \ln(55.5)$ (Gurney, 1953). For a bimolecular process (κ =2) this gives a value of 2.6 kcal (10.9 kJ) per mol at 324 Kelvin. When the enzyme is saturated with substrate, the rate of hydrolysis is limited by the value of $k_{+2,n,i}$. This value is either assumed constant for all possible reactions (MacGregor et al., 1994)), or proportional to the number of subsites occupied (Allen and Thoma, 1976a; Thoma and Allen, 1976; Torgerson et al., 1979) in the following way:

$$k_{+2,n,i} = k_{+2} \exp(\Delta G_a / RT) \quad , \qquad (4)$$

in which ΔG_a is an acceleration factor proportional to the number of occupied subsites.
Since the absolute value of k_{+2} is unknown, only relative rates of production can be considered. In this Monte Carlo simulation the relative rates of production of all products conceivable from a mixture of polymers are considered. When the ratio between the products formed (equation 2) from two different saccharides (with degrees of polymerization n and o) is considered this becomes:

$$\frac{d[P_m]}{d[P_p]} = \frac{d[P_{n-m}]}{d[P_{o-p}]} = \frac{k_{+2,i,n}[S_n]K_{i,n}}{k_{+2,j,o}[S_o]K_{j,o}}. \qquad (5)$$

Note that the denominator of equation 2 is eliminated. Substituting equation 3 and 4 in equation 5 leads to:

$$\frac{d[P_m]}{d[P_p]} = \frac{d[P_{n-m}]}{d[P_{o-p}]} = \frac{e^{\frac{\Delta G_{a,i,n}}{RT}}[S_n]e^{\frac{-\Delta G_{b,i,n}}{RT}}}{e^{\frac{\Delta G_{a,j,o}}{RT}}[S_o]e^{\frac{-\Delta G_{b,j,o}}{RT}}} = \frac{[S_n]e^{\frac{\Delta G_{a,i,n}-\Delta G_{b,i,n}}{RT}}}{[S_o]e^{\frac{\Delta G_{a,j,o}-\Delta G_{b,j,o}}{RT}}}. \qquad (6)$$

The absolute values of k_{+2} and ΔG_{mix} become unimportant since they are eliminated.

When a subsite map without an acceleration factor is considered (subsite map BLA-F and BLA-D from Table I), ΔG_a is set to zero. With equation 6 the relative rate of production of saccharides in a polymer mixture can be calculated.

When the product ratios of a limited number of substrates are considered, it is practical to solve all the differential equations (Torgerson et al., 1979). However, the amount of differential equations increases dramatically with increasing degree of polymerization of the starting material since each saccharide with degree of polymerization n leads to n-1 different products. The total number of differential equations that has to be considered in order to simulate the hydrolysis of a polymer with degree of polymerization x (only the productive complexes have to be considered) is:

$$\text{number of equations} = \sum_{n=1}^{x}\sum_{j=1}^{n-1} n_j. \qquad (7)$$

The number of differential equations to be solved simultaneously increases from 45 (hydrolysis of DP10) to half a million when the product ratio of the hydrolysis of DP1000

is modeled. Therefore a Monte Carlo simulation was chosen to model the hydrolysis of potato amylopectin (DP 200,000).

Monte Carlo simulation

Amylopectin, the substrate for the hydrolysis reaction, was modeled in a two dimensional matrix as described in part I of this article (chapter 5). The average % of β-hydrolysis of the modeled amylopectin is 54%, with an A to B chain ratio of 0.93. Within the molecule a normal distribution of the branching characteristics is assumed (range 52-56% of β-hydrolysis). See part I for more details.

The enzyme moves through the matrix at random. The chance of a productive complex with a linear substrate (with degree of polymerization n) is proportional to (n-1) times the concentration of this substrate in the matrix. This means that the chance of forming a productive complex is proportional to the amount of possible productive complexes of a substrate (n), which makes this approach equivalent to the analytical approach described above.

In a Monte Carlo simulation the relative rates of hydrolysis of the saccharides have to be converted to discrete events. The rate of hydrolysis of a saccharide is proportional to $k_{+2,i,n}K_{i,n}$ (equation 5). The highest value for $k_{+2,i,n}K_{i,n}$ is obtained for the highest negative sum of $(\Delta G_{a,i,n} - \Delta G_{b,i,n})$. For the subsite maps BLA-F and BLA-D (Table I) this value is obtained when all 8 subsites are occupied with glucose units. For the subsite maps BLA-B and BLA-N this highest value is obtained if the subsites 1 to 9 are occupied with glucose units. This highest value for the rate of hydrolysis of a saccharide (highest $k_{+2,i,n}K_{i,n}$) is translated to a chance of hydrolysis of 1. The chance of hydrolysis of all other values for $k_{+2,i,n}K_{i,n}$ is correlated to this maximum in the following way:

$$p(\text{hydrolysis}) = \frac{k_{+2,i,n}K_{i,n}}{(k_{+2,i,n}K_{i,n})_{max}}. \qquad (8)$$

In the model there are only two possibilities, i.e. a linkage can be hydrolyzed or not. So, the probability of hydrolysis has to be translated to a discrete action. For example, a probability of hydrolysis of 0.1 means that on average one in every ten times the linkage is actually hydrolyzed. With a random generator (standard available in Delphi) a random number (0 ≤1) is selected. If this number is smaller or equal to the calculated chance of hydrolysis (equation 8), the glucose linkage between subsite number 6 and 7 of the enzyme in the matrix is hydrolyzed, the matrix is adjusted accordingly, and the enzyme moves to the next point in the matrix at random. If it is decided not to hydrolyze, the enzyme simply moves to the next random point in the matrix without cleavage of the polymer.

The number of cleavages together with the degree of polymerization of the starting molecule (DP_n) determine the number-average molecular mass (M_n) of the starch hydrolysate:

$$M_n = \frac{162DP_n + 18(\text{cleavages}+1)}{(\text{cleavages}+1)}, \qquad \left[\frac{g}{mol}\right] \qquad (9)$$

in which 162 is the molecular weight of the repeating unit [g/mol] and 18 is the molecular weight of H_2O [g/mol]. The term (cleavages+1)x18 originates from the fact that each time a glucosidic linkage is hydrolyzed water is added, and the mass of the solute increases (see also Marchal and Tramper (1999a) for more information about hydrolytic gain). In the starch industry the dextrose equivalent (DE) is normally measured in order to obtain information about the M_n of a starch hydrolysate. The DE ranges from almost zero (starch) to 100 (glucose). Whenever in this article the term DE is mentioned, the theoretical dextrose equivalent defined as (180/number-average molecular mass of the starch hydrolysate)×100 is meant. Substituting this in equation 9 leads to:

$$DE = \frac{180(\text{cleavages}+1)}{162DP_n + 18(\text{cleavages}+1)} \times 100. \qquad [-] \qquad (10)$$

In the model simulation, each time a linkage is hydrolyzed, the dextrose equivalent increases with a small value. The extent of the increase in DE upon additional cleavage depends on the degree of polymerization of the starting molecule (DP_n) and the number of cleavages so far. During hydrolysis the number of cleavages is between 0 at the start of the hydrolysis, and (DP_n-1) when all the linkages in the polymer (DP_n) are hydrolyzed. For potato amylopectin (DP_n 200,000) as considered in this model, the increase in DE with each additional cleavage is in between 5.56×10^{-4} (start of the hydrolysis) and 4.50×10^{-4} (DE =100, end of the hydrolysis) DE units. At set intervals (normally 0.5 DE units), the saccharide composition of the matrix is determined and stored to file, either as mass % (taking into account hydrolytic gain), or as mol fraction.

α(1→6)-linked glucose units

An α-amylase can not cleave α(1→6)-linked glucose units (slightly over 4% of the glucose linkages in potato amylopectin). Furthermore the glucose units adjacent to an α(1→6)-linked glucose unit are inaccessible to the enzyme (Hizukuri, 1996). This means (French et al., 1972) that whenever a branch point is located at position 6 or 7 of the subsite map, hydrolysis is not possible and the smallest branched oligosaccharide liberated from amylopectin by an α-amylase has therefore a degree of polymerization of 5 (French et al., 1972).

There is no information on the influence of nearby α(1→6) linkages on the value of $k_{+2,i,n}K_{i,n}$ of productive enzyme substrate complexes. Neither is there kinetic data available on the hydrolysis of branched oligosaccharides by an α-amylase. It is known, however, that it takes a high dosage of enzyme and prolonged incubation to produce branched maltopentaose (French et al., 1972). This means that restrictions must apply. The nearest α(1→4) linkage an α-amylase is capable to hydrolyze is at 2 linkages from an α(1→6) linkage. Thus in order to hydrolyze this α(1→4) linkage the α(1→6)-linked glucose unit has to be at position 8 or 5 in the subsite map. Figure 3 illustrates this in a schematic way and the coding of the factors is explained in the legend. The influence of various

restrictions of a nearby α(1→6) linkage on the model predictions are evaluated. This is done by multiplying equation 8 with $(1-k_{br\_in})$. An inhibition factor (k_{br_in}) of 0 is equivalent to no inhibition and 1 to infinite inhibition. Inhibition constants for each of the three possible positions (Y8, T8, and T5 in Figure 3) are evaluated independently with respect to their fit. A branch point at position 4 or 9 or even further away from the catalytic site in the subsite map could also lead to an inhibition of the rate of hydrolysis.

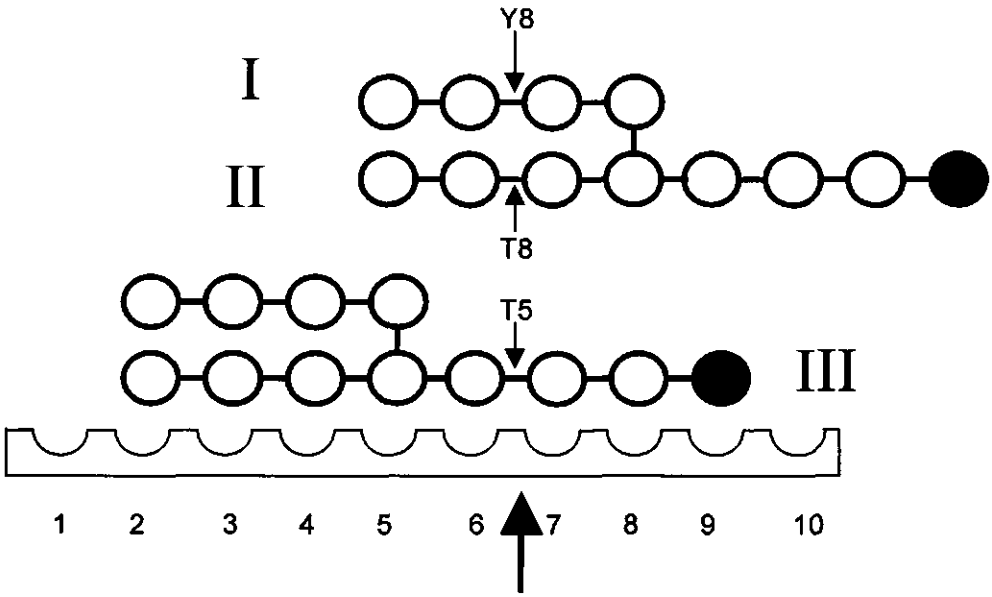

Figure 3: Visual representation of the three possible ways that α-amylase can hydrolyze α(1→4) linkages close to a branch point. The nomenclature of the hydrolysis possibilities (T8, Y8, T5) denotes to the position and nature of the branched glucose unit in the subsite map and is analogous to the nomenclature used to describe the glucose linkages in the matrix (see part I of this article). T refers to an α(1,4,6) linked glucose unit and Y to a glucose unit linked with (1) to the 6 position of another glucose unit. The number behind T and Y is the position of this linked glucose unit in the subsite map. ↑ Position of the catalytic site, ○ glucose unit, • reducing glucose unit, – α(1→4) or α(1→6) bond. The numbers I, II, and III denote the three different ways an α-amylase can approach a branch point.

It is assumed that the inhibition of a branch point will decrease with increasing distance from the catalytic site. In order to reduce the number of independent parameters to a minimum, the following equation (which describes an exponential decay in inhibition with increasing distance to the branch point) was used to describe the inhibition for each of the three types of approaching a branch point:

$$k_{br\_in} = 2 - e^{b_T \cdot y}, \qquad (11)$$

in which y is the amount of glucose units between the catalytic site and the branch point. The fit factor b_T (with T I, II, or III) is different for each of the three types of branch inhibition (Figure 3). Inhibition factors below zero are interpreted as 0. Inhibitions up to 4 glucose units between the catalytic site and the branch point (y=4) are considered. If a branch point is located outside the subsite map but inside the range of influence (y=4), inhibition is applied. Whenever more inhibition factors are valid at the same time (branched glucose units at both sides of the active site), the $(1- k_{br\_in})$'s are multiplied.

The influence of the branch factors on the model predictions are evaluated by varying each b_T value from 0.7 (no inhibition at all) to 0.1 (steps of 0.1). A b_T value of zero means 100% inhibition, which would contradict with the production of a branched maltopentaose (French et al., 1972). All the possible combinations of the three b_T types of inhibition are evaluated for each subsite map. The average of 3 simulation runs is taken.

Subsite-map fitting

An optimal subsite map would predict all the saccharides produced during hydrolysis as accurately as possible. By variation of the subsite energies a subsite map can be constructed that better describes the saccharides produced during α-amylolysis of amylopectin potato starch. A standard type of genetic algorithm was used for variation of the characteristics of such a subsite map. In general, a genetic algorithm treats an optimization by setting up a 'population' of possible solutions and then, after evaluating those solutions, produces a new

population of possible solutions (the next 'generation') by breeding from the best solutions of the parent population. Mutation is employed to give new information to the population (uncover new building blocks) and also prevents the population from premature convergence. The vector of parameters of one solution (individual) is coded as a bit string (the algorithm's equivalent of a chromosome). Desired resolution of each parameter (gene) dictates the amount of bits required. As with any algorithm, there are many variations to this basic theme. Since the primary purpose here is to investigate the potential of a genetic algorithm in this specific type of model, settings that are normally known to give good results are taken. See Banzhaf et al. (1998) and references cited therein for more information about the application of genetic algorithms.

The 4 subsite maps from literature (see Table I) together with the best inhibition factors determined so far (Table III) are taken as parents for the start of the genetic algorithm. The desired resolution together with maximum expected range of a parameter determines the amount of bits required for a gene. The resolution of the energy level of each subsite is set to 0.1 kJ/mol with a maximum energy possible of plus or minus 12.7 kJ/mol. These 255 different combinations can be described using 8 bits for each subsite ($2^8 = 256$). The resolution of the acceleration factor (maximum 5.11 kJ) and each inhibition factor (maximum 0.63) are both set to 0.01, which leads to 9 and 6 bits respectively. The total length of the 'chromosome' thus consists of a string of 91 bits. The population size is set to 50 individual solutions ('chromosomes'). After evaluation of a population, the best individual of each population is taken over, without mutation, into the next generation. The chance of selection of 'chromosomes' is proportional to its fit of the objective function. Given the selected 'chromosomes', pairs were chosen to mate with a 95% probability. A single cross-over was applied by exchanging genes from a point chosen at random along the length of the chromosome. To prevent premature convergence, single-point mutation was used with a minimum probability of 1% change per bit of a chromosome. The improvement in model fit over 100 generations was evaluated.

Results and discussion

Variance in model predictions between different hydrolysis simulations

The variation in model-predicted amount of saccharides between different Monte Carlo simulation runs is inversely proportional to the size of the starting amylopectin. A higher degree of polymerization of the starting amylopectin will lead to a lower variance. When the saccharides produced are evaluated on a mass basis, the variance of the predicted saccharide concentration increases with degree of polymerization of the saccharide considered. The variance in model predictions between different hydrolysis runs was generally very small for the evaluated oligosaccharides DP 1-10 and DP ≥ 11 (amount of rest-fraction of the HPLC analysis). The average of 20 simulation runs (buildup of amylopectin and subsequent hydrolysis), which gave very smooth model-predicted lines, was used in comparing the model predictions of the different subsite maps.

Comparing the different subsite maps of *B. amyloliquefaciens* α-amylase

First, the predicted saccharide composition using the 4 different subsites maps from Table I without any further constraints from nearby α(1→6) linkages were evaluated. Figure 4 gives the model and experimental values for the amount of maltohexaose (on mass basis the primary reaction product of *B. amyloliquefaciens* α-amylase) during the hydrolysis of amylopectin potato starch. Note that the x-axis is not time, but the time-related dextrose equivalent. The overall predictions agree reasonably well with the experimentally determined values. All subsite maps predict a maximum in the amount of maltohexaose after which the net amount of maltohexaose decreases again due to further hydrolysis.

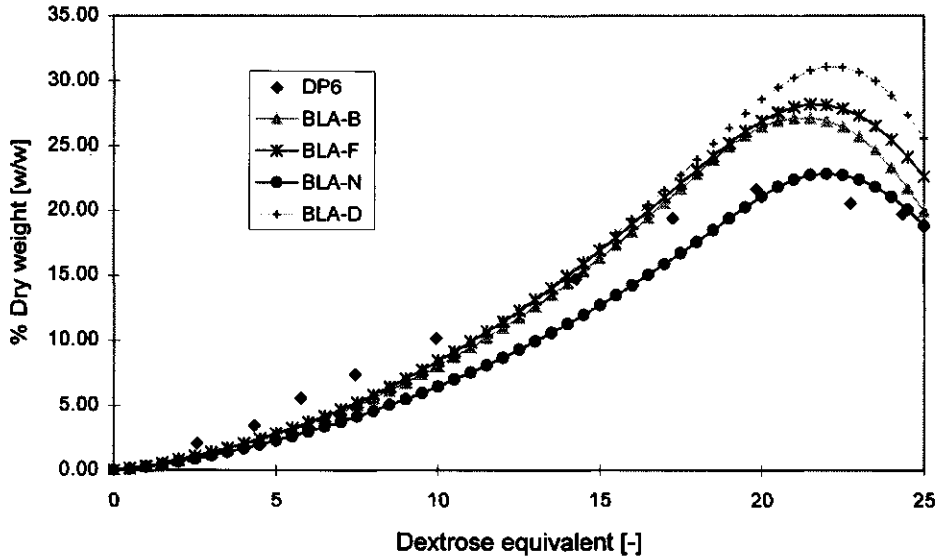

Figure 4: The predicted and experimentally determined amount of maltohexaose (DP6) for the hydrolysis of amylopectin potato starch (51°C, pH 6, 1% dry weight, *B. amyloliquefaciens* α-amylase). The abbreviations of the subsite maps used are the same as in Table I.

Figure 5 gives the predicted and experimentally determined amounts of DP5 (maltopentaose) and DP1 (glucose). Maltopentaose is predicted best by subsite map BLA-N, the subsite map BLA-D, on the other hand, predicted glucose the best. The model also can discriminate between linear and branched saccharides. Figure 6 gives the predicted amounts of linear and branched malto-octaose (DP8) as an example. With the experimental methods used (HPLC), only the total amount (linear plus branched) of a saccharide could be determined. The experimental amount of DP8 rose again after a minimum. As shown before (Marchal et al., 1999b), this second increase is most likely due to the net production of branched DP8 from the hydrolysis of structures with a higher degree of polymerization.

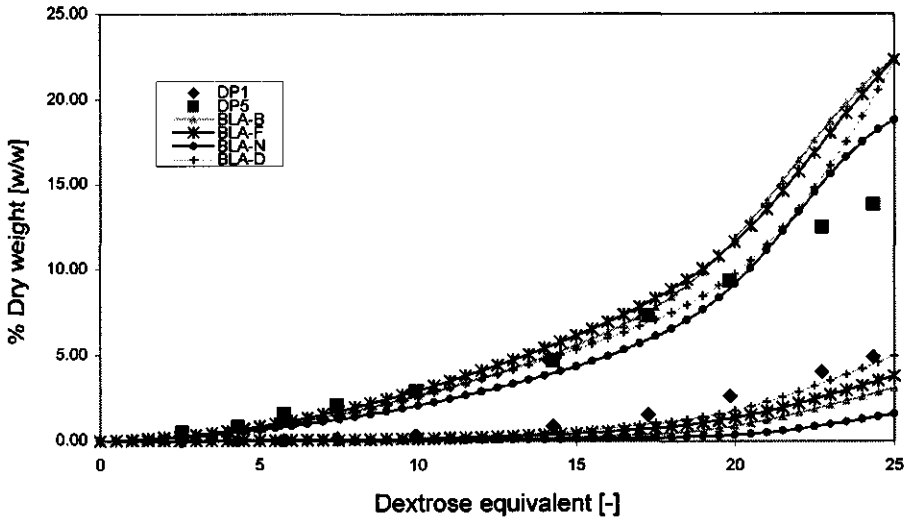

Figure 5: The predicted and experimentally determined amount of maltopentaose (DP5) and glucose (DP1) for the hydrolysis of amylopectin potato starch (51°C, pH 6, 1% dry weight, *B. amyloliquefaciens* α-amylase). The abbreviations of the subsite maps used are the same as in Table I.

The predicted increase in branched DP8 agreed very well with this finding. However, the predicted total amount of malto-octaose (production minus further hydrolysis) showed quite an overshoot, due to the net overproduction of linear malto-octaose. The predicted and experimental results of DP9 and DP10 gave similar results.

In general, the model overestimated the net production of larger linear saccharides (DP≥ 8) in the intermediate phase of the hydrolysis (DE range ≈ 5 to 20). This means that the affinity of the subsite maps to hydrolyze these linear saccharides (to smaller saccharides) is too small as compared to the hydrolysis of branched structures. Or, stated otherwise, the affinity to hydrolyze the branched saccharides is too high and restrictions have to be applied (see section below). For reason of occupying journal space, only a few figures are given here as an example. All figures (DP 1-10 and DP ≥ 11) and the figures with the

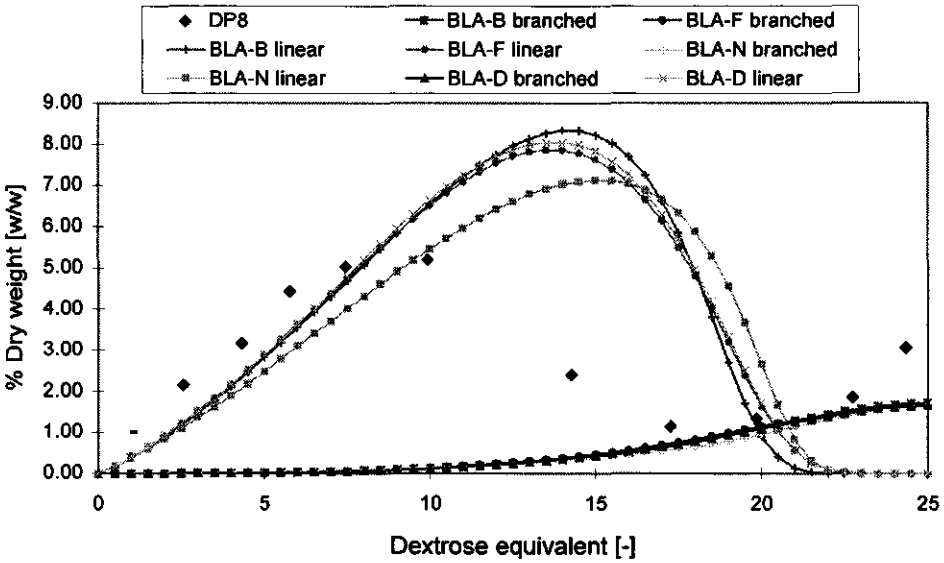

Figure 6: The predicted amount (linear and branched) and experimentally determined (total) amount of malto-octaose (DP8) for the hydrolysis of amylopectin potato starch (51°C, pH 6, 1% dry weight, *B. amyloliquefaciens* α-amylase). The abbreviations of the subsite maps used are the same as in Table I.

predicted linear and branched compositions can be found at:

http://www.spb.wau.nl/prock/maltodextrin/monte_carlo.htm

The dissimilarities in subsite map energies result in differences with respect to predicted amounts of various oligosaccharides (Table II). It is obvious that no single subsite map from literature gave acceptable model predictions for all the different saccharides. The subsite map BLA-B gave (on a molar basis) the best predictions overall.

Table II: The residual sum of squares (RSS) of model prediction (average of 20 simulation runs) minus experimental data (10 data points per saccharide). For ease of comparison, the lowest RSS of each saccharide is in bold. The sum of all the RSS for the different saccharides is given by s_mass. With the sum of all the RSS for the different saccharides on molar basis (mol), the RSS are weighted according to the molecular weight of the saccharide. Since the molecular weight of the rest fraction of the HPLC analysis (DP≥11) is unknown, the modeled average degree of polymerization of this rest fraction is used. Experimental conditions: 51°C, pH 6, 1% dry weight amylopectin potato starch, *B. amyloliquefaciens* α-amylase. The abbreviations of the subsite maps used are the same as in Table I.

DP	1	2	3	4	5	6	7	8	9	10	≥11	s_mass	s_mol
BLA_B	14.1	40.2	**26.9**	9.9	92.9	81.0	114.9	80.8	32.3	35.8	472.7	**1001.7**	**138.0**
BLA_N	30.4	54.6	326.1	37.8	**28.0**	**59.9**	160.1	**73.7**	**18.6**	**29.9**	498.0	1317.1	261.1
BLA_F	7.2	**10.8**	109.3	**6.1**	81.5	119.0	**107.8**	76.4	42.0	39.9	410.0	1009.9	145.4
BLA_D	**1.9**	17.4	131.0	7.9	50.9	236.8	114.2	76.9	45.3	40.4	**392.6**	1115.2	167.3

Influence of α(1→6)-linked glucose units

From the model predictions described above it was clear that additional constraints for the hydrolysis of branched saccharides had to be imposed. Various restrictions were evaluated by the residual sum of squares weighed on a molar basis for the various saccharides formed. The standard deviation in the RSS of one simulation was less then 2% of the average value from 100 simulations. This value dropped to below 0.8% when the average of 3 buildups, and below 0.6% when the average of 5 buildups was taken. The average of more simulations leads of course to more accurate predictions, but the calculation time required also increases more than proportional. Since the objective was to investigate the overall influence of inhibition constants, the average of three simulations was taken.

All (combinations of) inhibition constants led for all subsite maps to an improvement in the overall fit (on both mass and molar basis), thus indicating the validity of inhibition factors as such. The improvements in predictions on a molar basis were between 25 and 35%. Table III gives the b_T values that gave the best overall fit on molar basis.

Table III: The values of the inhibition constants (b_I, b_{II}, b_{III}) which gave, in the range investigated, the lowest overall residual sum of squares on a molar basis for each subsite map. Also the RSS of all the considered saccharides are given for these values of the inhibition constants. Other symbols and conditions are as given in the prefix of Table II.

DP	1	2	3	4	5	6	7	8	9	10	≥11	s_mass	s_mol
BLA_B	8.3	20.9	**32.6**	8.5	138.0	53.1	53.5	25.9	13.5	15.4	199.4	**569.0**	**93.7**
BLA_N	20.4	30.6	290.6	37.7	**65.2**	**38.3**	77.0	**19.5**	**5.6**	**8.9**	286.2	880.0	195.4
BLA_F	2.3	**2.9**	87.4	**5.0**	142.2	55.2	**51.2**	22.9	19.2	17.9	**199.3**	605.7	98.7
BLA_D	**0.2**	8.2	119.4	7.3	111.5	129.6	52.2	25.8	20.6	19.6	200.7	695.0	119.1

	b_I	b_{II}	b_{III}
BLA_B	0.3	0.1	0.1
BLA_N	0.1	0.2	0.4
BLA_F	0.3	0.1	0.1
BLA_D	0.5	0.1	0.1

As can be seen in this table, all RSS of the individual saccharides (with the exception of DP5) have a lower RSS than without restrictions. The net over production of larger linear saccharides in the intermediate phase of the hydrolysis (DE range ≈ 5 to 20) significantly decreased when inhibition constants were applied, thus improving the predictions. Figure 7 gives the predicted amount of malto-octaose (DP8) as an example. All other figures again can be seen at the URL given above. When the predicted amount of malto-octaose without (Figure 6) and with inhibition (Figure 7) are compared, the reduction in the net overproduction of the linear chains is evident. However, the predicted amount of linear malto-octaose still shows some overshoot and the predicted amount of branched malto-octaose decreases slightly. The linear saccharides (DP ≥ 6) are now more preferentially hydrolyzed to smaller saccharides than without inhibition for the branched saccharides. This leads to a net increase in the predicted amount of DP1, DP2, and DP5 in particular.

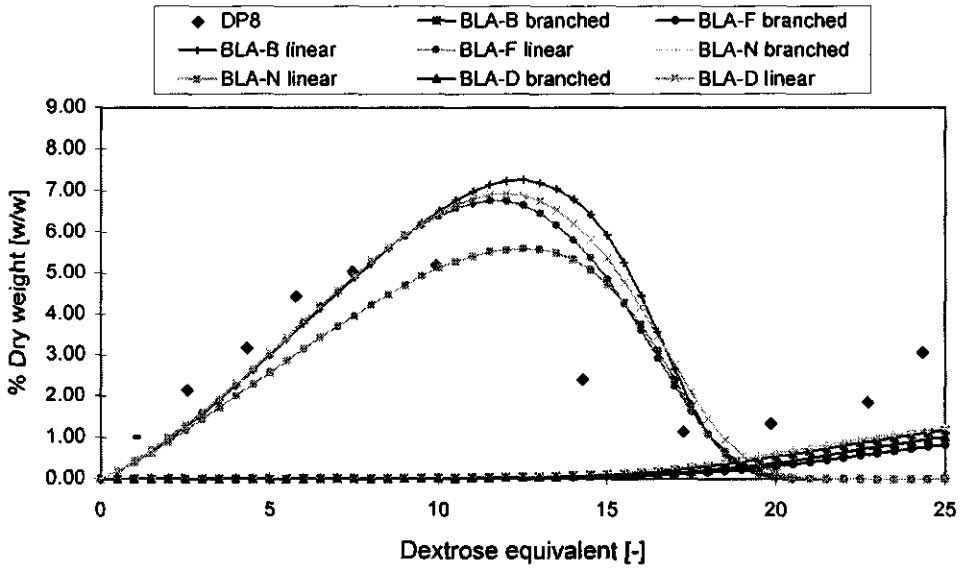

Figure 7: The predicted amount (linear and branched) of malto-octaose (DP8) for the subsite maps with the branch inhibition (b_T) factors as given in Table III. The abbreviations of the subsite maps used are the same as in Table I.

Since the predicted amount of DP5 without inhibition was already higher then the experimental values, this RSS deteriorates. The higher levels of DP1 and DP2 on the other hand lead to an improved fit of the model. The difference between the best inhibition values for each subsite map indicates that inhibition should always be seen together with the subsite map considered. The b_T values presented in Table III are not necessarily the ones that lead to the lowest RSS possible with these subsite maps from literature. A further refinement of the influence of inhibition constants would of course be possible, but those presented here already show the general trend quite clearly. Since here, as without inhibition constants, there is no single experimental subsite map that gives the best RSS for all the saccharides, the possibility was investigated to generate a superior hypothetical subsite map by a genetic algorithm.

Fitting an optimal subsite map

The subsite map is used in this model to predict the ratio of different saccharides that evolve during hydrolysis. Since only relative rates of production of saccharides are considered, the fitting procedure does not give information about the energy values of subsite 6 and 7 (which are always occupied in a productive hydrolysis). This means that the absolute value of subsite 6 and 7 become unimportant, and these were arbitrarily set to zero. The four subsite maps (BLA-B, N, D, and F) with the best b_T values (table III) were used as parents in the genetic fit procedure. The hypothetical subsite map was optimized towards the lowest RSS on molar basis, which was determined from the average of three simulation runs. After 50 generations the RSS on a molar basis decreases to around 40, which is an improvement of some 60% compared to the best fit so far (Table III). After 100 generations (5000 possible solutions checked), the RSS on a molar basis decreases to around 38. The reduction in RSS takes an ever-increasing number of generations, showing thus an exponential type of decay. To ensure that the fitting was not 'stuck' in a local minimum, several runs with different levels of mutations (mutation level 0.01, 0.02 and 0.03) were started with the same 4 parent subsites, but these all led to an RSS of around 38 after 100 generations. Additional generations (100) did not lead to a significant improvement. With this type of fitting procedure one can never be sure that the absolute minimum is obtained. However, a large number of solutions were evaluated in different runs that all led to similar overall RSS values. It can be expected therefore that further simulations do not lead to drastic improvements in the RSS.

Figure 8 gives four of the hypothetical subsites maps (arbitrarily numbered) as an example. Table IV gives the RSS for the saccharides evaluated with these maps. By comparing Figure 8 and Table IV it becomes clear that different hypothetical subsite maps can lead to similar overall model predictions. The subsite maps differ in the RSS for some of the individual saccharides, which originates from their difference in subsite map energies.

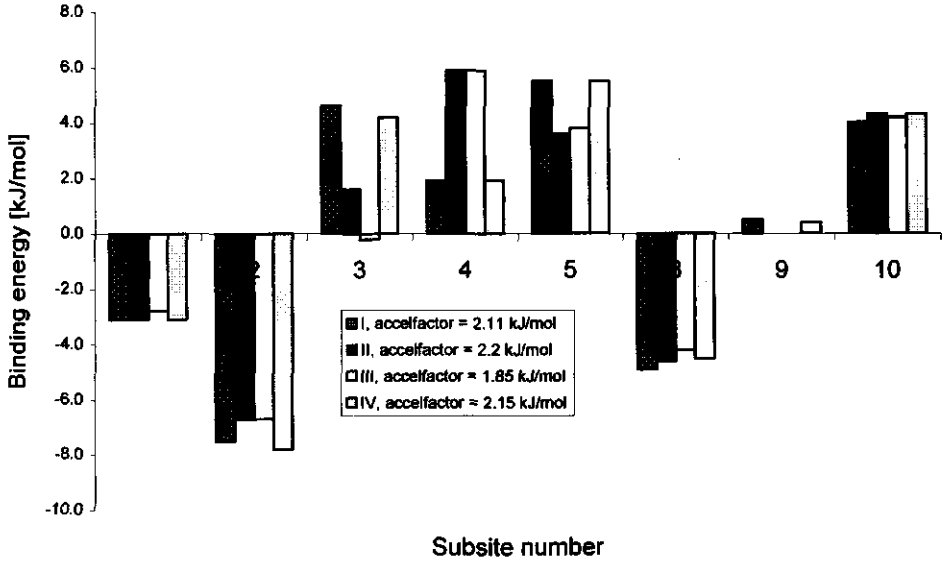

Figure 8: The energies of binding and acceleration factors of 4 different subsite maps obtained after the genetic fit procedure (see text for details). The value for the inhibition constants (b_I, b_{II}, b_{III}) for each subsite map are: subsite map I (0.07, 0.12, 0.15); subsite map II (0.07, 0.15, 0.08) subsite map III (0.07, 0.15, 0.13); subsite map IV (0.13, 0.09, 0.09).

Table IV: The residual sum of squares of the individual saccharides for four subsite maps from Figure 8. Other symbols and conditions are as given in the prefix of Table II.

DP	1	2	3	4	5	6	7	8	9	10	≥11	s_mass	s_mol
I	0.3	3.7	13.7	13.1	3.2	15.2	46.1	19.3	14.4	14.8	339.3	483.0	38.1
II	0.6	6.0	9.7	10.5	5.3	17.3	45.6	20.5	14.7	14.7	328.6	473.6	38.1
III	0.3	4.3	9.4	13.3	5.6	11.8	50.7	19.8	13.8	14.5	353.8	497.3	37.9
IV	0.8	4.0	11.9	14.4	2.8	17.6	46.1	20.1	14.3	14.5	311.7	458.2	37.9

From Table IV and Figure 8, it becomes clear that there is no single overall best subsite map. Rather there are groups of maps that predict the overall hydrolysis with the same RSS. These fits lead to improved model predictions for individual oligosaccharides, as illustrated in Figure 9 and 10. The predicted levels of the individual saccharides differ only

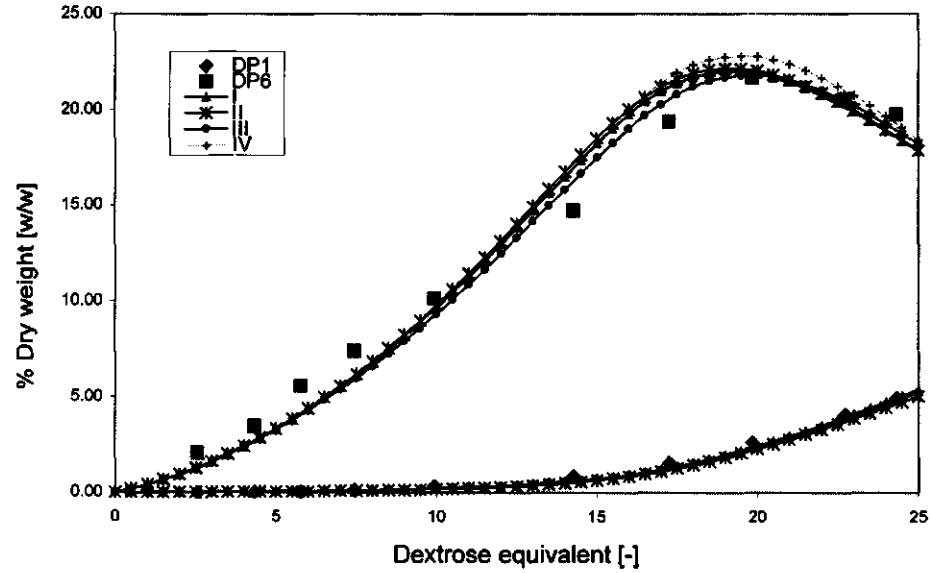

Figure 9: The predicted amount of glucose (DP1) and maltoheptaose (DP6) for the subsite maps as given in Figure 8.

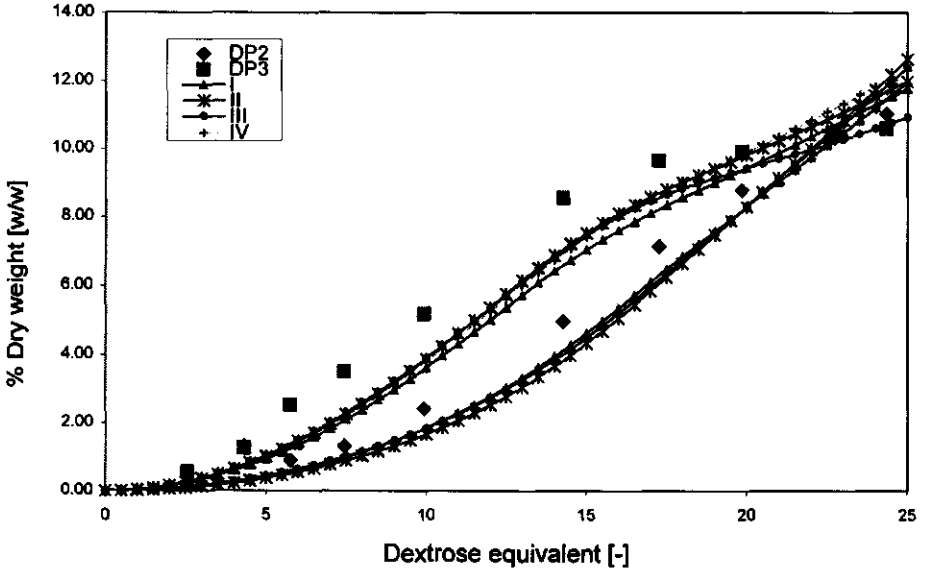

Figure 10: The predicted amount of maltose (DP2) and maltotriose (DP3) for the subsite maps as given in Figure 8.

slightly, which leads to some overlap in the model lines. All the other figures can be seen at the same Internet site cited above.

Model predictions

The advantage of this type of modeling over a regular fit is the additional information about the process during starch hydrolysis. With the approach presented here, in each simulation all the products that are produced during hydrolysis are described. This is illustrated in Figure 11 where the predicted amounts of the saccharides with of degree of polymerization of 15 and 20 are given.

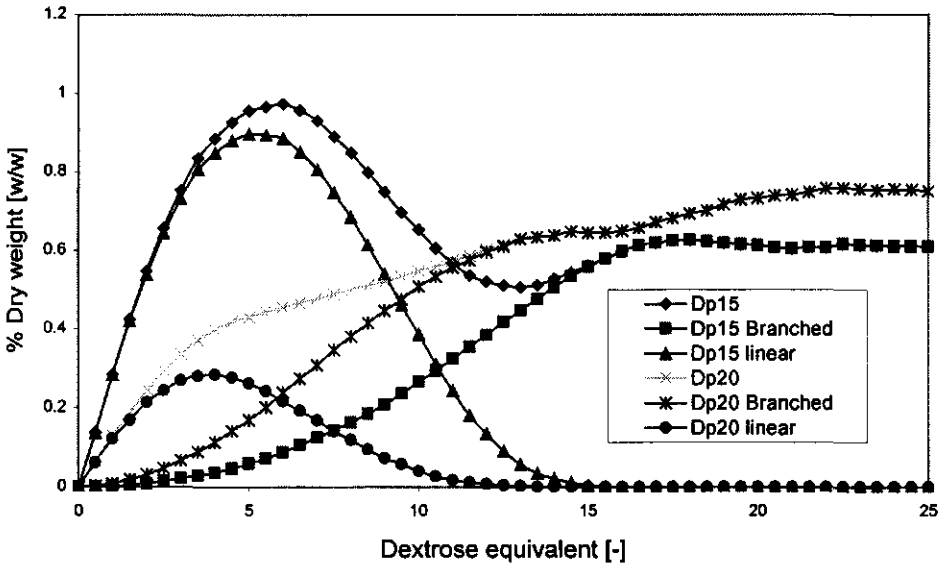

Figure 11: The predicted amount (average of 50 runs) of the saccharides with a degree of polymerization 15 (DP15) and 20 (DP20). The subsite map used is number IV (Table IV and Figure 8).

No experimental data is presented to validate these model predictions. The hydrolysis of starch however can be seen as a cascade of reactions that lead to "end"-products. A significant part of these "end"-products (small oligosaccharides) were evaluated by HPLC measurements. Since these "end"-products were modeled quite well, it is expected that the other saccharides, especially with a degree of polymerization close to the evaluated saccharides, are also modeled quite acceptable. These model predictions could for example be evaluated by an adequately calibrated high-performance anion-exchange chromatograph with a pulsed amperometric detector (HPAEC-PAD), combined with additional NMR measurements (to distinguish between linear and branched saccharides (Gidley, 1985)). However, calibration standards exceeding a degree of polymerization of 7 are not yet commercially available, which makes such a system laborious especially for industrial applications. The advantage of this type of simulation is thus that predictions outside the experimentally evaluated range seem feasible, unavailable in a black box model. This can be used to predict the complete saccharide composition of starch hydrolysis products. In the future, additional experimental data can be used to further refine the model predictions.

Conclusion

Despite the relative uncertainties in the overall structure of amylopectin, the modeled oligosaccharide composition during α-amylolysis is already quite satisfactory. The four different subsite maps, which are reported in literature for α-amylase from *B. amyloliquefaciens*, show different model predictions for the various saccharides. Evaluation of the model predictions with experimental data showed that the subsite with the best prediction for each saccharide differed. The subsite map as determined by Torgerson *et al.* (1979) showed the best overall fit on a molar basis for all the saccharides considered. Application of inhibition constants for a nearby α(1→6)-linked glucose unit on the rate of hydrolysis improved the overall fit for all investigated subsite maps, thus

indicating the validity of inhibition constants as such. With a genetic algorithm it was possible to generate hypothetical subsite maps (with inhibition constants) that gave further improvement. The major advantage of this type of modeling over a black box model is that all the different saccharides produced during hydrolysis are predicted, including those that are difficult to measure experimentally. The reaction considered here, hydrolysis of potato amylopectin with an α-amylase, could be seen as an example for many other reactions that can be modeled in a similar way.

Acknowledgements

The authors thank Stoffer Rustebiel (Avebe) for performing the HPLC analysis. Avebe and the Dutch Ministry of Economic Affairs (PBTS-Biotechnology Project No. BIO94043) funded this research.

References

Allen, J.D., Thoma, J.A. 1976a. Subsite mapping of enzymes. Application of the depolymerase computer model to two α-amylases. Biochem. J. **159:** 121-132.

Allen, J.D., Thoma, J.A. 1976b. Subsite mapping of Enzymes. Depolymerase computer modelling. Biochem. J. **159:** 105-120.

Banzhaf, W., Nordin, P., Keller, R.E., and Francone, F.D. 1998. Genetic programming. An introduction. Morgan Kaufmann Publishers, San Francisco.

Chipman, D.M., Sharon, N. 1970. Mechanism of Lysozyme action. Science. **165:** 454-465.

French, D., Smith, E.E., Whelan, W.J. 1972. The structural analysis and enzymatic synthesis of a pentasaccharide alpha-limit dextrin formed from amylopectin by *Bacillus substilis* alpha-amylase. Carbohydr. Res. **22:** 123-134.

Gidley, M.J. 1985. Quantification of the structural features of starch polysaccharides by N.M.R. spectroscopy. Carbohydr. Res. **139:** 85-93.

Gurney, R.W. 1953. Ionic processes in solution. McGraw-Hill Publishing company, Ltd, London.

Hiromi, K. 1970. Interpreatation of dependency of rate parameters of the degree of polymerization of substrate in enzyme-catalysed reactions. Evaluation of subsite affinities of exo-enzyme. Biochem. Biophys. Res. Commun. **40:** 1-6.

Hizukuri, S. 1996. Starch:Analytical Aspects, pp.347-429.In: Eliasson AC (eds.), Carbohydrates in food, Marcel Dekker, inc., New York.

Iwasa, S., Aoshima, H., Hiromi, K., Hatano, H. 1974. Subsite affinities of bacterial liquefying α-amylase evaluated from the rate parameters of linear substrates. J. Biochem. **75:** 969-978.

MacGregor, E.A., MacGregor, A.W., Macri, L.J., Morgan, J.E. 1994. Models for the action of barley alpha-amylase isozymes on linear substrates. Carbohydr. Res. **257:** 249-268.

Marchal, L.M., Tramper, J. 1999a. Hydrolytic gain during hydrolysis reactions; implications and correction procedures. Biotechnol. Tech. (in press).

Marchal, L.M., van der Laar, A.M.J., Goetheer, E., Schimmelpennink, E.B., Bergsma, J., Beeftink, H.H., Tramper, J. 1999b. The effect of temperature on the saccharide composition obtained after α-amylolysis of starch. Biotechnol. Bioeng. **63:** 344-355.

Thoma, J.A., Allen, J.D. 1976. Subsite mapping of enzymes: collecting and processing experimental data- a case study of an amylase-malto-oligosaccharide system. Carbohydrate Research. **48:** 105-124.

Thoma, J.A., Brothers, C.E., Spradlin, J.E. 1970. Subsite mapping of Enzymes. Studies on *Bacillus subtilis* Amylase. Biochemistry. **9:** 1768-1775.

Thoma, J.A., Rao, C.V., Brothers, C.E., Spradlin, J.E. 1971. Subsite mapping of Enzymes. Biochem. J. **246:** 5621-5635.

Torgerson, E.M., Brewer, L.C., Thoma, J.A. 1979. Subsite mapping of enzymes. Use of subsite map to simulate complete time course of hydrolysis of a polymer substrate. Archs. Biochem. Biophys. **196:** 13-22.

Chapter 8

Towards a Rational Design of Commercial Maltodextrins

L.M. Marchal, H.H. Beeftink, J. Tramper

to be submitted

Introduction

Maltodextrins, which are partially hydrolyzed starch products, have been on the market since the first commercial product Frodex 15 (later called Lo-Dex 15) was introduced by the American Maize Products Company in 1959 (Alexander, 1992). Starch hydrolysis products are commonly characterized by their degree of hydrolysis, expressed as dextrose equivalent (DE), which is the percentage of reducing sugar calculated as dextrose on dry-weight basis. The Unites States Food and Drug Administration defines maltodextrin as (21 CFR paragraph 184.1444): a non-sweet, nutritive saccharide polymer that consists of D-glucose units linked primarily by α-1,4 bonds and that has a DE (dextrose equivalent) of less than 20. In the 40 years since the first introduction, a range of commercial maltodextrins has become available and is used in a wide range of applications. Maltodextrins are used for example as carrier or bulk agent, texture provider, spray-drying aid, fat replacer, film former, freeze-control agent, to prevent crystallization, or to supply nutritional value. In these applications, various physical and biological properties are required. The dextrose equivalent of a maltodextrin has been shown inadequate to predict the product performance in various applications (Chronakis, 1998). Industrially produced maltodextrins (with a certain average degree of polymerization) normally consist of a broad distribution of both linear and branched (containing α(1→6) linkages) saccharides. Maltodextrins with the same DE can even have different properties in various applications that reflect differences in their molecular composition. (Chronakis, 1997; Kennedy et al.,

1985b; Raja et al., 1989). For reasons outlined below there is a growing interest with respect to the development of maltodextrins with a more defined (tailor-made) saccharide composition appropriate for a specific type of application.

1) The general interest in the functionality of food ("functional foods") has increased considerably in the last few years. Research focussed mainly on non-digestible oligosaccharides and resistant starch (Voragen, 1998), but it made the whole carbohydrate market increasingly aware of the relationship between molecular composition and the biological and physical functionality.
2) Progress with respect to the potential of commercially available analysis systems has improved the capability to analyze (oligo)saccharide compositions. These analysis systems include high-performance liquid chromatography (HPLC), high-performance anion-exchange chromatography combined with pulsed amperometric detection (HPAEC-PAD) (Johnson et al., 1993), gel permeation chromatography, NMR (Nelson, 1944) etc. The favorable price / performance ratio of these various analytical systems has contributed to a widespread use by both starch-hydrolysate producers and their customers, primarily the food industry, thus increasing the knowledge on the molecular composition of starch- hydrolysate products.
3) As a consequence of the increased availability of these molecular analytical tools more literature data on structure-function relations has become available both on physical and biological functionality of starch-hydrolysis products.
4) The number of different starch-hydrolysing enzymes has steadily increased since the commercial introduction in the seventies. These enzymes differ in their specificity towards the hydrolysis of starch (Nigam and Singh, 1995). Moreover, recent developments in genetic engineering techniques will further increase the variety of enzymes and decrease their price, enabling starch-hydrolysate producers to comply to customer demands more easily.

This review focuses on the production of maltodextrins with more defined saccharide compositions; glucose and maltose syrups, and cyclodextrins are not considered here. Both the design of the desired molecular composition and the production possibilities for maltodextrins are discussed. Tools in designing a production process and a final design strategy are presented.

Defining desired functionality on a molecular level

The saccharide composition of a maltodextrin determines both its physical and biological functionality. Several aspects related to both physical and biological functionality are discussed, as schematically illustrated in Figure 1. Several products are given to illustrate the need for a balanced saccharide composition.

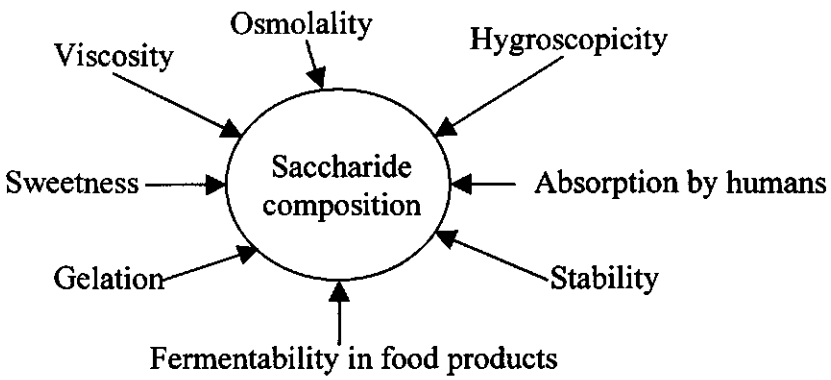

Figure 1: Aspects related to both physical and biological functionality, which determine the desired saccharide composition of starch hydrolysate product.

Hygroscopicity

Hygroscopicity is the ability to absorb moisture from the surrounding atmosphere. Several authors have investigated the hygroscopicity of individual oligosaccharides at various relative humidities and temperatures (Donnelly et al., 1973; Johnson and Srisuthep, 1975; Nakakuki and Kainuma, 1984; Nirkko et al., 1975). The hygroscopicity of glucose (degree of polymerization 1) and maltose (DP2) is very low as compared to the higher polymeric saccharides at all relative humidities. Maltotriose (DP3) shows the highest value for water absorption above a relative humidity of 60 %. The pattern of moisture absorption at 90 % relative humidity and 30°C with respect to the individual oligosaccharides (on mass basis) as determined by Donnelly et al. (1973) for example is:

$$DP3 > DP4 = DP7 > DP5 > DP6 > DP11 > DP2.$$

Although the exact reason for this decrease in hygroscopicity is not clear, it is obvious that oligosaccharides with a degree of polymerization > 9 (Johnson and Srisuthep, 1975) and ≤ 2 (Donnelly et al., 1973; Johnson and Srisuthep, 1975; Nirkko et al., 1975) are the least hygroscopic. The saccharide composition of a starch hydrolysate will thus determine its hygroscopicity. Starch hydrolysates with approximately the same dextrose equivalent, but composed of a different mixture of saccharides, were indeed shown to differ with respect to levels of moisture uptake (Kearsley and Birch, 1975).

Fermentability in food products

Shieh et al. (1973) examined the fermentability of maltooligosaccharides (DP2-DP8) by *Saccharomyces carlsbergensis* (brewers yeast) and *Saccharomyces cerevisiae* (bakers yeast). Neither the bakers nor the brewers yeast's could ferment oligosaccharides above DP3, nor did the presence of glucose stimulate their fermentation. But glucose stimulated all yeast's to ferment maltose and maltotriose. Maltose also prompted the fermentation of maltotriose.

Viscosity

In general, the viscosity will increase with the degree of polymerization of a polymer. Viscosity data for commercial maltodextrins are normally available from their manufactures, but information on the viscosity of individual saccharides is scarce. Johson and Srisuthep (1975) determined the specific viscosity of linear oligosaccharides with a degree of polymerization of 1 to 10 at various concentrations (Figure 2) Up to a degree of polymerization of 7, the viscosity increased approximately linear with both the DP and the concentration [w/v] of the saccharide. The specific viscosity for DP8 to DP10 increased curvilinearly with increasing concentrations. Detailed studies on synergistic effects in mixtures of saccharides and the viscosity of branched saccharides are still to be awaited.

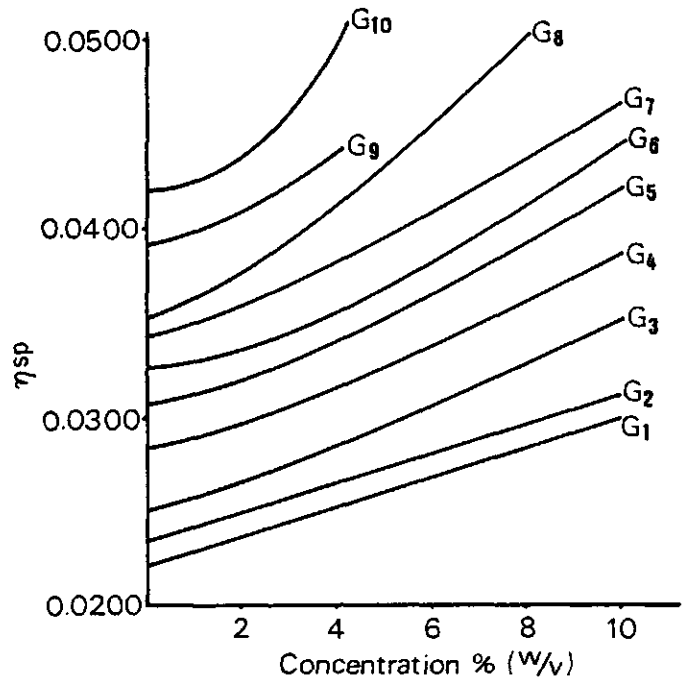

Figure 2: Relationship of the ratio of specific viscosity to concentration of maltooligosaccharides (adapted from Johnson and Srisuthep, 1975).

Sweetness

Although by definition maltodextrin is considered non-sweet, the sweetness of a starch hydrolysis product in general can be tailored by defining the amount and length of the oligosaccharides. In general, the sweetness of individual oligosaccharides (on a mass basis) decreases with increasing degree of polymerization of the oligosaccharide (Birch et al., 1991). Oligosaccharides above a degree of polymerization of 7 possess little or no sweetness (Kimura and Nakakuki, 1990c). The sweetness of a solution increases with increasing solid concentration (Loyd and Nelson, 1984). When for example the sweetness of different oligosaccharides (DP1-DP6) is compared on a molar basis, DP4 (maltotetraose) possesses the highest sweetness (Birch et al., 1991).

Stability

Maltodextrins are normally spray-dried and sold as dry products, which gives them good stability during shelf life. In certain applications, however, dissolved maltodextrins have to be stored for a prolonged period of time without any precipitation. Such applications are for example in clinical feed, where solutions containing up to 50% w/w maltodextrin have to be stored at low temperature (4°C). Kennedy et al. (1987) showed that the precipitate formed from a 50% w/w solution of maltodextrins was composed primarily of oligosaccharides with a degree of polymerization of 11 and above, with no evidence for the presence of oligosaccharides with a degree of polymerization up to 7. This is consistent with the findings of Gidley and Bulpin (1987) who determined that the DP required for precipitation of linear saccharides is at least 8 or 9 and Johson and Srisuthep (1975) who noted that linear saccharides above DP 7 had limited solubility as compared to the smaller saccharides.

Gelation

Low DE maltodextrins (DE < 5) are soluble in cold water and are low-viscous in solution, but at high concentrations (> 20% w/w) they are unstable and form gels that can be used as fat-mimics. The key physical characteristic associated with maltodextrins as fat replacement is their ability to form soft, spreadable gels with melt-in-the-mouth properties that give a fat-like mouth-feel of food products (Richter et al., 1976a,b). Gelation of maltodextrins is a complex phenomenon. The average molecular weight of a maltodextrin proved inadequate in the context of fat replacement. Rather, a molecular weight profile (giving molecular size and amount of each molecular species) can provide useful data that may, in the future, be correlated with functional (fat-mimetic) properties (Roller, 1996). What is clear is that for gelation both branched amylopectin fragments with a degree of polymerization around 50-100 and linear amylose fragments are important. Gidley and Bulpin (1987) showed that amyloses with mean DP values lower then 110 are particularly unstable and precipitate / retrograde faster than molecules having higher DP values (250-300). Amylose is known to accelerate the aggregation and gelation rate, with amylose with an average DP of 140 having the greatest effect (Schierbaum et al., 1984). The fact that a multimodal distribution of molecular weight is important for the gelation properties also becomes clear from the fact that none of the commercially available maltodextrins intended as fat-mimics are produced using acids, which gives a more homogeneous molecular distribution of saccharides upon hydrolysis (Roller, 1996). Rather α-amylases (primarily of *Bacillus* origin) are used. In the future, further improvement of the gelation properties of maltodextrins is anticipated using debranching enzymes (i.e. pullulanase and iso-amylase) in maltodextrin production processes (Chiu,1990,1994).

Osmolality

The osmolality of a solution is equal to the amount of moles dissolved per kg of water, implying that at the same dry-weight concentration, the osmolality increases with decreasing degree of polymerization of the saccharide. This means for example that a 10%

[w/w] solution of glucose has a ten times higher osmolality than a maltodextrin solution with an average degree of polymerization of 11.

Absorption by humans

Orally consumed maltodextrins are partially hydrolyzed by salivary α-amylase. The rate of further absorption of these saccharides is determined by the following factors:

1) The rate of gastric emptying

The pylorus of the stomach regulates the rate in which the ingesta (i.e. maltodextrin solution) leave the stomach to the intestine. The main factors of influence to this rate of gastric emptying are the concentration (a higher concentration gives a lower rate of gastric emptying), volume of the ingesta (a greater volume gives a higher rate of gastric emptying), and to a lesser extent the osmolality of the ingesta; a higher osmolality gives a lower rate of gastric emptying (Foster et al., 1980; Rehrer et al., 1989; Sole and Noakes, 1989).

2) The rate of absorption from the intestine.

The maltodextrins are further hydrolyzed by pancreatic α-amylase to lower saccharides and α-limit-dextrins. A number of membrane enzymes intrinsically bound to the epithelial cells of the intestinal mucosa such as maltase, sucrase, and α-dextrinase can further hydrolyze these linear and branched saccharides to glucose. Glucose at a low concentration enters the enterocytes rapidly by means of a sodium-dependent, energy-requiring carrier system. However, when the luminal sugar concentration is high, absorption may be almost entirely passive (Storey and Zumbe, 1995). Jones and coworkers (1983) studied the rate of absorption of different isotonic oligosaccharide solutions administered directly in the human small intestine. They found that small linear oligosaccharides were absorbed faster than larger (>DP10) oligosaccharides which contained α(1→6) linkages. Furthermore, maltose and maltotriose were absorbed faster than glucose. The authors found that the most probable explanation for the increased glucose absorption from maltose and other α(1→4)

linked oligosaccharides is that the production of monosaccharides by brush-border enzymes gives rise to higher local concentrations at glucose transport sites.

Bacteria in the colon ferment all carbohydrates that are not absorbed in the small intestine (Cummings and Macfarlane, 1991). An excess of fermentable carbohydrates in the large intestine can lead to flatulence and abdominal cramps (Storey and Zumbe, 1995).

It is also known that osmolality influences the rate of water absorption / secretion in the small intestine. In comparing a 17% glucose solution (1233 mosm) and a 17% maltodextrin solution with a DE of 20 (301 mosm), the glucose solution led to a net water secretion while the maltodextrin solution led to a net water absorption from the intestine (Rehrer, 1990). This osmotically induced fluid entry into the small intestine leads to an increased intestinal hurry (osmotic diarrhea) which leads to loss of fluid and electrolytes and can lead to gripping pain (Menzies, 1983).

In general one could state that soluble maltodextrins are well absorbed in the human body, but during more extreme conditions, such as sporting exercise or sickness, a more balanced carbohydrate composition can be an advantage.

Example products

To illustrate the translation of basic knowledge on the behavior of saccharides (best stored using some sort of computer database) to the formulation of actual products, three examples are given:

Sport drinks

A drink consumed during activities that require a great deal of effort has to provide a burst of energy and water to compensate for fluid loss from transpiration. From the above it is obvious that a balanced carbohydrate composition is essential to obtain such a result. An optimal drink would probably contain short linear oligosaccharides with a degree of

polymerization 3-6, since they are absorbed at the highest rate (Storey and Zumbe, 1995) and keep the osmolality at moderate levels, thus preventing fluid loss and possible side effects such as diarrhea and cramps.

Liquid beverages with limited solubility

Maltodextrins are often added to beverages to increase the viscosity. However, in some beverages containing alcohol (e.g. liqueur) the stability of a maltodextrin with a high degree of polymerization can give problems with respect to the stability of the solution. The addition of low-molecular-weight saccharides such as glucose or maltose on the other hand leads to a significant increase in sweetness, which may be undesirable. Furthermore these low-molecular-weight saccharides can be substrate for fermentation by yeast present in, for example, low-alcohol or alcohol-free beer. By balancing the degree of polymerization of the saccharides a non-sweet, viscous, but still stable maltodextrin can be designed for the specific application.

Parental and enteral fluids

Parental solutions are meant to maintain a patient's health and provide nutrition when he or she cannot be fed via the normal digestive system. Since these solutions are directly infused into the veins of a patient, they preferable should be isotonic to blood and therefore the amount of glucose is limited. To provide a daily energy requirement of 10,000 kJ, 14 liter of isotonic glucose solution (5% w/v of glucose) would be required. Clearly such an infusion of water would over-hydrate the patient. Alternatively, hypertonic glucose or fructose 10 to 20% w/v solutions can be injected to provide concentrated energy, but this leads to complications when provided over a prolonged period of time (Ramsay et al., 1980). It is possible to administer linear saccharides with a degree of polymerization between 2 and 5 since these saccharides are hydrolyzed by maltase in the kidney and the liberated glucose is reabsorbed (Watanabe et al., 1993). Using short linear oligosaccharides, sufficient energy can be administered with an isotonic solution, without

over-hydrating the patient (Ramsay et al., 1980). Since oligosaccharides below a degree of polymerization of 7 were shown to be stable in solution over a prolonged period of time (Gidley and Bulpin, 1987), varying the degree of polymerization between 2 and 7 in an infusion product can determine the amount of (excess) liquid provided to a patient at a constant level of energy admission.

Enteral nutrition fluids are beverages that may be either used orally or administered by some form of tube feeding into either the stomach or the small intestine. With enteral fluids, nutrition is the most important function; sweetness and flavor are relevant only for orally consumed beverages. One of the main problems associated with enteral fluids is diarrhea, caused by a high osmolality (Alexander, 1997). In principle the same solution as with sport drinks could be used to solve this problem. Currently maltodextrins, which consist of a complex mixture of linear and branched (containing $\alpha(1\rightarrow6)$ linkages) saccharides, with a DE of 10-20 are used (Alexander, 1992).

Factors influencing the saccharide composition

For the basic concepts of the production of starch hydrolysates we refer to two excellent textbooks on this subject (Kearsley and Dziedzic, 1995; Schenck and Hebeda, 1992). Here we focus on various factors influencing the saccharide composition of a starch hydrolysate product. The basic phenomena influencing the produced saccharide composition are summarized in Figure 3.

Enzymes

The most important tool in providing a saccharide with a specific composition is the use of enzymes with different specificity towards hydrolyzing starch. The three most widely used α-amylases are all isolated from *Bacillus*, i.e. *B. amyloliquefaciens*, *B. licheniformis*, and *B. stearothermophilus*, and differ with respect to the specificity by which they hydrolyze the

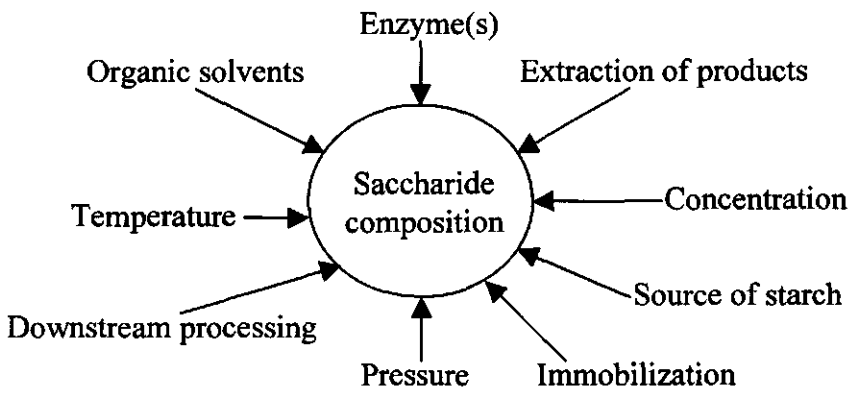

Figure 3: Aspects that influence the saccharide composition obtained during hydrolysis of starch.

α(1→4) linkages in starch. Their temperature optimum is in the range 60-90°C and the pH optimum is approximately 6 to 7. Pullulanases, capable of specifically cleaving the α(1→6) linkages in starch (branchpoints), have a lower pH (5)- and temperature (60°C) optimum. Pullulanase and α-amylase are so-called endo-enzymes, since they are capable to cleave glucose linkages inside the saccharide chain.

There are also hydrolytic enzymes that need to start at a non-reducing end of the saccharide chains and successively release oligosaccharides upon hydrolysis, the so-called exo-enzymes. Two exo-enzymes used in glucose and maltose syrup production are glucoamylase (capable of both cleaving α(1→4) and α(1→6) glucose linkages) which releases glucose, and β-amylase (capable of cleaving α(1→4) linkages) releasing maltose. Furthermore, there is a commercial α-amylase from *Bacillus megaterium* with enhanced transglycosylation activity (Brumm et al.,1991a,b; David et al., 1987) and fungal α-amylases (primary hydrolysis product maltose) both intended for glucose and maltose production.

All enzymes mentioned so far are relatively cheap and are easily obtained from enzyme supplying companies.

Some endo-acting α-amylases are capable of producing small linear oligosaccharides such as maltotriose (Wako et al., 1979), maltotetraose (Kainuma et al., 1972; Kimura and Nakakuki, 1990c; Kobayashi et al., 1991; Parkany Gyarfas and Vamos Vigyazo, 1979; Sakano et al., 1983), and maltohexaose (Fogarty et al., 1991; Monma et al., 1983) from the hydrolysis of starch. The gene encoding for maltotetraose-forming α-amylase from *Pseudomonas stutzeri* has been cloned recently (Hayashibara, Okayama, Japan), which may enhance commercial availability (Kubota et al., 1995). Furthermore, isolation of various α-amylases with specific properties, for example high transglycosylation activity, have been reported (Kimura and Horikoshi, 1990a; Nishimura et al., 1994). Genetic engineering (i.e. site-directed mutagenesis) is providing an increasing number of hydrolytic enzymes with different product specificity (Candussio et al., 1991; Conrad et al., 1995; Matsui et al., 1992; Svensson, 1994; Wind et al., 1998). Genetically engineered α-amylases are appearing on the market, for example Spezyme delta AA (Genencor, Rochester NY) designed to be used at a lower pH, lower calcium levels or higher temperatures (Crabb and Mitchinson, 1997) and Termamyl LC (Novo Nordisk, Bagsvaerd, Denmark) designed for a lower calcium dependency. Furthermore, an enormous range of different hydrolytic enzymes have been isolated from various higher (Nakatani and Kobayashi, 1996), psychrophilic (Feller et al., 1994; Kimura and Horikoshi, 1990b), but especially thermophilic organisms (Leuschner and Antranikian, 1995; Sunna et al., 1997). Cloning into generally used production organisms however remains a must since in general the original organisms show rather low growth rates, require complex media and special handling equipment. Furthermore, the enzyme producers can than benefit from their experience with fermentation and downstream processing of these production organisms. Uncertainty about market potentials has so far restricted the commercial availability of these enzymes.

As an alternative to α-amylases, acid hydrolysis, generally regarded as a more random type of hydrolysis, can be used in starch liquefaction. Low DE conversion products of acid hydrolysis contain more glucose than their enzymatically produced counterparts at the

same DE. This leads to increased sweetness and susceptibility to color development upon heating, generally undesirable for this type of product (Reeve, 1992). Furthermore, they have a low stability caused by the presence of linear chains that have not been shortened sufficiently. Nevertheless acid hydrolysis can be considered as an additional tool in producing a defined saccharide composition, especially in combination with additional enzyme reactions or chromatographic separations (Caboche, 1993; Fouachee née Ducroquet and Duflot, 1995).

Source of starch

Starches from various botanical origins (i.e. potato, corn, wheat, and tapioca) differ slightly in: amylose content, chain-length distribution, molecular weight, and the number of chains per cluster, amongst others. The overall molecular features of these starches, however, are more or less the same. These starches also differ in levels of impurities such as lipids, proteins, pentosans, and ash content (Swinkels, 1985), which may require further downstream processing to eliminate these components (Bowler et al., 1985; Matser and Steeneken, 1998). Low DE conversion products of waxy varieties, containing low-levels of amylose compared to their regular counterparts containing approximately 20% amylose, are more stable in solution, since the amount of linear saccharides is low due to the virtual absence of amylose (Lauro et al., 1993). In the future genetic engineering may provide new (e.g. highly branched) starches that will further enhance the possibilities to produce maltodextrins with different saccharide compositions.

Concentration

Starch hydrolysis products are industrially produced by enzyme reactions from a dissolved solution of starch (up to 40% [w/w]). However, the concentration at which the hydrolysis reaction takes place influences the saccharide composition. The best-known example for this is the production of glucose with a glucoamylase. At very low concentrations (around 1% [w/w]) a nearly 100% conversion of starch to glucose is possible, but at higher dry

weight concentrations, the maximum amount of glucose reached decreases (Reeve, 1992). This decrease in yield of glucose is caused by transglycosylation reactions. In normal industrial practice a 30-32% dry weight solution, which gives around 94% of glucose, is used (Crabb and Mitchinson, 1997; Loyd and Nelson, 1984). It is less well known that the saccharide composition during hydrolysis of starch with an α-amylases is also influenced by the substrate concentration (Fogarty et al., 1991). One of the factors involved is the concentration-dependent transglycosylation reaction by α-amylase (Ajandouz et al., 1992; Graber and Combes, 1990; Kimura and Horikoshi, 1990a). From our own (unpublished) work on the hydrolysis of amylopectin potato starch at 1% [w/w] and 10% [w/w] with *Bacillus amyloliquefaciens* α-amylase, it was also noted that the substrate concentration influences the saccharide composition obtained during hydrolysis (Figure 4).

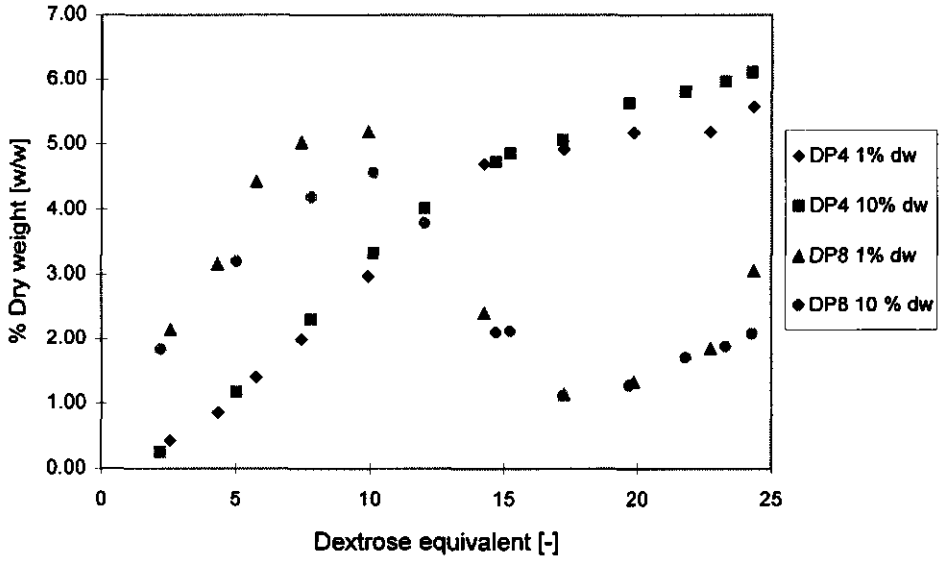

Figure 4: The amount (as weight percentage of total) of maltotetraose (DP4) and malto-octaose (DP8) as a function of the dextrose equivalent. Experimental conditions: 1 and 10% dry weight [w/w] amylopectin potato starch (Avebe, Veendam, The Netherlands), pH 6, 51°C, *Bacillus amyloliquefaciens* α-amylase (BAN 240L, Novo Nordisk, Bagsvaerd, Denmark).

Temperature

The first indications that the temperature at which α-amylolysis is executed influences the saccharide composition were reported by Dobreva et al. (1994) and Ramesh and Lonsane (1989). In both studies, however, there were substantial differences in the degree of hydrolysis between the different temperatures investigated. Recently (Marchal et al., 1999a) we found that the saccharide composition at the end of hydrolysis of amylopectin potato starch with *B. licheniformis* α-amylase (DE around 30) was significantly influenced by the reaction temperature. The temperature was found to have a distinct influence on the oligosaccharide composition during the whole hydrolysis of amylopectin potato starch with *B. amyloliquefaciens*, *B. licheniformis*, and *B. stearothermophilus* α-amylases (Marchal et al., 1999b). A higher temperature led to a less heterogeneous molecular-weight distribution during the initial phase of the hydrolysis with *B. licheniformis* α-amylase. The observed influence of temperature on the rate of hydrolysis is at least a combination of the following aspects:

1) A decrease in product specificity of the α-amylase with increasing temperature.
2) An increase in amount of transglycosylation products with increasing temperature.
3) A change, with the temperature of hydrolysis, between the ratio of the rates of hydrolysis of different linear oligosaccharides with a different DP.

The way in which temperature effects the saccharide composition found for amylopectin potato starch will also hold for other starches, although differences in molecular structure will affect the exact composition of the hydrolysate.

Organic solvents

Addition of organic solvents such as ethanol or polyols influences the saccharide composition obtained upon α-amylolysis of starch (Blakeney and Stone, 1985; Graber and Combes, 1990; Pazlarova, 1995). Although the exact mechanism is still unclear, it was shown that it is possible to decrease the levels of smaller oligosaccharides (glucose to

maltotetraose) produced by addition of various levels of ethanol during the hydrolysis of starch with an α-amylase (Karube and Morita, 1996).

Pressure

The application of high pressure (100-300 MPa) was shown to influence the ratio between the different reaction products (substrate specificity) to which maltohexaose was hydrolyzed by porcine pancreatic α-amylase (Matsumoto et al., 1997). Further research on the influence of pressure on the hydrolysis of higher molecular saccharides (i.e. starch) and industrially more relevant thermostable α-amylases is awaited.

Immobilization

The saccharide profiles obtained after hydrolysis of starch with either soluble enzyme or immobilized enzyme were shown to differ (Hisamatsu et al., 1996; Ivanova and Dobreva, 1994; Kennedy et al., 1985a). The most obvious reason for a different saccharide composition is of course diffusion limitation (Kennedy et al., 1985a; Tarhan, 1989), which increases with the degree of polymerization of the saccharide, enhancing heterogeneous hydrolysis. However, this is not the only reason for different saccharide profiles. Ivanova and Dobreva (1994) showed that the hydrolysis products of maltohexaose changed as a result of immobilization of α-amylase on silica supports. The increased product specificity of the α-amylase caused by immobilization resembles the increase in product specificity with decreasing temperature of hydrolysis (Marchal et al., 1999b), supporting the postulate that an increase in enzyme rigidity increases the substrate specificity.

Downstream processing

The best known example of downstream processing in starch hydrolysis is chromatographic fractionation of dextrose / fructose mixtures (obtained after enzymatic isomerization of dextrose to fructose) to produce syrups with a fructose level above 50% [w/w] (White, 1992). Several other applications are reported in which chromatographic

separation is used to decrease the polymolecularity index (ratio between mass and number-average molecular weight) of hydrolysis products with low DE (Fouachee née Ducroquet, 1998) or to enhance levels of one specific oligosaccharide from a starch hydrolysate by chromatographic methods (Jacques, 1998; Pankratz, 1977; Sakai et al., 1987). Another possibility for further refinement of the saccharide composition is fermentation to remove smaller oligosaccharides (maltose and or glucose) from a starch hydrolysis product (Yoo et al., 1995).

Extraction of products during hydrolysis

Extraction of hydrolysis products (which in turn can be substrate for further hydrolysis) during the hydrolysis of starch can be used to influence the saccharide composition obtained. Systems reported include aqueous two-phase systems and ultrafiltration systems (Larsson et al., 1989; Sims and Cheryan, 1992; Slominska et al., 1998).

Tools in hydrolysis design

When confronted with a demand for the production of a maltodextrin with a specific saccharide composition two computer-based tools, namely databases and hydrolysis models, can be of great assistance.

Databases

A database containing the influence of various enzymes, starches, and process conditions on the saccharide composition can be compiled using literature data combined with own measurements. Literature data provides the cheapest and quickest source of information on saccharide profiles. However, the vast majority of publications on hydrolysis of starch only expresses the decrease in average molecular weight expressed as DE, or only shows the saccharide composition at the 'end' of the hydrolysis reaction. Nevertheless, publications

exist in which the saccharide composition as a function of the degree of hydrolysis is given (Inglett, 1987; Ivanova et al., 1991; Lee et al., 1995; LovsinKukman et al., 1998; Marchal et al., 1999c; Nebesny, 1992,1993; Pasari et al., 1988; Shetty and Allen, 1988; Steverson et al., 1984). Furthermore, publications can be found in which the saccharide compositions are given for combinations of various hydrolytic enzymes and substrate concentrations (Atkins and Kennedy, 1985a,b; Nebesny, 1989,1990a,1990b,1996; Sprienat and Antranikian, 1992; Zackova and Kvasnicka, 1994). This valuable source of information alone, however, may be inadequate to provide a solution for a specifically desired saccharide composition.

Hydrolysis models

When a database with (empirical) recipes for hydrolyzing starch to a certain saccharide composition does not provide a direct answer, hydrolysis models may be useful. However, most kinetic models only express the decrease in average degree of polymerization as a function of process conditions such as temperature and substrate concentration (Fujii et al., 1988; Henderson and Teague, 1988; Komolprasert and Ofoli, 1991; Park and Rollings, 1994). There are kinetic models, however, that describe the hydrolysis in terms of individual saccharides produced, but only for small linear oligosaccharides as a starting material (Dubreucq et al., 1989; Heymann and Guenther, 1994; Iwata et al., 1990; Nakatani, 1997), or for larger ones but still only linear saccharides (amylose) (Kondo et al., 1980; Mazur, 1984; Thoma, 1976a). Since starch normally consists for about 80% of branched amylopectin, the usefulness of these models is limited. Recently, a two-step-approach was presented by us to overcome this problem. In the first step (chapter 5), the branched structure of amylopectin (degree of polymerization ~ 200,000) was modeled in a computer matrix using a Monte Carlo simulation. The chain-length distribution, length and width of a cluster of the amylopectin molecule were used as input variables in the model. Independent literature values related to the structure of amylopectin (% β-hydrolysis and ratio of A to B chains) were then used for evaluation of the branching characteristics

(length of branch area and chance of branching) of the modeled amylopectin. In a second step (chapter 7), the use of this computer-generated model of amylopectin in solution was demonstrated by simulating the hydrolysis with *B. amyloliquefaciens* α-amylase in a Monte Carlo simulation, using the subsite maps presented in literature to describe the enzyme specificity. The predicted saccharide composition, evaluated with experimentally determined values, was acceptable. The influence of an α(1→6) linkage on the rate of hydrolysis of nearby α(1→4) linkages by the α-amylase was evaluated using various inhibition constants. Furthermore, it was demonstrated that it was possible to fit hypothetical subsite maps (with inhibition constants) on a limited set of experimental data, using a genetic type of algorithm. The major advantage of this type of modeling over fitting of experimental data points is that all the different saccharides produced during hydrolysis are predicted, including the ones that are difficult to measure experimentally. Although not perfect yet, at least a reasonable prediction of the saccharides during hydrolysis is obtained. Using the various subsite maps of hydrolytic enzymes available in literature (Iwasa et al., 1974; MacGregor et al., 1994; Matsui et al., 1991; Sano et al., 1985; Seigner et al., 1987; Suganuma et al., 1978; Thoma and Allen, 1976b), a quick overview of the saccharide profiles produced using (combinations of) these enzymes can be obtained. This pre-selection can decrease the number of experiments required to produce a desired saccharide composition. Hydrolysis models can be combined with process models on for example the extraction of saccharides during hydrolysis with ultrafiltration, to predict the resulting saccharide profile.

Production strategy

Despite the fact that an optimal saccharide composition may be designed, it is highly important to produce at an acceptable price, since especially in the food industry, being a bulk market, cost price of a product is always an issue. This implies that the increased

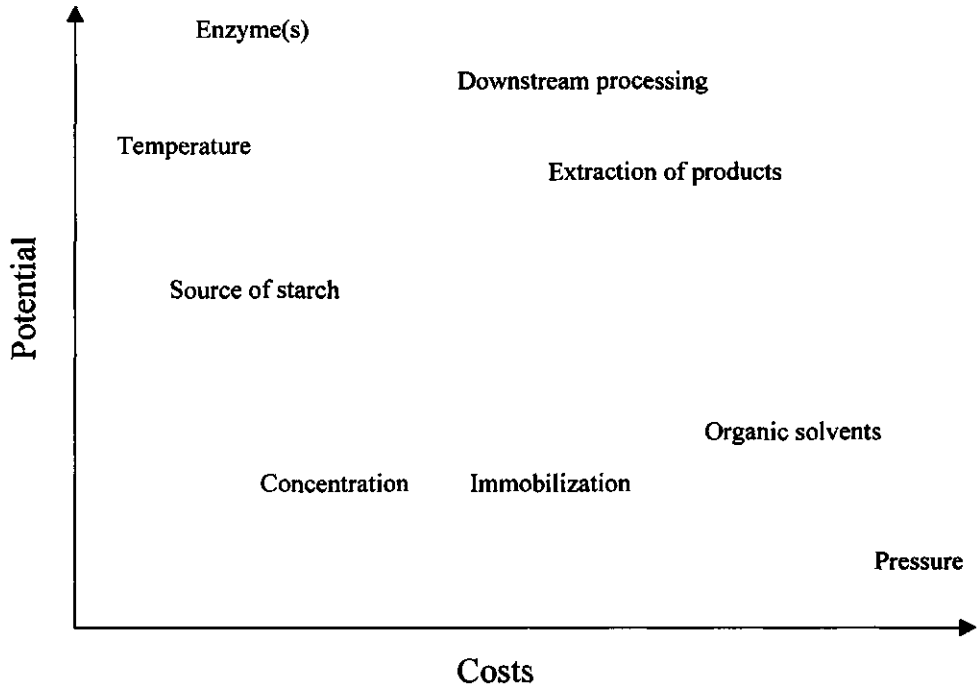

Figure 5: Different ways to influence the saccharide composition of a starch hydrolysate grouped according to potential and costs.

performance must always be balanced by the increased price. Figure 5 shows the different ways to influence the saccharide composition of a starch hydrolysate discussed above, grouped according to potential and costs. In choosing the way to produce a desired saccharide composition, the best production strategy is of course to first investigate the production methods with the highest potential and lowest costs. Production of tailor-made starch hydrolysis products in standard equipment already available to the starch manufacturer significantly reduces the costs. Tailoring a saccharide composition with a relatively simple combination of different enzymes, temperature, and source of starch is

therefore preferred above more laborious, costly methods. The substrate concentration can influence the saccharide composition, but a lower dry-weight concentration has a negative effect on the cost price since it decreases the output of a reactor and increases the drying cost (more evaporation of water for the same amount of product). Immobilized enzyme systems all suffer from increased costs due to immobilization procedures and materials used for normal relatively cheap enzymes. Furthermore, since hydrolyzed starch is an excellent microbial substrate, it is hard to maintain the process microbial stable over a prolonged period. Large-scale application of immobilized hydrolysis systems in the starch industry has so far been limited to the relatively expensive intracellular glucose-isomerase enzyme (White, 1992). Downstream processing (chromatography, separation with ceramic membranes, fermentation of low oligosaccharides) is a very potent tool in chancing the saccharide composition. With the increasing performance and decreasing costs of ceramic membranes, their application for extracting products during hydrolysis, or in down-stream processing, is very likely to increase. A major problem that needs to be addressed, however, is the fouling of the membrane due to non-starch components such as protein (Singh and Cheryan, 1998). The application of organic solvents will be limited because of the adjustments it requires to the standard hydrolysis equipment for safety reasons, and the negative image of organic solvents, other then ethanol, in food production. The use of pressure to influence the saccharide composition is not only expensive, but also little effect has been shown until now.

Future developments and research needs

The global (food) market is characterized by an ever-decreasing lifetime of a specific product. This has forced manufacturers to reduce the time needed to bring a possible product to the market (leap time). This consequently will force the starch manufactures to a quicker response to the demands of their consumers, in the case of maltodextrins primarily

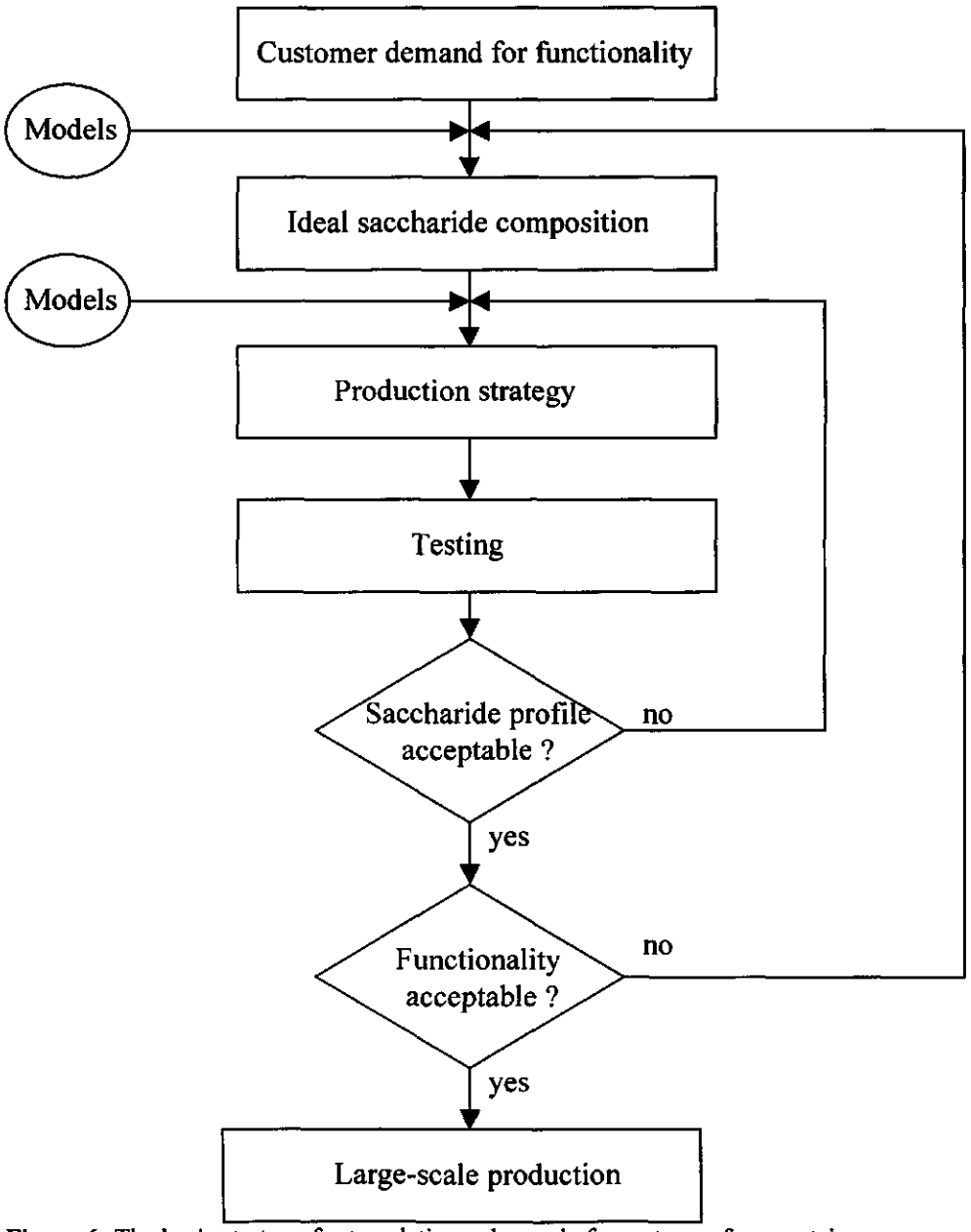

Figure 6: The basic strategy for translating a demand of a customer for a certain functionality of a starch hydrolysate product to actual production. Processes between <> denote decisions.

the food industry. Producers who respond fast will win considerable market share for these (in this bulk industry) high-added-value products. Figure 6 outlines a general strategy from a customer demand for a specific functionality to the actual (large-scale) production. A fast approach would heavily rely on the use of computer-based models and databases to decrease the number of experiments needed to obtain results. These models are likely to increase in number and capability in the near future, since computational performance keeps steadily increasing and database applications and model-building languages are getting more and more user-friendly.

The current state of models is therefore limited to a large extent by the actual knowledge on the structure of starch, the physical and biological properties of saccharides and the exact enzyme specificity. These are exactly the research needs to be addressed in the near future.

Acknowledgements

The authors thank Jack Bergsma and Bert Franke (Avebe), and Kees de Gooijer (WAU) for careful reading of the manuscript and their useful comments. Avebe and the Dutch Ministry of Economic Affairs (PBTS-Biotechnology Project No. BIO94043) funded this research.

References

Ajandouz, E.H., Abe, J., Svensson, B., Mouren, G.M. 1992. Barley malt-α-amylase. Purification, action patern and subsite mapping of isozyme 1 and two members of the isozyme 2 subfamily using p-nitrophenylated maltooligosaccharide substrates. Biochim. Biophys. Acta. **1159:** 193-202.

Alexander, R.J. 1992. Maltodextrins:production, properties and applications, pp.233-276.In: Schenck FW and Hebeda RE (eds.), Starch hydrolysis products; Worldwide technology, production, and applications, VCH Publishers, New York.

Alexander, R.J. 1997. Sweetners used in nutritional beverages. Cereal-Food-World. **42:** 105-106.

Atkins, D.P., Kennedy, J.F. 1985a. A comparison of the susceptibility of two commercial grades of wheat starch to enzymic hydrolysis and their resultant oligosaccharide product spectra. Starch. **37:** 421-427.

Atkins, D.P., Kennedy, J.F. 1985b. The influence of pullulanase and alpha-amylase upon the oligosaccharide product spectra of wheat starch hydrolyzates. Starch. **37:** 126-131.

Birch, G.G., Azudin, M.N., Grigor, J.M. 1991. Solution properties and composition of dextrins, pp.261-272.In: Friedman RB (eds.), Biotechnology of Amylodextrin Oligosaccharides, American Chemical Society, Washington.

Blakeney, A.B., Stone, A.B. 1985. Activity and action pattern of *Bacillus licheniformis* α-amylase in aqueous ethanol. FEBS Letters. **186:** 229-232.

Bowler, P., Towersey, P.J., Galliard, T. 1985. Some effects of the minor components of wheat starch on glucose syrup production. Starch. **37:** 351-356.

Brumm, P.J., Hebeda, R.E., Teague, W.M. 1991a. Purification and characterization of the commercialized, cloned *Bacillus megaterium* alpha-amylase. Part I: purification and hydrolytic properties. Starch. **43:** 315-319.

Brumm, P.J., Hebeda, R.E., Teague, W.M. 1991b. Purification and characterization of the commercialized, cloned *Bacillus megaterium* alpha-amylase. Part II: transferase properties. Starch. **43:** 319-323.

Caboche, J.J. Production of polysaccharide with low digestibility. European patent. 0,561, 090 A1. 1993.

Candussio, A., Schmid, G., Böck, A. 1991. Comparative study of the structure/function relationschip of wild-type and structurally modified maltopentaose-producing amylase. Eur. J. Biochem. **199:** 637-641.

Chiu, C.W. Partially debranched starches and enzymatic process for preparing the starches. European Patent. 0,372,184 A1. 1990.

Chiu, C.W. Foods opacified with debranched starch. European Patent. 0,616,778 A1. 1994.

Chronakis, I.S. 1997. Structural-functional and water holding properties of biopolymers in low fat content spreads. Lebensmittel Wissenschaft und Technologie. **30:** 36-44.

Chronakis, I.S. 1998. On the molecular characteristics, compositional properties, and structural-functional mechanims of maltodextrins: A review. Critical Reviews in Food Science. **38:** 599-637.

Conrad, B., Hoang, V., Polley, A., Hofemeister, J. 1995. Hybrid *Bacillus amyloliquefaciens* X *Bacillus licheniformis* alpha-amylases: Construction, properties and sequence determinants. European Journal of Biochemistry. **230:** 481-490.

Crabb, W.D., Mitchinson, C. 1997. Enzymes involved in the processing of starch to sugars. TIBTECH. **15:** 349-352.

Cummings, J.H., Macfarlane, G.T. 1991. A review: The control and consequences of bacterial fermentation in the human colon. J. Appl. Bacteriol. **70:** 443-459.

David, M.H., Guenther, H., Roeper, H. 1987. Catalytic properties of *Bacillus megaterium* amylase. Starch. **39:** 436-440.

Dobreva, E., Ivanova, V., Emanuilova, E. 1994. Effect of temperature on some characteristics of the thermostable alpha-amylase from *Bacillus licheniformis*. World J. Microbiol. Biotechnol. **10:** 547-550.

Donnelly, B.J., Fruin, J.C., Scallet, B.L. 1973. Reactions of oligosaccharides. III. Hygroscopic properties. Cereal. Chem. **50:** 512-519.

Dubreucq, E., Boze, H., Nicol, D., Moulin, G., Galzy, P. 1989. Kinetics of the alpha-amylase of *Schwanniomyces castelli*. Biotechnol. Bioeng. **33:** 369-373.

Feller, G., Payan, F., Theys, F., Qian, M., Haser, R., Gerday, C. 1994. Stability and structural analysis of α-amylase from the antartic psychrophile *Alteromonas haloplanctis* A23. Eur. J. Biochem. **222:** 441-447.

Fogarty, W.M., Bealin Kelly, F., Kelly, C.T., Doyle, E.M. 1991. A novel maltohexaose-forming alpha-amylase from *Bacillus caldovelox*: patterns and mechanisms of action. Appl. Microbiol. Biotechnol. **36:** 184-189.

Foster, C., Costill, D.L., Fink, W.J. 1980. Gatric emptying characteristics of glucose and glucose polymer solutions. Res. Q. **51:** 299-305.

Fouachee née Ducroquet, C. Process for the manufacture of a starch hydrolysate of low polymolecularity index, obtention and use of novel starch hydrolysate in peritoneal dialysis. United States Patent. 5,837,060. 1998.

Fouachee née Ducroquet, C., Duflot, P. Starch hydrolyzate production with low polymolecularity index. European Patent. 667,356 A1. 1995.

Fujii, M., Homma, T., Taniguchi, M. 1988. Synergism of alpha-amylase and glucoamylase on hydrolysis of native starch granules. Biotechnol. Bioeng. **32:** 910-915.

Gidley, M.J., Bulpin, P.V. 1987. Crystalilisation of Malto-oligosaccharides as model of the crystalline forms of starch: minumum chain length requirement for the formation of double helices. Carbohydr. Res. **161:** 291

Graber, M., Combes, D. 1990. Action pattern of alpha-amylase from *Aspergillus oryzae* in concentrated media. Biotechnol. Bioeng. **36:** 12-18.

Henderson, W.E., Teague, W.M. 1988. A kinetic model of *Bacillus stearothermophilus* alpha-amylase under process conditions. Starch. **40:** 412-418.

Heymann, H., Guenther, S. 1994. Calculation of subsite affinities of human small intestinal glucoamylase-maltase. Biol. Chem. Hoppe-Seyler. **375:** 451-455.

Hisamatsu, M., Hirata, M., Sakamoto, A., Teransihi, K., Yamada, T. 1996. Partial hydrolysis of waxy maize amylopectin by isoamylase immobilized on magnetic support. Starch. **48:** 6-9.

Inglett, G.E. 1987. Action pattern of *Bacillus licheniformis* alpha-amylase on ordinary, waxy, and high amylose corn starches and their hydroxypropyl derivatives. Journal of Food Biochemistry. **11:** 249-258.

Ivanova, V., Dobreva, E. 1994. Catalytic properties of immobilized purified thermostable alpha- amylase from *Bacillus licheniformis* 44MB82-A. Process Biochemistry. **29:** 607-612.

Ivanova, V., Emanuilova, E., Sedlak, M., Pazlarova, J. 1991. HPLC study of starch hydrolysis products obtained with alpha- amylase from *Bacillus amyloliquefaciens* and *Bacillus licheniformis*. Applied Biochemistry and Biotechnology. **30:** 193-202.

Iwasa, S., Aoshima, H., Hiromi, K., Hatano, H. 1974. Subsite affinities of bacterial liquefying α-amylase evaluated from the rate parameters of linear substrates. J. Biochem. **75:** 969-978.

Iwata, K., Ohnishi, M., Hiromi, K. 1990. Glucose production from Maltohexaose as a Substrate by the Bacterial α-amylase-catalyzed Reaction. Its Time Courses Obtained by a Theoretical and an Experimental Approaches. Starch. **42:** 147-151.

Jacques, C.J. High dextrose content starch hydrolysate preparation by liquefaction of starch milk using alpha-amylase, inhibiting amylase, saccharification, molecular sieving and hydrolysate recovery. French Patent. 2,762,616. 1998.

Johnson, D.C., Dobberpuhl, D., Roberts, R., Vandeberg, P. 1993. Pulsed amperometric detection of carbohydrates, amines and sulfor species in ion chromatography- the current state of research. J. Chromatogr. **640:** 79-96.

Johnson, J.A., Srisuthep, R. 1975. Physical and chemical properties of oligosaccharides. Cereal. Chem. **52:** 70-78.

Jones, B.J.M., Brown, B.E., Loran, J.S., Edgerton, D., Kennedy, J.F., Stead, J.A., Silk, D.B.A. 1983. Glucose absorption from starch hydrolysates in the human jejunum. Gut. **24:** 1152-1152.

Kainuma, K., Kobayashi, S., Ito, T., Suzuki, S. 1972. Isolation and action pattern of maltohexaose producing amylase from *Aerobacter aerogenes*. FEBS Letters. **26:** 281-285.

Karube, I., Morita, T. Method for the producing an higher oligosaccharide of a higher polymerization degree. United States Patent. 5,580,762. 1996.

Kearsley, M.W., Birch, G.G. 1975. Selected physical properties of glucose syrup fractions obtained by reverse osmosis. II. Hygroscopicity. J. Fd. Technol. **10:** 625-635.

Kearsley, M.W., Dziedzic, S.Z. 1995. Handbook of starch hydrolysis products and their derivatives. Blackie academic & professional, London.

Kennedy, J.F., Cabral, J.M.S., Kalogerakis, B. 1985a. Comparison of action patterns of gelatin-entrapped and surface- bound glucoamylase on an alpha-amylase degraded starch substrate: a critical examination of reversion products. Enzyme Microb. Technol. 7: 22-28.

Kennedy, J.F., Noy, R.J., Stead, J.A., White, C.A. 1985b. Oligosaccharide component composition and storage properties of commercial low DE maltodextrins and their further modification by enzymatic treatment. Starch. **37:** 343-351.

Kennedy, J.F., Noy, R.J., Stead, J.A., White, C.A. 1987. Composition of the low temperatuure precipitate from commercial high dextrose equivalent maltodextrins and the kinetics of its formation. Starch. **39:** 171-178.

Kimura, T., Horikoshi, K. 1990a. Characterization of pullulan-hydrolyzing enzyme from an alkalopsychrotrophic *Micrococcus sp* . Appl. Microbiol. Biotechnol. **34:** 52-56.

Kimura, T., Horikoshi, K. 1990b. Purification and characterization of alpha-amylases of an alkalopsychrotrophic *Micrococcus sp*. Starch. **42:** 403-407.

Kimura, T., Nakakuki, T. 1990c. Maltotetraose, a new saccharide of tertiary property. Starch. **42:** 151-157.

Kobayashi, S., Okemoto, H., Hara, K., Hashimoto, H., Yamasato, K. 1991. Preparation and some properties of novel maltotetraose-forming enzyme of *Pseudomonas saccharophila.* DEnpun Kagaku. **38:** 27-36.

Komolprasert, V., Ofoli, R.Y. 1991. Starch hydrolysis kinetics of *Bacillus licheniformis* alpha-amylase. J. Chem. Technol. Biotechnol. **51:** 209-223.

Kondo, H., Nakatani, H., Mutsuno, R., Hiromi, K. 1980. Product distribution in Amylase-catalysed hydrolysis of amylose. J. Biochem. **87:** 1053-1070.

Kubota, M., Nakada, T., Sakai, S. Polypeptide possessing maltotetraose-forming amylase activity, and its uses. European patent. 0,298,645 B1. 1995.

Larsson, M., Arasaratnam, V., Mattiason, B. 1989. Integration of bioconversion and downstream processing: starch hydrolysis in an aqueous two-phase system. Biotechnol. Bioeng. **33:** 758-766.

Lauro, M., Lappalainen, A., Suortti, T., Autio, K., Poutanen, K. 1993. Modification of barley starch by α-amylase and pullulanase. Carbohydrate Polymers. **21:** 151-152.

Lee, S.J., Yoo, S.H., Kim, M.J., Kim, J.W., Seok, H.M., Park, K.H. 1995. Production and characterization of branched oligosaccharides from liquefied starch by the action of *B. licheniformis* amylase. Starch. **47:** 127-134.

Leuschner, C., Antranikian, G. 1995. Heat-stable enzymes from extremely thermophilic and hyperthermophilic microorganisms. World J. Microbiol. Biotechnol. **11:** 95-114.

LovsinKukman, I., ZelenikBlatnik, M., Abram, V. 1998. Quantitative estimation of the action of alpha-amylase from bacillus subtilis on native corn starch by hplc and hptlc. Zeitschrift Fur Lebensmittel Untersuchung Und Forschung A Food Research And Technology. **206:** 175-178.

Loyd, N.E., Nelson, W.J. 1984. Glucose- and fructose-containing sweeteners from starch, pp.611-660.In: Whistler RL, Bemiller JN, and Paschall EF (eds.), Starch Chemistry and Technology, 2nd: Academic Press, Orlando.

MacGregor, E.A., MacGregor, A.W., Macri, L.J., Morgan, J.E. 1994. Models for the action of barley alpha-amylase isozymes on linear substrates. Carbohydr. Res. **257:** 249-268.

Marchal, L.M., Jonkers, J., Franke, G.Th., de Gooijer, C.D., Tramper, J. 1999a. The effect of process conditions on the α-amylolytic hydrolysis of amylopectin potato starch. an experimental-design approach. Biotechnol. Bioeng. **62:** 348-357.

Marchal, L.M., van der Laar, A.M.J., Goetheer, E., Schimmelpennink, E.B., Bergsma, J., Beeftink, H.H., Tramper, J. 1999b. The effect of temperature on the saccharide composition obtained after α-amylolysis of starch. Biotechnol. Bioeng. **63:** 344-355.

Matser, A.M., Steeneken, P.A.M. 1998. Origins of the poor filtration characteristics of wheat starch hydrolysates. Cereal. Chem. **75:** 289-293.

Matsui, I., Ishikawa, K., Matsiu, E., Miyairi, S., Fukai, S., Honda, K. 1991. Subsite structure of saccharomycopsis α-amylase secreted from *Saccharomyces cerevisiae*. J. Biochem. **109:** 566-569.

Matsui, I., Ishikawa, K., Miyairi, S., Fukui, S., Honda, K. 1992. A mutant α-amylase with enhanced activity specific for short substrates. FEBS Letters. **310:** 216-218.

Matsumoto, T., Makimoto, S., Taniguchi, Y. 1997. Effect of pressure on the mechanism of hydrolysis of maltotetraose, maltopentaose, and maltohexaose catalyzed by porcine pancreatic alpha-amylase. Biochimica Et Biophysica Acta Protein Structure And Molecular Enzymology. **1343:** 243-250.

Mazur, A.K. 1984. Most-probable distribution at enzyme depolymerization of polysaccharides. Biopolymers. **23:** 859-876.

Menzies, I.S. 1983. Medical importance of sugars in the alimentary tract, pp.89-117.In: Grendy TH, Parker KJ, and Lindley MG (eds.), Developments in sweetners, vol 2: Applied Sciences, London.

Monma, M., Nakakuki, T., Kainuma, K. 1983. Formation and hydrolysis of maltohexaose by an extracellular exo-maltohexaohydrolase. Agric. Biol. Chem. **47:** 1769-1774.

Nakakuki, T., Kainuma, K. 1984. Present and future of development of maltooligosaccharides. Chemical Economy & Engineering Review. **16:** 23-29.

Nakatani, H. 1997. Monte carlo simulation of multiple attack mechanism of beta- amylase-catalyzed reaction. Biopolymers. **42:** 831-836.

Nakatani, H., Kobayashi, I. 1996. Enzymatic properties of α-amylase from Sea Urchin, *Strongylocentrotus*. Comp. Biochem. Physiol. **113B:** 383-386.

Nebesny, E. 1989. Carbohydrate compositions and molecular structure of dextrins in enzymatic high conversion starch syrups. Starch. **41:** 431-435.

Nebesny, E. 1990a. Carbohydrate compositions and molecular structure of dextrins in enzymatic high-maltose syrups. Starch. **42:** 437-444.

Nebesny, E. 1990b. Changes of carbohydrates and molecular structure of dextrins during enzymatic hydrolysis of starch with maltogenase participation. Starch. **42:** 432-436.

Nebesny, E. 1992. Changes of carbohydrates and molecular structure of dextrins during enzymatic liquefaction of starch. Starch. **44:** 398-401.

Nebesny, E. 1993. Changes of Carbohydrate compositions during enzymatic hydrolysis of starches of various orgin. Starch. **45:** 426-429.

Nebesny, E., Pierzgalski, T., Brenzifiki, S. 1996. Changes of carbohydrate composition during enzymatic hydrolysis of starch with mycolase participation. Starch. **48:** 263-266.

Nelson, N. 1944. A photometric adaptation of the somogyi method for the determination of glucose. J. Biol. Chem. **153:** 375-380.

Nigam, P., Singh, D. 1995. Enzyme and microbial systems involved in starch processing. Enzyme Microb. Technol. **17:** 770-778.

Nirkko, V.P., Gál, S., Giovanoli, R., Signer, R. 1975. Der Einfluß des Polymerisationgrades von Oligosacchariden auf die Wasserdampfsorption und ihre Hysterese. Starch. **27:** 278-280.

Nishimura, T., Kometani, T., Takii, H., Terada, Y., Okada, S. 1994. Acceptor specificity in the glucosylation reaction of *Bacillus subtilis* X-23 alpha-amylase towards various phenolic compounds and the structure of kojic acid glucoside. J. Ferment. Bioeng. **78:** 37-41.

Pankratz, T.J. Process for producing maltopentaose. United States Patent. 4,039,383. 1977.

Park, J.T., Rollings, J.E. 1994. Effects of substrate branching characteristics on kinetics of enzymatic depolymerization of mixed linear and branched polysaccharides: I. Amylose/Amylopectine alpha-amylolysis. Biotechnol. Bioeng. **44:** 792-800.

Parkany Gyarfas, A., Vamos Vigyazo, L. 1979. Determination of amylase activity in corn using a chromogenic substrate. Starch. **31:** 328-332.

Pasari, A.B., Korus, R.A., Heimsch, R.C. 1988. Kinetics of the amylase system of *Schwanniomyces castelli*. Enzyme Microb. Technol. **10:** 156-160.

Pazlarova, J. 1995. Activity and hplc measured action pattern of *Bacillus amyloliquefaciens* alpha-amylase in water-soluble organic solvents. Biotechnology Letters. **17:** 503-506.

Raja, K.C.M., Sankarikutty, B., Sreekumar, M., Jayalekshmy, S., Narayanan, S. 1989. Material characterization studies on maltodextrin sample for use of wall material. Starch. **41:** 298-303.

Ramesh, M.V., Lonsane, B.K. 1989. End product profiles of starch hydrolysis by bacterial alpha-amylases at different temperatures and pH values. Biotechnol. Lett. **11:** 649-652.

Ramsay, A.B., Luebke, D.R., Guzek, D.T., Hsieh, C.L., Roteman, R., Leathem, W.D. High calorie solutions of low molecular weight glucose polymer mixtures useful for intravenous administration. United States. 4,182,756. 1980.

Reeve, A. 1992. Starch hydrolysis: processes and equipment, pp.70-120.In: Schenck FW and Hebeda RE (eds.), Starch hydrolysis products; Worldwide technology, production, and applications, VCH Publishers, New York.

Rehrer, 1990. Limits to fluid availability during exercise. University of Maastricht, the Netherlands.

Rehrer, N.J., Beckers, E.J., Brouns, F., Hoor, F., Saris, W.H.M. 1989. Exercise and training effects on gastric emptying of carbohydrate beverages. Med. Sci. Sports. Exerc. **21:** 540-549.

Richter, M., Schierbaum, F., Augustat, S., Knoch, K.D. Method for producing starch hydrolysis products for use as food additives. United States Patent. 3,962,465. 1976a.

Richter, M., Schierbaum, F., Augustat, S., Knoch, K.D. Process for the production of starch hydrolysis products. United Kingdom Patent. 1,423,780. 1976b.

Roller, S. 1996. Starch-derived fat mimetics: maltodextrins, pp.99-118.In: Roller S and Jones SA (eds.), Handbook of fat replacers, CRC Press, Boca Raton.

Sakai, S., Shibuya, T., Miyake, T. Crystalline maltopentaose and process for producing the same. United States Patent. 4,652,640. 1987.

Sakano, Y., Kashiyama, E., Kobayashi, T. 1983. Purification of alpha-maltotetraose-forming exo-amylase of *Pseudomonas stutzeri*; two-forms of the amylase and their enzymatic properties. Agric. Biol. Chem. **47:** 1761-1768.

Sano, M., Sakano, Y., Kobayashi, T. 1985. Subsite structure and action mode of the α-amylase from *Thermoactinomyces vulgaris*. Agric. Biol. Chem. **49:** 2843-2846.

Schenck, F.W., Hebeda, R.E. 1992. Starch hydrolysis products. VCH, New York.

Schierbaum, F., Kettlitz, B., Radosta, S., Reuther, F., Richter, M., Vorwerg, W. 1984. Zum stand der kenntnisse über struktur-eigenschafts-beziehungen von maltodextrinen. Acta Alimentaria Polonica. **10:** 69-99.

Seigner, C., Prodanov, E., Mouren, G.M. 1987. The determination of subsite binding energies of porcine pancreatic α-amylase by comparing hydrolytic activity towards substrates. Biochim. Biophys. Acta. **913:** 200-209.

Shetty, J.K., Allen, W.G. 1988. An Acid-stable, thermostable alpha-amylase for starch liquefaction. Cereal-Food-World. **33:** 929-934.

Shieh, K.K., Donnelly, B.J., Scallet, B.L. 1973. Reaction of oligosaccharides. IV Fermentability by yeasts. Cereal. Chem. **50:** 169-175.

Sims, K.A., Cheryan, M. 1992. Continuous production of glucose syrup in an ultrafiltration reactor. Journal of Food Science. **57:** 163-166.

Singh, N., Cheryan, M. 1998. Membrane technologgy in corn refining and bioproduct-processing. Starch. **50:** 16-23.

Slominska, L., Grajek, W., Grzeskowiak, A., Gocalek, M. 1998. Enzymatic starch saccharification in an ultrafiltration membrane reactor. Starch. **50:** 390-396.

Sole, C.C., Noakes, T.D. 1989. Faster emptying for glucose-polymer and fructose solutions than for glucose in humans. Eur. J. Appl. Physiol. **58:** 605-612.

Sprienat, A., Antranikian, G. 1992. Analysis of the amylolytic enzyme system of Clostridium thermosulfurogenes EM1. Starch. **44:** 305-311.

Steverson, E.M., Korus, R.A., Admassu, W., Heimsch, R.C. 1984. Kinetics of the amylase system of *Saccharomycopsis fibuliger*. Enzyme Microb. Technol. **6:** 549-554.

Storey, D.M., Zumbe, A. 1995. Physiology, metabolism and tolerance of digestible and low-digestible carbohydrates, pp.178-229.In: Kearsley MW and Dziedzic SZ (eds.), Handbook of starch hydrolysis products and their derivatives, Blackie academic & professional, London.

Suganuma, T., Matsuno, R., Ohnishi, M., Hiromi, K. 1978. A study of the mechanism of action of Taka-amylase on linear oligosaccharides by product analysis and computer simulation. J. Biochem. **84:** 293-216.

Sunna, A., Moracci, M., Rosi, M., Antranikian, G. 1997. Glycosyl hydrolases from hyperthermophiles. Extremophiles. **1:** 2-13.

Svensson, B. 1994. Protein engineering in the alpha-amylase family: catalytic mechanism, substrate specificity, and stability. Plant. Mol. Biol. **25:** 151-157.

Swinkels, J.J.M. 1985. Composition and properties of commercial native starches. Starch. **37:** 1-5.

Tarhan, L. 1989. The effect of substrate diffusion factor on immobilized alpha-amylase. Starch. **41:** 315-318.

Thoma, J.A. 1976a. Models for depolymerizing Enzymes. Application to α-Amylases. Biopolymers. **15:** 729-746.

Thoma, J.A., Allen, J.D. 1976b. Subsite mapping of enzymes: collecting and processing experimental data- a case study of an amylase- malto- oligosaccharide system. Carbohydr. Res. **48:** 105-124.

Voragen, A.G.J. 1998. Technological aspects of functional food-related carbohydrates. Trends in Food Science & Technology. **9:** 328-335.

Wako, K., Hashimoto, S., Kubomura, S., Yokota, K., Aikawa, K., Kanaeda, J. 1979. Purification and some properties of a maltotriose-producing α-amylase. DEnpun Kagaku. **26:** 175-181.

Watanabe, S., Maruo, S., Mukai, H., Morino, A. 1993. Utilization of intravenously infused maltooligosaccharides in rabbits. Biological & Pharmaceutical Bulletin. **16:** 1044-1045.

White, J.S. 1992. Fructose syrups: production, properties, and applications, pp.177-199.In: Schenck FW and Hebeda RE (eds.), Starch hydrolysis products; Worldwide technology, production, and applications, VCH Publishers, New York.

Wind, R.D., Buitenlaar, R.M., Dijkhuizen, L. 1998. Engineering of factors determining α-amylase and cyclodextrin glycosyltransferase specificity in the cyclodextrin glycosyltransferase from *Thermoanaerobacterium thermosulfurigens* EM1. Eur. J. Biochem. **253:** 598-605.

Yoo, S.H., Kweon, M.R., Kim, M.Y., Auch, J.H., Jung, D.S., Kim, J.R., Yook, C., Kim, J.W., Park, K.H. 1995. Branched oligosaccharides concentrated by yeast fermentation and effectiveness as a low sweetness humectant. Journal of Food Science. **60:** 516-519.

Zackova, J., Kvasnicka, F. 1994. A contribution to the raw wheat starch hydrolysis. Potrav Vedy. 445-455.

Summary

Industrially produced starch is used for various applications mainly in the food, paper and textile industries. A considerable quantity of this starch is modified (chemically, physically, or enzymatically) before use. The most important modifications are polymer degradation, oxidation, cross-linking, and substitution with various groups, and combinations thereof. This thesis deals with one of these modifications, the partial enzymatic degradation of starch to a saccharide mixtures. These partially hydrolyzed starches (maltodextrins) are used in a wide variety of products, primarily in the food industry. A general introduction to starch and maltodextrin production is given in chapter 1. Maltodextrins are normally characterized by the dextrose equivalent (DE), which is a measure for the number-average molecular weight. Chapter 2 describes the determination of the theoretical dextrose equivalent by measuring the osmolality (mol dissolved particles / kg H_2O) by freezing-point depression. Relations for DE and increase in dry weight during hydrolysis were derived as a function of molality and amount of dry weight at the start of the hydrolysis. With freezing-point depression it was possible to determine the theoretical DE of oligosaccharides (dextrose to maltoheptaose), whereas a traditional titration method (Luff-Schoorl) overestimates 20-50%. The overestimation of DE by Luff-Schoorl titration was also evident during the hydrolysis of amylopectin potato starch. With freezing-point depression it was possible to determine the degree of hydrolysis of starch in a fast, reliable and above all accurate way. The relation for the increase of dry weight during the hydrolysis of starch with an α-amylase was experimentally validated. Throughout the work presented in this thesis osmometry was used.

The hydrolysis of amylopectin potato starch with *Bacillus licheniformis* α-amylase was studied (chapter 3) under industrially relevant conditions (i.e. high dry-weight concentrations). The following ranges of process conditions were chosen and investigated by means of an experimental design: pH [5.6-7.6]; calcium addition [0-120 μg/g]; temperature [63-97°C]; dry-weight concentration [3 - 37% [w/w]]; enzyme dosage [27.6-372.4 μl/kg] and stirring [0-200 rpm]. The rate of hydrolysis was followed as a function of the theoretical DE. The highest rate

(at a DE of 10) was observed at high temperature (90°C) and low pH (6). At a higher pH (7.2), the maximum temperature of hydrolysis shifted to a lower value. Also, high levels of calcium resulted in a decrease of the maximum temperature of hydrolysis. The pH, temperature, and the enzyme dosage showed interactive effects on the observed rate of hydrolysis. No product or substrate inhibition was observed. Stirring did not effect the rate of hydrolysis. The temperature at which the starch was hydrolyzed was found to influence the saccharide composition obtained at the end of the hydrolysis. The number-average molecular weight of these hydrolysates was the same, but their saccharide composition differed. The level of maltopentaose [15-24% [w/w]], a major product of starch hydrolysis catalyzed by *B. licheniformis* α-amylase, was influenced the most by temperature.

The temperature effects were investigated in more detail in chapter 4. *B. licheniformis* α-amylase was added to 10% [w/w] gelatinised amylopectin potato starch solutions. The hydrolysis experiments were done at 50, 70, and 90°C. Samples, taken at defined DE-values were analysed with respect to their saccharide composition. At the same DE the oligosaccharide composition depended on the temperature of hydrolysis. This implies that at the same net number of bonds hydrolysed by the enzyme, the saccharide composition was different. The temperature at which hydrolysis was performed also influenced the initial overall molecular-weight distribution. Higher temperatures led to a more homogenous molecular weight distribution. Similar effects were observed for α-amylases from other microbial sources such as *Bacillus amyloliquefaciens* and *Bacillus stearothermophilus*. The pH of the reaction (5.1, 6.2, and 7.6) at 70 °C did not significantly influence the saccharide composition obtained during *B. licheniformis* α-amylase hydrolysis. The underlying mechanisms for *B. licheniformis* α-amylase were studied using pure linear oligosaccharides, ranging from maltotriose to maltoheptaose as substrates. Activation energies for the hydrolysis of individual oligosaccharides were calculated from Arrhenius plots at 60, 70, 80, and 90°C. Oligosaccharides with a degree of polymerisation exceeding that of the substrate could be detected. The contribution of these oligosaccharides increased as the degree of polymerisation of the substrate decreased and the temperature of hydrolysis increased. The product specificity decreased with increasing

temperature of hydrolysis, which led to a more equal distribution between the possible products formed. Calculations with the subsite map as determined for the closely related α-amylase from *B. amyloliquefaciens* reconfirmed this finding of decreased substrate specificity with increased temperature of hydrolysis. The reaction temperature proved to be a valuable tool for the production of starch hydrolysate products with more defined saccharide compositions. A model, capable of describing the hydrolysis of starch in terms of the saccharide produced, can be a potent tool for the development of tailor-made maltodextrins. Since no suitable models were available, work was initiated on the development of such a model (chapter 5). The branched structure of potato amylopectin (degree of polymerization ~ 200,000) was modeled in a computer matrix. For the amylopectin molecule the chain-length distribution, the length of a cluster and its width were used as input variables in the model. Independent literature values related to the structure of amylopectin (% β-hydrolysis and ratio of A to B chains) were used for evaluation of the branching characteristics (length of branch area and chance of branching) of the modeled amylopectin. The structural parameters predicted by the model agreed very well with data from literature. The chain-length distribution and values for the % of β-hydrolysis were the two most important parameters required to model the structure of amylopectin. This computer-generated model of potato amylopectin in solution can be used to simulate various enzymatic (i.e. α-amylase, β-amylase, glucoamylase, pullunanase) or chemical reactions (i.e. acid hydrolysis, hypochlorite oxidation). The modeling approach is also suitable for a starch structurally different from amylopectin potato starch as obtained from other botanical sources (i.e. corn, wheat, tapioca). When this modeled amylopectin structure was evaluated with independent literature values related to the structure of amylopectin (i.e. % β-hydrolysis), it was recognized that these values were not corrected for the hydrolytic gain during hydrolysis. This overestimation of the actual percentage of β-hydrolysis can however be corrected for (chapter 6). Some of the structural parameters of starch (i.e. % beta- or gluco-hydrolysis) were influenced by the increase in mass during the hydrolysis reactions (hydrolytic gain). Procedures were derived to correct this apparent percentage of hydrolysis to actual percentage of hydrolysis. These analytically derived

equations are not only valid for the hydrolysis of starch but also for the hydrolysis of lower molecular weight saccharides (e.g. α-limit dextrin). With a minor modification, these equations can be used to correct for hydrolytic gain that occurs during the hydrolysis of other (bio)polymers.

An application of the computer-generated model of amylopectin in solution is given in chapter 7 by evaluation of the saccharides produced upon hydrolysis with an α-amylase, the principle enzyme used in maltodextrin production. The four different subsite maps presented in literature for α-amylase originating from *B. amyloliquefaciens* were used to describe the hydrolysis reaction in a Monte Carlo simulation. The saccharide composition predicted by the model was evaluated with experimental values. Overall, the model predictions were acceptable, but no single subsite map gave the best predictions for all saccharides produced. The influence of an α(1→6) linkage on the rate of hydrolysis of nearby α(1→4) linkages by the α-amylase was evaluated using various inhibition constants. For all subsite maps considered the use of inhibition constants led to an improvement in the predictions (decrease of residual sum of squares), indicating the validity for the use of inhibition constants as such.

As without inhibition constants, no single subsite map gave the best fit for all saccharides. The possibility of generating a hypothetical subsite map by fitting was therefore investigated. With a genetic algorithm it was possible to construct hypothetical subsite maps (with inhibition constants) that gave further improvements in the average prediction for all saccharides. The advantage of this type of modeling over a regular fit is the additional information about all the saccharides produced during hydrolysis, including the ones that are difficult to measure experimentally. The final chapter deals with the design procedure for more tailor-made starch hydrolysate products. The saccharide composition of a maltodextrin determines both its physical and biological functionality. Aspects related to the saccharide composition such as hygroscopicity, fermentability in food products, viscosity, sweetness, stability, gelation, osmolality, and adsorption by humans are discussed. The translation of basic knowledge on the behavior of saccharides to the formulation of actual products is illustrated by three examples: a sport drink, maltodextrins

in liquid beverages with limited solubility, and parental and enteral fluids. Various factors that can be used to influence the saccharide composition produced during starch hydrolysis are different hydrolytic enzymes, source and concentration of the starch, temperature of hydrolysis, addition of organic solvents, pressure, immobilization of the hydrolytic enzymes, downstream processing, extraction of products during hydrolysis, and combinations thereof. Tools in designing the production process for a maltodextrin with a specific saccharide composition are databases with saccharide compositions obtained at various hydrolysis conditions and hydrolysis models, which can be used to predict new saccharide compositions. A production strategy for desired saccharide compositions at acceptable prices is discussed and future research needs are pointed out.

Samenvatting

Industrieel geproduceerd zetmeel wordt in veel applicaties gebruikt, voornamelijk in de voedsel-, papier- en textielindustrie. Een groot gedeelte van dit zetmeel wordt gemodificeerd voor gebruik (chemisch, fysisch, of enzymatisch). De belangrijkste modificaties zijn polymeer-degradatie, oxidatie, cross-linken en substitutie met verschillende groepen, en combinaties hiervan. Dit proefschrift behandelt één van deze modificaties, de gedeeltelijke afbraak van zetmeel tot een saccharidenmengsel. Deze gedeeltelijk afgebroken zetmeelhydrolysaten (maltodextrinen) worden gebruikt in een grote verscheidenheid aan producten, voornamelijk in de levensmiddelenindustrie. Hoofdstuk 1 geeft een algemene inleiding over zetmeel- en maltodextrineproductie. Maltodextrinen worden normaal gekarakteriseerd door hun dextrose-equivalent (DE), wat een maat is voor het aantalsgemiddeld molecuulgewicht. Hoofdstuk 2 beschrijft de bepaling van de theoretische dextrose-equivalent door meting van de osmolaliteit (mol opgeloste deeltjes per kilogram water) door meting van de vriespuntsverlaging. Relaties voor DE en toename van het gehalte aan droge stof tijdens de hydrolyse zijn afgeleid als functie van de molaliteit en de hoeveelheid droge stof aan het begin van de hydrolyse. Met behulp van de vriespuntsverlagingsmeting was het mogelijk om de theoretische DE van oligosacchariden (dextrose tot en met maltoheptaose) te bepalen, waar traditionele titratiemethoden (Luff-Schoorl) 20 tot 50 % overschatten. De overschatting van de DE door Luff-Schoorl titratie was ook evident tijdens de hydrolyse van amylopectine-aardappelzetmeel. Met behulp van de vriespuntsverlagingsmeting was het mogelijk om de graad van afbraak van zetmeel op een snelle, betrouwbare, maar bovenal nauwkeurige manier te bepalen. De relatie voor toename in het droge-stofgehalte tijdens de hydrolyse van zetmeel werd experimenteel gevalideerd. Osmometrie is voor al het in dit proefschrift beschreven werk gebruikt.

De hydrolyse van amylopectine-aardappelzetmeel met *Bacillus licheniformis* α-amylase onder industrieel relevante condities (in het bijzonder hoge droge-stofconcentraties) staat

beschreven in hoofdstuk 3. De volgende range van procescondities werd gekozen en onderzocht met behulp van een experimenteel design: pH [5.6-7.6]; calciumtoevoeging [0-120 µg/g]; temperatuur [63-97°C]; droge-stofconcentratie [3 - 37% [w/w]]; enzymdosering [27.6-372.4 µl/kg] en roeren [0-200 omwentelingen per minuut]. De hydrolysesnelheid werd gevolgd als functie van de theoretische DE. De hoogste hydrolysesnelheid (bij een DE van 10) werd waargenomen bij hoge temperatuur (90°C) en lage pH (6). Bij een hogere pH (7.2) verschoof de optimale hydrolysetemperatuur naar een lagere waarde. Voorts resulteerden hogere niveaus van calciumtoevoeging in een verlaging van de optimale hydrolyse-temperatuur. De pH, temperatuur, en enzymdosering vertoonden interacties met betrekking tot de waargenomen hydrolysesnelheid. Product- noch substraatremming werden waargenomen. Roeren beïnvloedde de hydrolysesnelheid niet. De hydrolysetemperatuur bleek de saccharidensamenstelling op het einde van de hydrolyse te beïnvloeden. Het aantalsgemiddeld molecuulgewicht van de hydrolysaten was hetzelfde, maar de saccharidensamenstelling was anders. Het gehalte aan maltopentaose [15-24% [w/w]], op massabasis het belangrijkste product van de zetmeelhydrolyse met *B. licheniformis* α-amylase, werd het meest beïnvloed door de hydrolysetemperatuur.

De temperatuureffecten werden in meer detail in hoofdstuk 4 onderzocht. *B. licheniformis* α-amylase werd toegevoegd aan een 10% [w/w] verstijfselde amylopectine-aardappel-zetmeeloplossing. Hydrolyse-experimenten werden uitgevoerd bij 50, 70 en 90°C. Op gezette DE-waarden werden monsters genomen en geanalyseerd op de saccharidensamen-stelling. Bij een zelfde DE hing de oligosaccharidensamenstelling af van de hydrolyse-temperatuur. Dit impliceert dat bij een zelfde netto aantal verbroken bindingen door het enzym, de saccharidensamenstelling anders was. De hydrolysetemperatuur beïnvloedde ook de initiële algemene molecuulgewichtsverdeling Een hogere hydrolyse-temperatuur leidde tot een homogenere molecuulgewichtsverdeling. Soortgelijke effecten werden ook waargenomen voor α-amylases van andere microbiële oorsprong zoals *Bacillus amyloliquefaciens* and *Bacillus stearothermophilus*. De pH tijdens de reactie (5.1, 6.2 en 7.6) bij 70°C beïnvloedde de saccharidensamenstelling door hydrolyse met *B. licheniformis*

α-amylase niet. De achterliggende mechanismen voor *B. licheniformis* α-amylase werden bestudeerd met behulp van zuivere lineaire oligosacchariden als substraat, variërend van maltotriose tot en met maltoheptaose. De activeringsenergieën voor de hydrolyse van de individuele oligosacchariden werden berekend met behulp van Arrhenius grafieken voor 60, 70, 80 en 90°C. Oligosacchariden met een hogere polymerisatiegraad dan het substraat werden waargenomen. Het aandeel van deze oligosacchariden met een hogere polymerisatiegraad nam toe met afnemende polymerisatiegraad van het substraat en toenemende reactietemperatuur. De productspecificiteit nam af bij toenemende hydrolysetemperatuur, wat tot een gelijkmatiger distributie tussen de mogelijk te vormen producten leidde. Berekeningen met de subsitemap voor de nauw verwante α-amylase van *B. amyloliquefaciens* bevestigden deze bevinding van een afnemende substraatspecificiteit bij toenemende hydrolysetemperatuur.

De reactietemperatuur bleek een waardevol hulpmiddel te zijn voor de productie van zetmeelhydrolysaten met een beter gedefinieerde saccharidensamenstelling. Een model dat in staat is om de hydrolyse van zetmeel te beschrijven in termen van geproduceerde sacchariden, kan een waardevol hulpmiddel zijn bij het ontwikkelen van zulke klantgerichte maltodextrinen.

Aangezien er geen geschikte modellen voorhanden waren, werd begonnen aan de ontwikkeling van zo'n model (hoofdstuk 5). De vertakte structuur van amylopectine-aardappelzetmeel (polymerisatiegraad ~ 200.000) werd gemodelleerd in een computer-matrix. Voor het amylopectinemolecuul werden de ketenlengtenverdeling, lengte van een cluster en zijn breedte gebruikt als input-parameters voor het model. Onafhankelijke literatuurwaarden gerelateerd aan de structuur van amylopectine (het percentage β-hydrolyse en de ratio van de A en B ketens) werden gebruikt voor de evaluatie van de vertakkarakteristieken (lengte van een vertakgebied en kans op vertakking) van het gemodelleerde amylopectine. De door het model voorspelde structurele parameters kwamen zeer goed overeen met de literatuurwaarden. De ketenlengtedistributie en de waarden voor het percentage β-hydrolyse waren de twee belangrijkste parameters nodig om

de structuur van amylopectine te modelleren. Dit computergegenereerde model van aardappelamylopectine in oplossing kan gebruikt worden om allerlei enzymatische (bijvoorbeeld met α-amylase, β-amylase, glucoamylase, pullunanase) of chemische reacties (bijvoorbeeld een zure hydrolyse of hypochloriet-oxidatie) te simuleren.

Deze modelaanpak is ook geschikt voor zetmelen die qua structuur verschillen van amylopectine-aardappelzetmeel, zoals zetmelen verkregen uit andere botanische bron (bijvoorbeeld maïs, tarwe en tapioca).

Tijdens het evalueren van het gemodelleerde amylopectine met onafhankelijke literatuurwaarden gerelateerd aan de structuur van amylopectine (in het bijzonder het percentage β-hydrolyse) bleek dat deze waarden niet gecorrigeerd waren voor de hydrolysewinst tijdens de hydrolyse. Voor deze overschatting van het werkelijke percentage β-hydrolyse kan echter gecorrigeerd worden (hoofdstuk 6). Enkele van de structurele parameters van zetmeel (bijvoorbeeld het percentage bèta- of gluco-hydrolyse) werden beïnvloed door de toename in droge stof tijdens de hydrolysereactie (hydrolysewinst). Procedures werden afgeleid om deze schijnbare hydrolysepercentages te corrigeren naar werkelijke hydrolysegehaltes. Deze analytisch afgeleide vergelijkingen waren niet alleen geldig voor de hydrolyse van zetmeel, maar ook voor de hydrolyse van lager-moleculaire sacchariden (bijvoorbeeld α-grensdextrines). Deze vergelijkingen kunnen, met enkele kleine aanpassingen, ook gebruikt worden om voor de hydrolysewinst bij enkele andere (bio)polymeren te corrigeren.

Een voorbeeld van de toepassing van dit computergegenereerd model van amylopectine in oplossing, de sacchariden die geproduceerd worden tijdens de hydrolyse met een α-amylase (het voornaamste enzym voor maltodextrineproductie), wordt gegeven in hoofdstuk 7. De 4 verschillende subsitemaps uit de literatuur voor α-amylase geïsoleerd uit *B. amyloliquefaciens* werden gebruikt om de hydrolysereactie te beschrijven in een Monte Carlo simulatie. De door het model voorspelde saccharidensamenstelling werd geëvalueerd met experimentele waarden. In het algemeen waren de modelvoorspellingen acceptabel, maar geen enkele subsitemap gaf de beste voorspelling voor alle geproduceerde

saccharіden. De invloed van een α(1→6)-binding op de hydrolysesnelheid van nabij gelegen α(1→4)-bindingen door het α-amylase werd geëvalueerd met behulp van verschillende inhibitieconstanten. Voor alle subsitemaps leidde de toepassing van inhibitie-constanten tot een verbetering in de voorspelling (vermindering van de kwadratensom van de rest), wat de validiteit van het gebruik van inhibitieconstanten als zodanig ondersteunt. Net als in het geval zonder inhibitieconstanten gaf geen enkele subsitemap de beste fit voor alle saccharіden. De mogelijkheid om een hypothetische subsitemap te fitten werd daarom onderzocht. Met een genetisch algoritme was het mogelijk om hypothetische subsitemaps (met inhibitieconstanten) te construeren die een verdere verbetering van de gemiddelde voorspelling van alle saccharіden gaven. Het voordeel van dit type van modellering boven een normale fit is dat additionele informatie wordt verkregen over alle tijdens de hydrolyse geproduceerde saccharіden, inclusief diegene die moeilijk experimenteel te meten zijn.

Het laatste hoofdstuk gaat over een ontwerpprocedure om meer klantgerichte zetmeelhydrolysaten te produceren. De saccharidensamenstelling van een maltodextrine bepaalt zowel de fysische als biologische functionaliteit. Aspecten gerelateerd aan de saccharidensamenstelling zoals hygroscopiciteit, fermentabiliteit in levensmiddelen, viscositeit, zoetheid, stabiliteit, gelering, osmolaliteit en opname door mensen worden besproken. De vertaling van fundamentele kennis over het gedrag van saccharіden naar de formulering van daadwerkelijke producten wordt geïllustreerd aan de hand van drie voorbeelden: een sportdrank, maltodextrinen in vloeibare dranken en sonde- en etheranale voeding. De verschillende factoren die de geproduceerde saccharidensamenstelling kunnen beïnvloeden zijn verschillende hydrolytische enzymen, oorsprong en concentratie van het zetmeel, hydrolysetemperatuur, additie van organische oplosmiddelen, druk, immobilisatie van hydrolytische enzymen, opwerking en extractie van producten tijdens de hydrolyse, en combinaties hiervan.

Hulpmiddelen bij het ontwerp van het productieproces voor maltodextrinen met een specifiekere samenstelling zijn databases met saccharidensamenstellingen verkregen onder verschillende hydrolysecondities en hydrolysemodellen, welke gebruikt kunnen worden om

nieuwe saccharidensamenstellingen te voorspellen. Een productiestrategie voor het ontwerp van een gewenste saccharidensamenstelling tegen een acceptabele prijs en toekomstige onderzoeksbehoeften worden besproken.

Publications

Marchal, L.M., Jonkers, J., Tramper, J. 1996. The use of freezing point depression to determine the theoretical dextrose equivalent. Starch. **48:** 220-224.

dos Santos, V.A.P.M., Marchal, L.M., Tramper, J., Wijffels, R.H. 1996. Modeling and evaluation of an integrated nitrogen removal system with microorganisms co-immobilized in double-layer gel beads. Biotechnol. Prog. **12,** 240-248.

Jonkers, J., Marchal, L.M. 1998. α-Amylolytische hydrolyse van amylopectine-aardappelzetmeel. VMT. **1/2**, 11-14.

Marchal, L.M., Jonkers, J., Franke, G.Th., de Gooijer, C.D., Tramper, J. 1999. The effect of process conditions on the α-amylolytic hydrolysis of amylopectin potato starch. an experimental-design approach. Biotechnol. Bioeng. **62:** 348-357.

Marchal, L.M., van der Laar, A.M.J., Goetheer, E., Schimmelpennink, E.B., Bergsma, J., Beeftink, H.H., Tramper, J. 1999. The effect of temperature on the saccharide composition obtained after α-amylolysis of starch. Biotechnol. Bioeng. **63:** 344-355.

Marchal, L.M., Tramper, J. 1999. Hydrolytic gain during hydrolysis reactions; implications and correction procedures. Biotechnol. Tech. **13:** 325-328.

Marchal, L.M. 1999. Partial hydrolysis of starch to maltodextrins on the laboratory scale, pp.119-127. In: Bucke,C. (ed.), Carbohydrate Biotechnology, Humana Press, New York.

Publications

Marchal, L.M., Zondervan, J., Bergsma, J., Beeftink, H.H., Tramper, J. Monte Carlo simulation of the α-amylolysis of amylopectin potato starch. Part I: Modeling of the structure of amylopectin. submitted to Biotechnol. Bioeng.

Marchal, L.M., Ulijn, R.V., de Gooijer, C.D., Franke, G.Th., Tramper, J. Monte Carlo simulation of the α-amylolysis of amylopectin potato starch. Part II: α-amylolysis of amylopectin. submitted to Biotechnol. Bioeng.

Marchal, L.M., Beeftink, H.H., Tramper, J. Towards a rational design of commercial maltodextrins. to be submitted

Curriculum vitae

Leon Marchal werd geboren 7 januari 1970 te Sittard. In 1989 behaalde hij het VWO diploma aan de Groenenwald te Stein, waarna hij aan de studie Moleculaire wetenschappen aan de Landbouwuniversiteit van Wageningen (LUW) begon. Na het behalen van het propaedeutisch examen in 1990 veranderde hij van studie en begon met de studie Bioprocestechnologie, eveneens aan de LUW. Tijdens de doctoraal fase werd het eerste afstudeervak gevolgd bij de sectie Proceskunde (Prof. Tramper) en het tweede afstudeervak bij de sectie Meet- Regel- en Systeemtechniek (Prof. Van Straten), beiden aan de LUW.
De stage werd volbracht bij The Department of Chemical Engineering (Prof. Willson) aan The University of Houston, Texas, USA. In maart 1995 slaagde hij (cum laude) voor het doctoraal examen. Van februari 1995 tot maart 1999 was hij werkzaam als assistent in opleiding bij de Bioprocestechnologie groep van de sectie Proceskunde van Prof. Tramper. Het onderzoek werd uitgevoerd bij de afdeling Process Research van Avebe in Veendam en de resultaten staan beschreven in dit proefschrift. Vanaf maart 1999 is Leon Marchal werkzaam als procestechnoloog bij Avebe.